

TECHNICAL REPORT

EARLY DETECTION OF SPOTS HIGH WATER SATURATION FOR LANDSLIDE PREDICTION USING THERMAL IMAGING ANALYSIS

KAMARUL HAWARI BIN GHAZALI
MOHD FALFAZLI BIN MAT JUSOF
BADARUDDIN BIN MUHAMMAD
MOHD SHAWAL BIN JADIN
FTKEE
kamarul@ump.edu.my

Faculty of Electrical & Electronics Engineering Technology

UNIVERSITI MALAYSIA PAHANG

ABSTRACT

Landslide hazard often found discussed in electronic media and newspapers. Due to this problem, the government needs to bear millions of Malaysia ringgit to repair the infrastructures and utilities that had ruined and give compensation to the victims involved. Early warning system is one of the effective ways to reduce damage caused by landslides. Based on the literature found, there are many conventional methods to predict landslide had been done previously such as remote sensing, wireless sensor network and many more. Basically, the landslide happened due to the many factors such as slope gradient factor, geological weathering and human-related activities such as deforestation. The main factor for landslide is water saturated caused by heavy rain. Our naked eyes cannot see the water saturated in the soil. Hence, to solve this issue, this study investigates a new method to detect water saturation spots which is integrated with a thermal image camera to provide early detection of landslide. Thermal camera is selected because it provides accurate prediction where landslide is occurs. Thermal imaging is a technique that converts the invisible radiation into visible image for analysis and feature extraction. The images are process using image processing software. Performance of image processing software is based on how accurate Region of Interest (ROI) detection to eliminate unwanted pixels from an image. There are three segmentation algorithm used in this study such as HSV, K-Means and Feature Matching. The performance of these segmentation algorithms are measured using misclassification error. The result reveals that HSV color space technique provides the best segmentation with average misclassification error equals to 0.00165 for abnormal images, 0.0061 for normal images and 0.0014 for combination of abnormal and normal images. Furthermore, the prediction method should make decision and classify the images into correct groups. Therefore, after the ROI has been detected, feature extraction and classification must be performed. Statistical based featured namely minimum, maximum, mean and standard deviation were extracted from each image channels. The results show that the classifications using linear thresholding perform the image into correct group successfully.

The logo for UIMP (Universiti Malaysia Perlis) is a large, stylized letter 'V' shape. The left side of the 'V' is light blue, and the right side is light green. The letters 'UIMP' are written in white, bold, sans-serif font across the center of the 'V'.

TABLE OF CONTENT

TITLE PAGE	
ACKNOWLEDGEMENTS	Error! Bookmark not defined.
ABSTRAK	Error! Bookmark not defined.
ABSTRACT	iii
TABLE OF CONTENT	iv
LIST OF TABLES	vii
LIST OF FIGURES	ix
LIST OF SYMBOLS	xii
LIST OF ABBREVIATIONS	xiii
CHAPTER 1 INTRODUCTION	1
1.1 Introduction	1
1.2 Problem Statement	4
1.3 Research Objectives	5
1.4 Scope of Study	5
1.5 Thesis Overview	6
CHAPTER 2 LITERATURE REVIEW	7
2.1 Introduction	7
2.2 History of landslides	7
2.2.1 Landslide caused by water infiltration	9
2.2.2 Types of Landslides	11
2.2.3 Properties of soil	13

2.3	Current technology in landslide monitoring	14
2.3.1	Remote Sensing	14
2.3.2	Interferometric Synthetic Aperture Radar (InSAR)	16
2.3.3	Geo Information System	17
2.3.4	Photogrammetric	19
2.3.5	Optical Fiber Sensing System	20
2.3.6	Wireless Sensor Network	21
2.4	Thermal Camera Application	23
2.5	Thermal Image Analysis	26
2.6	Image Segmentation	27
2.6.1	Color-Based Segmentation using K-means Clustering	29
2.6.2	K- Means Clustering	29
2.6.3	Feature Matching	31
2.6.4	HSV Color Space	32
2.7	Feature Extraction	34
2.8	Summary	36
CHAPTER 3 METHODOLOGY		37
3.1	Introduction	37
3.2	Research Methodology	37
3.3	Study area	39
3.4	Image acquisition	41
3.4.1	Water Content in Soil	43
3.5	Image Segmentation for Water Spot Detection	46
3.5.1	Feature Matching	47
3.5.2	Color-based segmentation using K-Means	50

3.5.3	HSV	53
3.6	Feature Extraction	55
3.7	Classification	56
3.8	Misclassification Error Measurement	57
CHAPTER 4 RESULTS AND DISCUSSION		58
4.1	Introduction	58
4.2	Effectiveness of image segmentation algorithm	58
4.3	HSV Color Space Technique	Error! Bookmark not defined.
4.4	Color-based segmentation using K-Means	65
4.5	Feature Matching	64
4.6	Statistical Analysis	76
4.6.1	Classification	92
4.7	Water content in soil	94
4.7.1	The result of water content in soil	95
CHAPTER 5 CONCLUSION		97
5.1	Introduction	97
5.2	Recommendation for further research	97
REFERENCES		98

LIST OF TABLES

Table 2.1	List of major landslide phenomenon in 2010 – 2015	8
Table 2.2	List of landslide in Malaysia in 2007 – 2015	8
Table 2.3	Type of landslides	11
Table 2.4	Properties of soil particle	13
Table 2.5	Minimum size of objects to be recognized in various types of Remote sensing imagery	15
Table 3.1	Technical specification of FLIR A615	42
Table 3.2	The groups for classification using Linear thresholding	56
Table 4.1	Misclassification error of HSV techniques	59
Table 4.2	Misclassification error of Color- Based Segmentation using K-Mean clustering techniques	60
Table 4.3	Misclassification error of Feature Matching techniques	61
Table 4.4	Average misclassification error of HSV, K-Means and Feature Matching techniques	62
Table 4.5	Percentage of accuracy of misclassification error of HSV, K-Means and Feature Matching techniques	62
Table 4.6	Hue and its values for red, green and blue in colors	69
Table 4.7	20 data of abnormal condition for HSV technique	76
Table 4.8	20 data of normal condition for HSV technique	77
Table 4.9	20 data of combination normal and abnormal condition for HSV Technique	78
Table 4.10	The statistical analysis for HSV abnormal images results	78
Table 4.11	The statistical analysis for HSV normal images results	78
Table 4.12	The statistical analysis for HSV normal and abnormal images results	79
Table 4.13	20 data of abnormal condition for K-Means technique	79
Table 4.14	20 data of normal condition for K-Means technique	80
Table 4.15	20 data of combination normal and abnormal condition for K-Means Technique	81
Table 4.16	The statistical analysis for K-Means abnormal images results	81
Table 4.17	The statistical analysis for K-Means normal images results	81
Table 4.18	The statistical analysis for K-Means normal and abnormal images results	82
Table 4.19	20 data of normal condition for Feature Matching technique	82
Table 4.20	20 data of abnormal condition for Feature Matching technique	83

Table 4.21	20 data of combination normal and abnormal condition for Feature Matching technique	84
Table 4.22	The statistical analysis for Feature Extraction normal images results	84
Table 4.23	The statistical analysis for Feature Extraction abnormal images results	84
Table 4.24	The statistical analysis Feature Extraction normal and abnormal images results	85
Table 4.25	The percentage of water content and the quantity of water	94
Table 4.26	Experimental condition of soils	96



UMIP

LIST OF FIGURES

Figure 2.1	Field Infiltration Test	10
Figure 2.2	The major types of landslides movement	12
Figure 2.3	The comparison of sizes between sand, clay and silt	13
Figure 2.4	GIS- based conceptual system integrated with data mining for landslide hazard assessment.	18
Figure 2.5	The invention and use of different photogrammetrical methods with respect to time.	19
Figure 2.6	Landslide monitoring configuration based on distributed-fiber sensors	21
Figure 2.7	Sensor Column	22
Figure 2.8	(a) Thermal image of the slope (b) Original photo of the slope	24
Figure 2.9	(a) Photo taken at the daylight (b) Thermal image	24
Figure 2.10	Clustering Procedure	29
Figure 2.11	HSV Color Space	32
Figure 2.12	Classification of shape representation and description techniques	35
Figure 3.1	General proposed methodology of early detection of high water saturation spots for landslide prediction using thermal imaging analysis	38
Figure 3.2	Location of first study area	39
Figure 3.3	The location of second study area	40
Figure 3.4	The location of third study area	40
Figure 3.5	The process converts the video into image	41
Figure 3.6	Thermal Imaging Camera FLIR A615	41
Figure 3.7	The location at Jalan Gambang, Pahang	43
Figure 3.8	Crushing the aggregated soils	44
Figure 3.9	The drying oven	44
Figure 3.10	The crush sample	45
Figure 3.11	The Portable Sieve Shaker	45
Figure 3.12	300 strongest feature points found in the target image	48
Figure 3.13	The putatively matched features image	48
Figure 3.14	The detected box	49
Figure 3.15	Cluster the image into three clusters using Euclidean distance metric	51
Figure 3.16	Water spots segmentation using K-means Clustering	52
Figure 3.17	Flow Diagram for HSV Color Space technique	54

Figure 3.18	The perimeter calculation for the object	55
Figure 4.1	Original photo of concrete wall	70
Figure 4.2	The landslide phenomenon happened in Indera Mahkota 8	70
Figure 4.3	Original thermal images. (a), (b), (c) Abnormal images, (d), (e), (f) normal images (g), (h), (i) combination between abnormal and normal images	71
Figure 4.4	(a) – (i) The images that have been process using HSV color space technique	72
Figure 4.5	(a) and (b) The segmented images using ranges between 0.33 and 0.66	73
Figure 4.6	(a) and (b) The segmented images using ranges between 0 – 0.33	73
Figure 4.7	(a) and (b) The segmented RGB images using color threshold. (c) and (d) the segmented HSV images	74
Figure 4.8	The dialog box displays the options for user.	65
Figure 4.9	Segmentation result when number of cluster is set to 2.	66
Figure 4.10	Segmentation result when number of cluster is set to 3	66
Figure 4.11	Segmentation result when cluster is set to 4	67
Figure 4.12	(a) The abnormal image segmented result using K-Means technique (b) the normal image segmented result using K-Means technique. (c) the abnormal image segmented result using HSV technique (d) the normal image segmented result using HSV technique.	68
Figure 4.13	(a) the segmented result for abnormal image using Feature Matching technique (b) the segmented result normal image using Feature Matching technique.	64
Figure 4.14	The comparison using area features between abnormal and normal condition for HSV technique.	86
Figure 4.15	The comparison using perimeter features between abnormal and normal condition for HSV technique	87
Figure 4.16	The comparison using intensity features between abnormal and normal condition for HSV technique	88
Figure 4.17	The comparison using area features between abnormal and normal condition for K-Means technique	88
Figure 4.18	The comparison using perimeter features between abnormal and normal condition for K-Means technique	89
Figure 4.19	The comparison using intensity features between abnormal and normal condition for K-Means technique	90
Figure 4.20	The comparison using area features between abnormal and normal condition for Feature Matching technique	90
Figure 4.21	The comparison using perimeter features between abnormal and normal condition for Feature Matching technique.	91

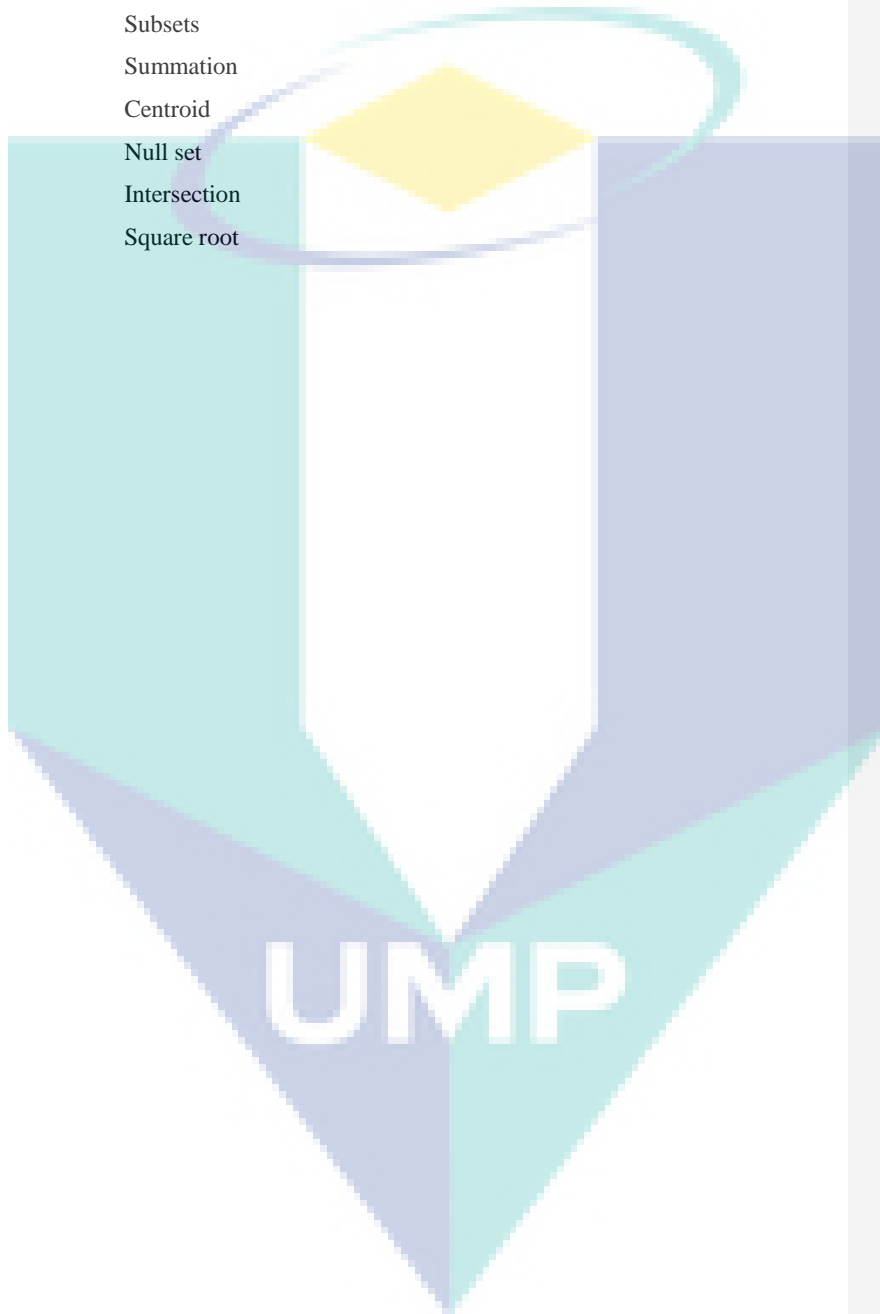
Figure 4.22	The comparison using intensity features between abnormal and normal condition for Feature Matching technique	91
Figure 4.23	The detection result for the proposed technique	92
Figure 4.24	The intensity value for abnormal condition	93
Figure 4.25	The intensity value for normal condition	93
Figure 4.26	The results of laboratory experiment to prove thermal image for water content	95
Figure 4.27	The graph of particle size distribution curve	96




UMP

LIST OF SYMBOLS

F	Set of all pixels
S	Subsets
Σ	Summation
μ_i	Centroid
\emptyset	Null set
\cap	Intersection
$\sqrt{\quad}$	Square root



LIST OF ABBREVIATIONS



JKR	Public Work Department of Malaysia
GPS	Global Positioning System
UWB	Ultra Wideband
InSAR	Interferometric Synthetic Aperture Radar
GIS	Geo Information System
OTDR	Optical Time Domain Reflectometry
WSN	Wireless Sensor Network
MRI	Magnetic Resonance Imaging
SURF	Speeded Up Robust Features
SIFT	Scale Invariant Feature Transform
ASIFT	Affine SIFT
DAS	Driver Assistance Systems
HSV	Hue, Saturation, Value
JPEG	Joint Photographic Experts Group

CHAPTER 1

INTRODUCTION

1.1 Introduction

This study is to explore the Computer Vision technology in developing a system which capable in detecting high water saturation spots for landslide prediction by using thermal imaging analysis. The term of landslide prediction means to determine the potential hazardous location. Landslides are one of the common phenomenon and most frequent in Malaysia. The main factor of landslides is slope failure. Slope failure is occur when soil particles become loose because of the presence of water. Every year, there must be at least a landslide disaster occurs in Malaysia. The problem during this phenomenon is the warnings from an existing landslide, areas of potential failure and initial slope movement are failed to recognize. According to the inventory record from JKR (Public Work Department of Malaysia), the total estimated loss due to the landslides from 1973 to 2007 reached to RM 4.0 Billion (De Wrachien, 2010). It is included loss of life, injury cost, vehicle damage and property damage.

Due to the damage and loss as stated above, it is important to develop an early warning system. A new approach and method to detect spots of high water saturation will be developed which then to be integrated with a thermal camera system to provide an early detection of the landslide. Thermal camera is a device that detects infrared energy which is heat and converts it into an electronic signal. Then, it is processed to produce a thermal image or thermal video. Thermal imaging camera can detect radiation in infrared range of electromagnetic spectrum in the range of 0.78 to 1000 μ m (Krishnamurthy et al., 2009). Thermal imaging cameras are becoming a current tool in industrial field. The research show that thermal imaging camera is use in various field of application, such as electrical and electronic engineering, mechanical engineering, medical and military application (Gowen, Tiwari, Cullen, McDonnell & O'Donnell,

2010; Kastek, Dulski, Trzaskawka & Bieszczad, 2010; Ring & Ammer, 2012). This tool can make the user predict any failure or fault and monitor the process.

Current practice on landslide monitoring and prediction is based on sensor warning networks where it is located and installed in the area of the potential of landslide. The existing monitoring systems for early warning are available in terms of monolithic systems. This is a very cost-intensive way considering installation as well as operational and personal expenses. A very complex emergency plan is usually executed in case of warning. This requires a disciplined adherence to an information chain. Meanwhile, this study is using thermal imaging camera to predict landslide which is very practical in term of mobility. It is easy and can be use anywhere without any installation.

Another new method of landslide detection is using Multi-Band Orthogonal Frequency Division Multiplexing. For this case, the information sequence is modulated on a carrier frequency. Then, the receiver demodulates the information from the carrier frequency. For example, this system is used in GPS (C/A Code). This method has a problem with multipath effects. The ultra-wide band has the possibility to send information with or without a carrier frequency. The absolute bandwidth is more than 500 MHz. The relative bandwidth is a quarter of the middle frequency. The frequency ranges between 0.1 – 0.96 GHz and 3.1 – 10.6 GHz but the information is sent with a low-power (max. -41.3 dBm/MHz). However, the technology that used radiowaves as a medium to detect any change of land has a few disadvantages. The maximum range of monitoring coverage is only 50 m where it is not practical when involved with monitoring in huge area. The other drawback of the system is the UWB transmitter could disrupt other frequencies of radio transmission. For thermal imaging camera, there is no limit of usage. It is because thermal imaging camera detects infrared energy which is heat. The higher the object temperature, the greater the infrared radiation emitted.

From the recent studies, each has its advantages and its drawbacks. This research is proposed approach and method use thermal camera provides accurate predict where landslide going to occur. Thermal camera can be used to detect spots of higher water saturation, a key component that contributes to landslide activity. Such spots of high water saturation are prime candidates for landslide activity when certain

Comment [k1]: ?? what is the advantage ? and drawback ? discuss it. not just giving a general statement like this.

make a table of summarize of the system

Comment [k2]: be carefull with this statement. you are not developing a system

other criteria are met. Thermal camera is able to identify spot of intense saturation, a red flag of a landslide, before any actual damage is done. It is because thermal camera is a device that forms an image using infrared radiation. All object emit infrared energy which is heat as function of their temperature. Then, the device collect the infrared radiation from object in scene and create an electronic image based on info about temperature different because object rarely precisely the same temperature as other object around them. For use in temperature measurement the brightest means the warmest parts of the image are customarily coloured white, intermediate temperatures reds and yellows, and the dimmest means the coolest part is black. The spots of water saturation must appear dark in colour because of different temperature between the soil and saturated water.

The image acquired using thermal camera FLIR A615. The camera is placed nearest to the landslide. The position of thermal camera is not static. It is for searching the high risk spots in that area. The parameters use is focus lens, camera positioning and distances. The camera resolution is 640 x 480. After the image is acquired, the image is process using image processing. Image processing is the backbone of the computer vision system and it is involve with a series of steps. The images of the water spots are focus on the segmentation techniques. Image segmentation is to simplify the representation of image into something that is more meaningful. The comparison between three segmentations is being analyses and the highest accuracy is chooses as the best segmentation technique.

Comment [k3]: ?? rewrite or remove... not appropriate explanation here

Introduction should explain

1. Background of your study. Focus more on image processing not on application and system
2. explain also the motivation on image processing.

1.2 Problem Statement

Nowadays, landslide phenomenon has become a serious problem in Malaysia.

The problem during the landslide phenomenon is the area of potential failure is failed to recognize. The area of potential failure is based on water saturation spots. In determining the regions of the water spots using thermal camera, the main thing need to be considered is the accuracy of the segmented image. This is because the color in the segmented image must be blue color. Blue color is the thermal image color representation for coldest area. Blue color is represents water saturated inside the soil. Besides, thermal camera processes the image manually and it is difficult to visualize the image. Hence, it need image processing to do the decision. Another problem is to classify the regions into normal and abnormal. Normal means it is not danger and abnormal is lead to landslides. Most studies in the field of image processing for landslide have only focused on remote sensing image (Fauzi, Wibowo, Lim & Tan, 2015; P. Ganesan, Rajini, Sathish & Shaik, 2014; K. E. Joyce, Dellow & Glassey, 2008). They use segmentation stage to detect landslide regions from satellite image. None of researchers reported about image processing for thermal image.

Another concern during monitoring the landslide mechanism is the efficiency in term of time and budget. Previously, there are traditional methods that use to monitor landslide phenomena such as remote sensing or satellite technique, geodetic methods, geotechnical methods. In Malaysia, the investigation is carried out after the incident occurs by the government sectors such as Department of public worker and Mineralogy and Geological Survey Department. They used geological method and geotechnical method using inclinometer techniques on landslide area (Jamaludin, Zainuddin, Abdullah & Jaafar, 2011). These methods take longer time to identify the rate if landslide movement.

Besides, there are also methods for landslide monitoring and prediction based on wireless sensor networks where it is installed in the area of potential of landslide. This method is very cost-intensive way considering operational and personal expenses. The conventional technique also has its own limitation such as communication issues. Another concern during landslide monitoring is about specialized in that field. They need to have extra knowledge to use the tools.

Comment [k4]: repeating, just straight forward explain problem statement.

continue explanation in 1.0 introduction

Rewrite your problem statement by focusing on image processing so that it syn with objective. do not high light on system, application.

Comment [k5]: please, you do not do anything with budget and time.

Hence, to overcome this problem, this study investigates a new method to detect spots of high water saturation which is integrated with a thermal camera system to provide early detection of landslide. The thermal camera is selected because it provides accurate predict where landslide going to occur. Thermal camera can be used to detect spots of high water saturation which is a key component that contributes to landslide activity.

1.3 Research Objectives

Based on the problem statement in subchapter 1.2, this study embarks on the following objectives in order to achieve the goal for landslide prediction using thermal camera based on image processing algorithms. The objectives outlined as follows:

- (i) To develop an image processing algorithm based on thermal color of water spots for landslide.
- (ii) To apply region properties technique for feature extraction method.
- (iii) To classify normal and abnormal of water spot region using linear thresholding technique.

1.4 Scope of Study

Most of techniques used are based on image processing techniques that can be applied on Matlab R2013a. The image of landslide will be processed to get the region of the water spots. Thus, the focuses of this project are detection of water spot that saturated in soil. There are two places were used to collect data in this experiment. First batch of data is acquired from Universiti Malaysia Pahang, Pekan, Pahang. The second batch is collected at Bandar Indera Mahkota, Kuantan, Pahang.

Furthermore, this study is for early prediction of landslide. It used image processing analysis which is segmentation and feature extraction technique to process the water spots images. The results of segmented images is to detect whether the water spots is abnormal or normal. The abnormal water spots has high possibilities landslide to happen.

1.5 Thesis Overview

The remainder of this thesis is organized as follows. The first chapter presents an overview of the research such as background of project, problem statements, research objectives, scope of study and thesis outline.

Chapter 2 presents each stage involved in computer vision system. It also contained the literature review of the landslides, current techniques for landslides application, thermal camera application and image processing application.

Chapter 3 explains the research methodology used in this thesis to detect water saturation spots for landslides prediction.

Chapter 4 covers results obtained from the experiment. The discussion and analysis on the results are presented in details.

Chapter 5 concludes all the work and contribution are highlighted. There are further works recommendations are suggested at the end of this chapter.

The publications generated from this thesis are listed in the appendix.



UMP

CHAPTER 2

LITERATURE REVIEW

2.1 Introduction

This chapter briefly discusses about the landslides and current application techniques that used for predict landslide. This is followed by the discussion of application using thermal imaging camera and image processing techniques. This research is focus in image segmentation on how to detect the water saturation spots in landslides. All the segmentation techniques literature review is presented. A summary is presented at the end of this chapter.

2.2 History of landslides

The term of landslide has many definitions. Encyclopedia of Natural Hazard considered landslide as the failure and movement of mass of rock, soil, sediment under the influence of gravity (Clague, 2013). Refer to the (Jongmans & Garambois, 2007), landslide is a large variety of mass movement which is the range from very slow slides in soils to rock avalanches. According to the previous research by (Bobrowsky & Couture, 2014), 'landslide is a movement of mass of soil or rock'. This geological phenomenon can be triggered by natural environment changes or by human activities (Brunetti, Guzzetti & Rossi, 2009). It also can be divided into six factors which are geomorphology, geological, meteorological soil, land use, land cover and hydrologic conditions (Alkhasawneh, Ngah, Tien & Isa, 2012). The factors of geomorphology, geological and meteorological are includes slopes aspect, gradient, weathering, depth and porosity.

The factors of landslide happen are earthquakes, volcanic activity, and heavy rains. Earthquakes affect landslide when it occur on areas with steep slopes. However, Malaysia is not affected by the earthquake. While for the factor caused by heavy rains, it is when water enters into the top soil which can make the soil become heavier. Soil is the heaviest to the effects of gravity when saturated. Landslide impacts in many aspects of human life and the natural environment.

Landslide can cause property damage, injury and death (Alimohammadlou, Najafi & Yalcin, 2013). It is estimated around 375 landslide occur every year and about 4600 people killed per year (Mihir, Malamud, Rossi, Reichenbach & Ardizzone, 2014). There are records of large landslide phenomenon all around the world. The lists of major world landslide phenomenon and the list of landslide that occur in Malaysia are summarized in Table 2.1 and Table 2.2 below respectively. Many methods are used as landslide disaster prevention. For example, an early warning system is the best solution in the prevention plan (Pascal, Thierry, Emmanuelle & Yves, 2013). This system is able to detect an early signs of failure or triggering factor.

Table 2.1 List of major landslide phenomenon in 2010 – 2015

Number	Date	Place	Casualties
1	1 Mar 2010	Bududa District, Uganda	100-300
2	8 August 2010	Gansu, China	1287
3	16 June 2013	Uttarakhand, India	5700
4	22 March 2014	Washington, United States	43
5	2 May 2014	Badakhshan Province, Afghanistan	350-500
6	20 August 2014	Hiroshima, Japan	50
7	13 December 2014	Java, Indonesia	32
8	23 April 2015	Badakhshan Province, Afghanistan	52
9	28 April 2015	Bahia, Brazil	14
10	13 November 2015	Zhejiang, China	38

Table 2.2 List of landslide in Malaysia in 2007 – 2015

Number	Date	Place	Casualties
1	26 December 2007	Kapit, Sarawak	2
2	12 February 2009	Bukit Ceylon, Kuala Lumpur	1
3	21 May 2011	Hulu Langat, Selangor	16
4	29 December 2012	Puncak Setiawangsa, Kuala Lumpur	-
5	4 January 2013	Putra Height	-
6	11 November 2015	Kuala Lumpur-Karak Highway	-

Table 2.2 above shows the landslide that happened in Malaysia from 2007 to 2015 (Ahmad, Lateh & Saleh, 2014). The tragic landslide in 2007 at Kampung Baru Cina, Kapit, Sarawak which resulted two villagers are buried alive and there are houses destroyed. Besides, another landslide reported in 2009 at 43-storey condominium Bukit Ceylon, Kuala Lumpur. One contract worker was killed at the construction site. In 2011, there was also tragedy happened at Hidayah Madrasah Al- Taqwa orphanage in FELCRA Semungkis, Hulu Langat, Selangor and it caused 16 people killed. In 2012, 88 residents of bungalows, shophouses and double storey terrace houses in the Puncak Setiawangsa, Kuala Lumpur were ordered to move out because of soil movement. Another landslides incident happened a year after that which is located at Putra Height. Construction at the Kingsley Hill housing project at Putra Heights has been halted temporarily because of landslide at the site that caused several vehicles to be submerged in mud. Lastly, in 2015, there is a landslide occurred at km 52.4 of the Kuala Lumpur – Karak Expressway between Lentang and Bukit Tinggi.

Slides and flows are the types of landslide that happened frequently in Malaysia. Malaysia has high average annual rainfall, it can caused the soil lose their strength. However, human also the main cause of the landslide phenomenon in Malaysia (Jebur, Pradhan & Tehrani, 2015; Qasim, Harahap, Osman & Baharom, 2013). Human factors like deforestation and poor construction are the reason of landslide occurrence. The stability of slope becomes worst when it affect with natural factor which is heavy rainfall. The heavy rain weakened the soil structure and increase the groundwater level which lead to landslide.

2.2.1 Landslide caused by water infiltration

Water infiltration has been considered one of the triggering mechanisms of slope failure and landslide and it is been investigated by a number of researchers (Capparelli, La Sala, Vena & Donato, 2015; Huat, Ali & Low, 2006; Iverson, 2000; C. W. Ng & Pang, 2000; Rahardjo, Ong, Rezaur & Leong, 2007; Thapa, 2016). The term of infiltration means the process by which water on ground surface enters the soil. It is usually happened in high seasonal rainfalls. The correlation between rainfall and infiltration are rainfall duration and intensity, slope surface factors, slope angle and degree of saturation (Huat et al., 2006).

When the rainwater infiltrates into the slopes, the soil become saturated. Even after rain has stopped, the rain water will continue to move into the soil. When water starts to infiltrated into the soil, the soil approaches saturated condition and the matric suction near the ground surface become zero. Matric suction is one of the main stress variables in unsaturated soil theory. It will increase the strength of soil (Fredlund, Morgenstern & Widger, 1978).

(Huat et al., 2006) used an infiltrometer in his research to determine the infiltration rate of the soil. The Geonor P-88 infiltrometer was used. The field test is shown in Figure 2.1 below is tested at the slope near the Kuala Lumpur International Airport, Kuala Lumpur, Malaysia. This method has the advantage which is easy to use and easy to interpret. However, it also has the limitation which is the water inside the infiltration can flows horizontally through the soil. This technique is sensitive to worm and root holes in the soil.

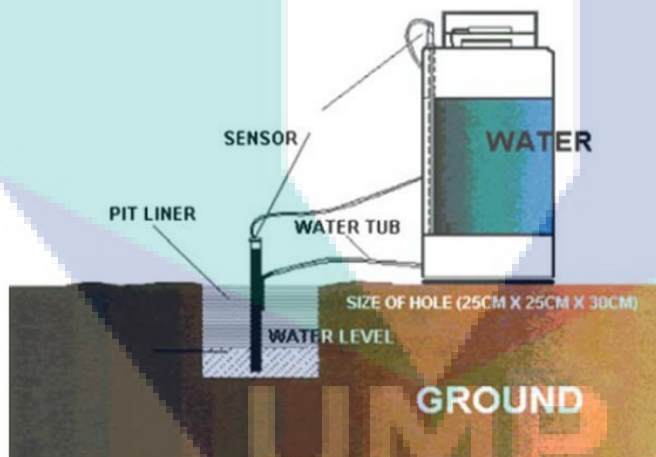


Figure 2.1 Field Infiltration Test

Source : (Huat et al., 2006)

Furthermore, (Chae & Kim, 2012) stated that an early warning system is needed to enable the early prediction of landslide indicators and timely evacuation of residents from landslide-prone areas. They proposed a monitoring system to observe the changes

of soils physical properties during landslide event. It used water content sensor to be installed at the upper, middle and lower parts of the valley at depths of 50 and 80cm.

In Thailand, there is also a study to understand the process of soil moisture changes in soil slope (Jotisankasa & Vathananukij, 2008). The method used is tensiometers to monitor the soil changes. They stated that the saturation of soil slope decrease the strength of the soil and matric suction, finally it will destabilized the slope. However, there are a few disadvantages of tensiometers such as it is slow reaction time due to hydraulic resistance of cup and surrounding soil and tensiometers measures matric potential only in the vicinity of the sensor, several units are needed to give a reliable spatial average.

2.2.2 Types of Landslides

The types of landslides can be differentiated by the kind of material involved and mode of movement. A classification system based on these parameters is shown in Table 2.3 below.

Table 2.3 Type of landslides

Type of movement	Type of material		
	Bedrock	Engineering Soils	
Falls	Rock fall	Predominantly coarse	Earth fall
Topples	Rock topples	Debris fall	Earth topple
Rotational	Rock slide	Debris topple	Earth slide
Translational	Rock slide	Debris slide	Earth slide
Lateral spreads	Rock spread	Debris spread	Earth spread
flows	Rock flow	Debris flow	Earth flow

Source: (Varnes, 1978)

The most common types of landslides are slides, topples, flows and creep. Slides are where there is a distinct zone of weakness that separates the slide material from more stable underlying material. There are two major types of slides which are rotational slides and translational slides. Rotational slide is a slide which the surface of rupture is curved concavely upward and the slide movement is roughly rotational about an axis that is parallel to the ground surface and across the slide. Translational slide is when the landslide mass is move along the roughly planar surface. The Figure 2.2 below illustrates the major types of landslide movement.

Besides slides, another types of landslides is topples. Toppling failures are distinguished by the forward rotation of unit, below in the unit, under the actions of gravity and by fluids in cracks. There is also type of landslides named flows. There are five basic categories of flows which are debris flow, debris avalanche, earthflow, mudflow and creep.

Debris flow is a form of rapid mass movement which is combination of loose soil, rock and water (Hung, Evans, Bovis & Hutchinson, 2001). Debris flows is caused by intense surface-water flow. Debris flows also commonly mobilize from the other types of landslides that occur on steep slopes. Debris avalanche is extremely rapid debris flow. Furthermore, earthflow is the slope material runs out and forming a depression at the head. The flow is usually occurs in fine-grained materials or clay-bearing rocks on moderate slopes and under saturated conditions. Mudflow is an earthflow that consist of wet material and flow rapidly. It contains at least 50% sand, silt and clay-sized particles. A last type of landslides is creep. Creep is slow, steady and downward movement of slope-forming soil. Creep is indicated by curved tree trunks, bent fences or retaining walls and small soil ripples.

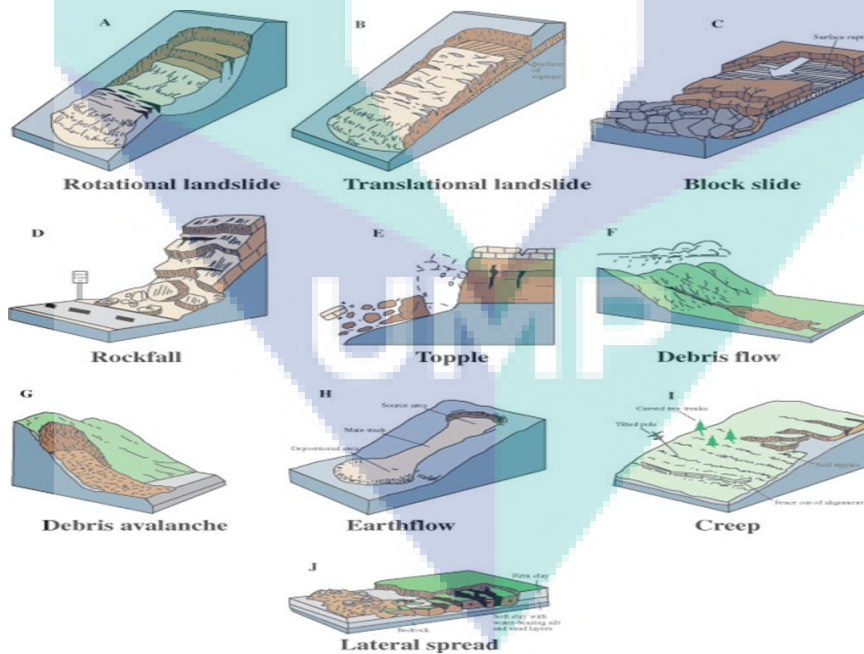


Figure 2.2 The major types of landslides movement

2.2.3 Properties of soil

The particles that make up the soil are categorized into three groups by size namely sand, silt and clay. Sand particles are the largest and clay particles are the smallest. Figure 2.3 below show the comparison of sizes between the three groups of soil.

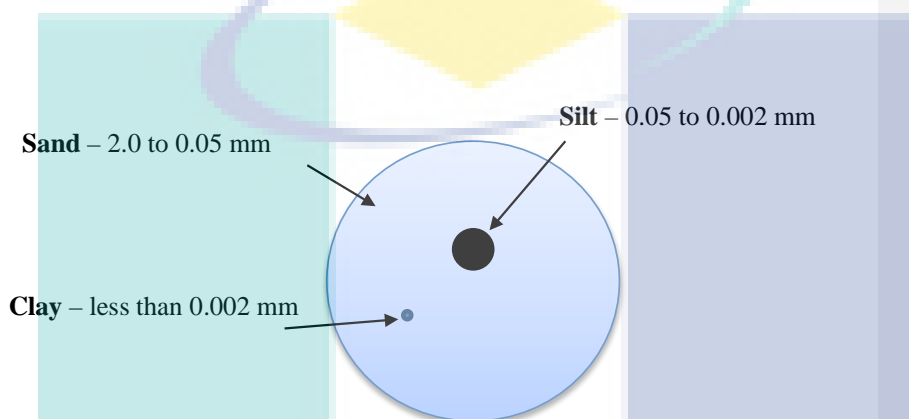


Figure 2.3 The comparison of sizes between sand, clay and silt

Source : (McCauley & Jones)

All soils have the ability to hold water. This ability is different from soil to soil and it relates to the texture of the soil. It also called as permeability which is the rate at water moves through the soil. Porosity is a structure and texture of the soil. Soil texture is important in determining the water holding capacity of soil. For example, fine textured soils hold more water compared to coarse textured soils. Fine grained are silt and clay while coarse grained is sand. The properties of the soil are summarized in the Table 2.4 below.

Table 2.4 Properties of soil particle

Properties of soil	Sand	Silt	Clay
Porosity	Large pores	Small pores	Small pores
Permeability	Rapid	Low to moderate	Slow
Water holding capacity	Limited	Medium	Very large
Soil particle surface	Small	Medium	Very large

2.3 Current technology in landslide monitoring

Previous subchapter had discussed about causes of landslide. Hence, there are a lot of applications nowadays that use to monitoring and preventing landslide. A lot of studies have been done to monitor landslide and the current practice method for the monitoring including remote sensing, geodetic, geotechnical, terrestrial laser scanner, geo-electrical, acoustic emission, optical fiber, suction measurement and sensor network. None of the studies use thermal camera as their tools to detect any land mass movement. Thermal imaging is defined as technique that using the heat given off by an object to produce an image or to locate it. Thermal imaging camera, also known as infrared thermometers, is used to obtain the temperature measurement. Thermal imaging is useful and reliable for single spot temperature reading as it enables us to observe the differences of temperature surface even in 0.01°C .

2.3.1 Remote Sensing

Remote sensing is the science of obtaining information of area or phenomenon through the analysis of data acquired by a device that is not contact with the object, phenomenon or area during the investigation (Lillesand, Kiefer & Chipman, 2014). Remote sensing is also use in monitoring landslide (Karen E Joyce, Belliss, Samsonov, McNeill & Glassey, 2009; Savvaidis, 2003). Landslide studies can classified into three stages. First is detection and classification of landslide, second is monitoring activity of existing landslide and lastly, analysis and prediction of slope failure. For the first stage, the frequent remote sensing tool for detection and classification of landslide is aerial photographs (S. Lee & Min, 2001). Other types are Radar imagery and Satellite imagery. Some most widely used remote sensing tools are shown in Table 2.5 below. The Table 2.5 below indicates the minimum sizes needs for features to be recognized in conditions of high contrast. It can be observed that the SPOT- 5, IKONOS, QUICKBIRD imageries and aerial photos are more suitable to recognize most of the landslides for higher spatial resolution.

Table 2.5 Minimum size of objects to be recognized in various types of Remote sensing imagery

Data source		Spatial resolution (m)	Landslide size (m)
LandSAT- 5	MSS	80	800
	TM	30	300
LandSAT- 7	ETM	30	300
	PAN	15	150
SPOT- 1,2,4	XS	20	200
	PAN	10	100
SPOT- 5	XS	10	100
	PAN1	5	50
	PAN2	2.5	25
IKONOS	XS	4	40
	PAN	1	10
QUICKBIRD	XS	2.44	25
	PAN	0.61	6
Aerial photos 1: 50,000		0.5	5
Aerial photos 1: 25,000		0.25	2.5
Aerial photos 1: 10,000		0.1	1

Source : (Zhiqiang, Huili, Wenji & Youquan, 2005)

Monitoring means the comparison of landslide conditions, such as areal extent, speed of movement, surface topography, and soil humidity from different periods in order to assess the activity of a landslide. For the monitoring of landslides, a wide range of techniques providing very detailed measurements of the surface topography can be used (Mantovani, Soeters & Van Westen, 1996). There are several techniques that used in this stage such as Global Position System (G.P.S) and Radar imagery. The Global Position System (G.P.S.) is a technique which uses a whole series of satellites to determine the X, Y, Z location. It has been recently applied in Italy in studies of monitoring of the Tessina landslide in the region of Veneto by the local Geological Department.

The third stage is to predict where failures are likely to occur. The limitation of the remote sensing technique is very expensive in term of the cost (Tucker & Sellers, 1986). The cost is include the cost for buying or renting the required instruments, the cost of processing software and hardware and the cost of man work (Scaioni, Longoni, Melillo & Papini, 2014). Besides, this technique also requires specialized training and it is complicated to whom that not expertise in this area to use remote sensing technique.

2.3.2 Interferometric Synthetic Aperture Radar (InSAR)

Another method to monitor landslide is Interferometric Synthetic Aperture Radar (InSAR) has demonstrated its potential for landslide deformation monitoring. (Fruneau, Achache & Delacourt, 1996; Jin, van Dam & Wdowinski, 2013; Motagh, Wetzel, Roessner & Kaufmann, 2013; Singhroy, Mattar & Gray, 1998). The data of InSAR is acquired from remote sensing (Riedel & Walther, 2008). InSAR has proven an effective instrument to monitor slow ground deformation. It is based on the quantitative comparison between paired and complex radar images of the same area, taken at different times, to produce interferograms representing pixel by pixel between two images (Zhiqiang et al., 2005). InSAR measures in the direction along straight line between SAR antenna and the ground. SAR satellite transmits and receives radio wave upward from the ground (Antonello et al., 2004).

Ground movement is three dimensional which are east and west, north and south and up and down. However, InSAR can measure one direction only. The absolute distance is not detected by InSAR, only the phase of a radio wave is measured. The reason is the phase only describes its position within one wave cycle, the number of waves which the phases contain is not available. Thus, the information is only represents the LOS direction which cannot directly reflect the actual movement of landslide and should be projected to the slope direction. Furthermore, the application of the InSAR technique is limited to the temporal decorrelation. Another drawback of InSAR is this method required a complete system of analyzing to identify any potential mass massive of landslide.

(Tantianuparp, Shi, Zhang, Balz & Liao, 2013) have investigated the application of inSAR techniques in landslide movement detection and analysis at Badong in the Three Gorges area. Using inSAR, they can detect the areas with high risks of slope failure in Badong and also time-series deformation of landslide bodies. However, they reported that this technique is difficult to be applied for long-term monitoring. There are also limitations due to geometrical and temporal decorrelations.

Besides, (Tarchi et al., 2003) also proposed a technique which provides a remotely sensed measurement of ground displacements. The technique named InSAR has been applied for monitoring the Tessina landslide in Italy. InSAR is allowed to

derive real-time maps showing the deformation field of those landslide sectors characterized by a good radar reflectivity and coherence. Furthermore, InSAR is used to locate and monitor landslide movement in the wide area of Wudonghe Hydropower Reservoir in Jinsha River, China (G. Wang, Xie, Chai, Wang & Dong, 2013). The moving state of the different area and the detailed displacement map of the study area in two time periods are obtained. They highlight that InSAR is one of the important approaches to monitoring of early-stage landslides.

2.3.3 Geo Information System

A Geo Information System (GIS) is a system designed to capture, store, manipulate, analyze, manage, and present all types of geographical data. Many studies have evaluated landslide susceptibility using geographic information system (GIS) technology, and many of these studies have used probabilistic models (Regmi, Giardino & Vitek, 2010) GIS has elevated good expectations as useful means of coping with natural disasters, for example landslides. The most fundamental aspect is to construct useful geospatial database in support of GIS applications.

Although GIS is widely applied in landslide, there are limitations to extract latent information from data collected for evaluating landslide susceptibility. For landslide investigation, there are amount of data have been collected on geology, geomorphological and hydrology which are contain useful information (Huabin, Gangjun, Weiya & Gonghui, 2005). Hence, these problems lead to the risk of losing data or misinterpreting data. There are methods and techniques for effective data management, analysis and information generation should be incorporated into GIS-based landslide assessment as shown in Figure 2.4 below.

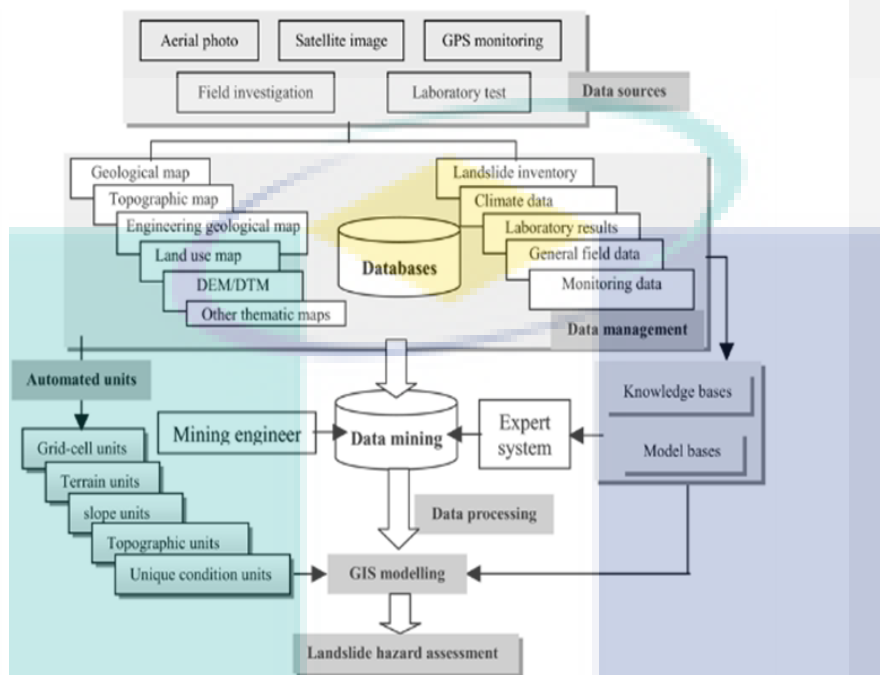


Figure 2.4 GIS- based conceptual system integrated with data mining for landslide hazard assessment.

Source : (Huabin et al., 2005)

Data mining, as an intersection of statistics, machine learning, database management and data visualization, is an exploratory for knowledge discovery in database which consists of six steps in data processing, selection of data, pro-processing of data, analysis and interpretation. There is a study from (C.-T. Lee, 2008) that used GIS as a tool to map storm- induced landslides from SPOT5 images. Digital elevation model (DEM) of 10m X 10m resolution was used to extract geomorphic landslide factors such as slope gradient, slope roughness, slope height and also wetness index. He claimed that GIS is a useful tool for the construction of landslide prediction model. Another study is carried by (Rajbhandari, Alam & Akther, 2002). They investigate the methods of application of GIS for landslide hazard zoning and disaster prone area mapping. They found that GIS is more effective in analyzing the landslide distribution spatially by overlaying with maps related with factors affecting landslide occurrence.

As GIS become one of the popular tools for landslide monitoring, thermal camera can become a complimentary method to perform an early detection of landslide going to occur. The limitation of GIS is its accuracy is depends on the open source data and how it is encoded to be data referenced.

2.3.4 Photogrammetric

Photogrammetry is the process of gaining surface data from a region with use of image analysis instead of direct physical contact (Schenk, 2005). It uses image matching to create 3 dimensional scenes. The image matching is done by triangulating points and sources from different image. The concept is similar as eyesight.

The history of photogrammetry is started from 1839. It is begin with stereo photogrammetry. Images were taken from offset positions and viewed with stereoscopic equipment. The invention of digital cameras and computers has created the present state of photogrammetry. Processing techniques are fast and resolution is increasing. The stages of photogrammetry are seen in Figure 2.5 below.

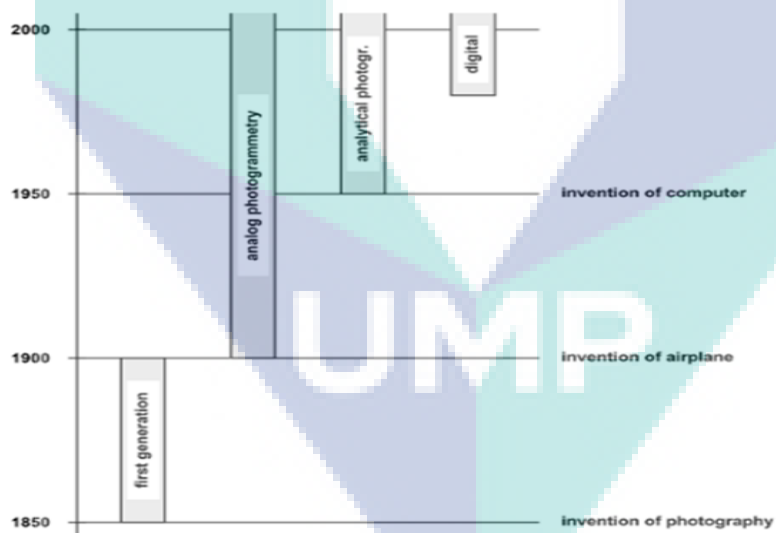


Figure 2.5 The invention and use of different photogrammetrical methods with respect to time.

Source : (Schenk, 2005)

For landslide monitoring, photogrammetry is used for two tasks (Saunders, 2014). Firstly, monitoring of landslide movement can use temporal photogrammetric data to track movement. It is cover different sized regions and image capture techniques. Second, photogrammetry is used for determining fracture orientation. Photogrammetric techniques have been extensively used in determining ground movements in ground subsidence studies in mining areas (Savvaiddis, 2003)

The main advantages of using photogrammetry are the reduced time of fieldwork, simultaneous three-dimensional coordinates and in principle an unlimited number of points can be monitored. Terrestrial photography is also being used for local-scale landslide monitoring. Sites that are too steep and too small to be confidently viewed from the air lend themselves to study on the ground. Terrestrial photogrammetry can effectively be used at unsafe or inaccessible sites, such as road cuttings and landslides. Besides the advantages for photogrammetric, there is also disadvantages for this techniques such as it is requires expensive instruments like metric aerial cameras, photogrammetric scanners and digital photogrammetric workstation (Bitelli, Dubbini & Zanutta, 2004).

2.3.5 Optical Fiber Sensing System

Fibre-optic sensors embedded in shallow trenches within slopes could help detect and monitor both large landslide and slow slope movements. Usually, electrical sensors have been used for monitoring the risk of landslides, but they are easily damaged. Fibre- optic sensor is economical and sensitive.

An investigation is carried by Public Research Institute in Japan and Institute di Recerca per la Protezione Idrogeologica in Italy (Higuchi, Fujisawa, Asai, Pasuto & Marcato, 2007). As one of the new technique, an optical fiber sensing system was installed in the Takisaka Landslide. The optical fiber sensing system has 18 sensors and was installed at the end of the Takisaka Landslide facing the Aga River. The OTDR (Optical Time Domain Reflectometry) method was selected at this site. The sensor is a mechanical device in which part of an optical fiber bends in response to landslide displacement. Figure 2.6 below shows the monitoring configuration. The sensor

comprises optical fibers inside the steel tubes. In application, vertical holes are drilled in the landslide body down to bedrock while the sensors are laid down in the holes.

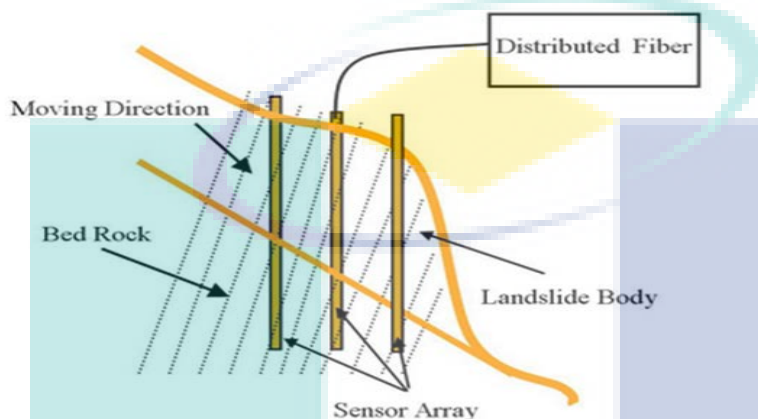


Figure 2.6 Landslide monitoring configuration based on distributed-fiber sensors

Several sensors are installed along the optical fiber measurement line, and OTDR detector detects the transmission loss of the light caused by bending of the optical fiber. Another monitoring system of fibre optic system is investigated by (Arslan, Kelam, Eker, Akgün & Koçkar, 2015). The system is composed of optical fiber cables with sensor and OTDR. OTDR is the device sending light into fiber and collecting the back-scattered light. They used JDSU MTS 6000 model OTDR. OTDR gave the exact location of reflection in the optical fiber system. The investigation shows that fiber optical technology can be utilized as a landslide monitoring tool.

However, Optical fiber sensing system has limitations. The limitation for this technique is complicated task. It needs installation for the system. The other problem is with the sensor. It is highly fragile nature in order to combine the different cables having different diameters. The sensors also leads to an amount of power loss and this causes the system detect that specific location only.

2.3.6 Wireless Sensor Network

A number of wireless sensor network researches have been reported recently (Mehta et al., 2007; M. V. Ramesh, 2009; Sheth et al., 2005; Terzis, Anandarajah,

Moore & Wang, 2006). Real time monitoring is an obligation for environment disasters. Wireless sensor network (WSN) is a technology that used real-time monitoring. The architecture of wireless sensor network has two-layer hierarchies which are the lower layer and upper layer of wireless sensor nodes. The function of lower layer wireless sensor nodes is to collect the heterogeneous data from sensor column and the data packets are transmitter to the upper layer (Maneesha Vinodini Ramesh, 2014).

The sensors that needed for monitoring rainfall induced landslides for this technique are pore pressure transducer and dielectric sensor. Those sensors also called as geophysical sensors. It is for detecting the change in pore pressure and moisture content. Besides, strain gauge and tiltmeter are used to measuring in-situ slope gradient changes. Other than that, geophone is used for analyzing the vibration. Figure 2.7 below shows the geophysical sensors were placed inside a sensor column and they were connected to the wireless sensor node via a data acquisition board.

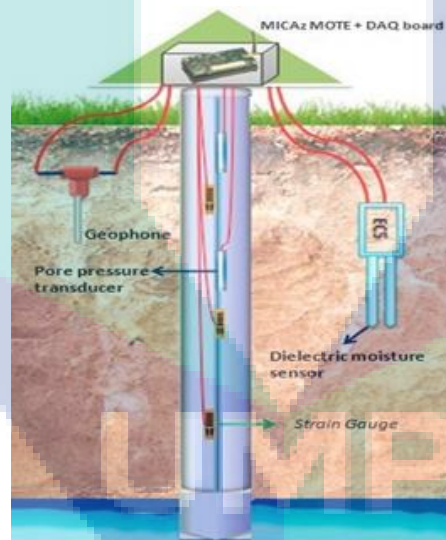


Figure 2.7 Sensor Column

In WSN, there are some challenges that summarized by (Giorgetti et al., 2016). First is long network lifetime is required such as battery replacement in hostile environment. Secondly, landslide detection is a rare event that needs continuous monitoring for long period. This makes energy consumption lower. Lastly, to manage

network lifetime and support event-driven mechanisms, network parameters need to be controlled and set up remotely and autonomously.

Furthermore, WSN has another limitation such as low memory, power and bandwidth. The other challenge is the environmental factors (Akyildiz & Stuntebeck, 2006). Water, temperature, animals, insects are risky to WSN device. It must be provided with proper protection. Processor, radio, power supply must be resilient to these factors.

comment

Comment [k6]: make a summarized, critics, find disadvantages etc

2.4 Thermal Camera Application

Based on the other application of landslide detection reviewed in subsection 2.4, it has been observed that the conventional tools that used to monitor or predict the landslide has their own limitations. The example of the limitations are some of the current tools need to be installed and take longer time, while thermal imaging camera is a handy camera and can bring to anywhere. Furthermore, some of the tools such as remote sensing and wireless sensor network need expertise to use the tools but for thermal imaging camera, it can be used by any person from any level of expertise. Hence, thermal imaging camera has a potential to become a complimentary method to perform an early detection of landslide. Thermal imaging cameras becoming a current tool in industry where they are being used to authenticate building performance to specifications, to fix upon insulation condition, detect leaks and discover moisture intrusion.

Comment [k7]: ???

Comment [k8]: summarized and discuss the limitation in 2.3

Comment [k9]: then, why you need this study?

(Liu, Xu, Wu, Ma & Liu, 2011) investigated an infrared imaging detection of landslide in Opencast Mine at China. They stated that rock or the soil in landslide area is looser and more fractured than the normal rock or soil, especially some faults are distributed at the edge of the landslide, and some water contained in the faults. Hence, the temperature in the landslide is different from the surrounding rock. Figure 2.8 below shows the result of infrared imaging detection of slope. It can be seen that temperature along the broken line is lower than other area. They analyzed the causes of the

temperature is lower. The reason is that loosening and fracturing soil contained more water in the area.

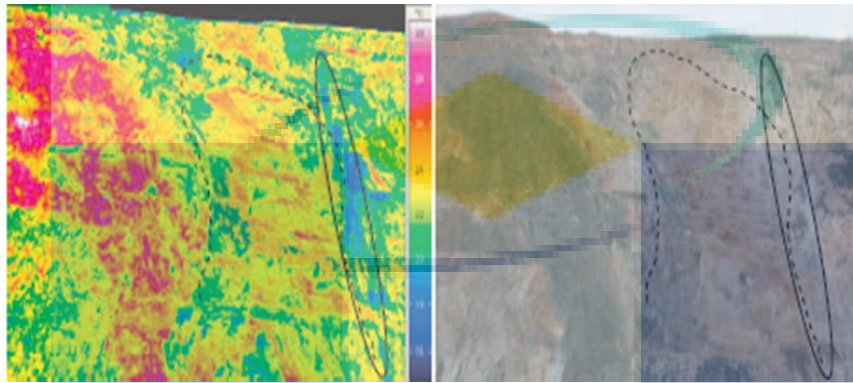


Figure 2.8 (a) Thermal image of the slope (b) Original photo of the slope

Comment [k10]: cite this image

Another example of using thermal camera for investigate instability of rock slope is by (Mineo, Pappalardo, Rapisarda, Cubito & Di Maria, 2015). Based on the Figure 2.9 below, the lowest value is detected at the top of the slope while maximum values at the area of past rockfalls. According to them, the lowest value is due to the water content in the soil.

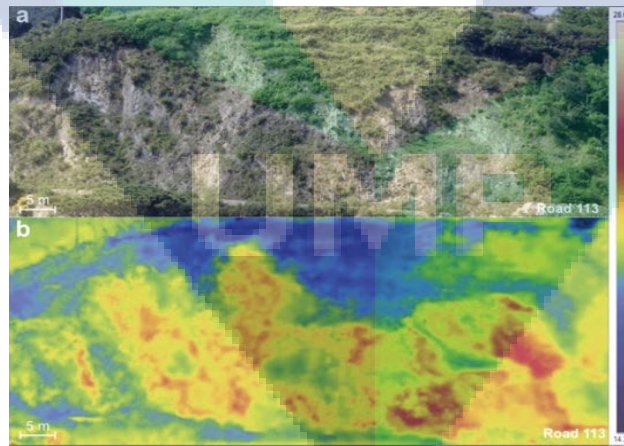


Figure 2.9 (a) Photo taken at the daylight (b) Thermal image

Another application using thermal cameras is to detect buried circular objects with a Rule-Based Fast Shape Detection Algorithm (Azak, Akgun, Azak & Torun, 2003). Abandoned buried objects are major problems for humanitarian and military purposes. A thermal camera has been used to receive thermal images from the soil surface where objects are buried in different depths and received thermal images were processed by a simple rule-based 'Fast Circular Shape Detection' algorithm that we have introduced.

Besides that, the application that uses infrared imaging is detection of diabetic foot hyperthermia (Vilcahuaman et al., 2014). It is easier to detect a possible hyperthermia by using thermal images. Hyperthermia is defined as temperature greater than 2.2°C in a given region of one of the foot compared to the temperature of the same region of contralateral foot.

Thermal camera also can detect roof leakage (Angaitkar, Saxena, Gupta & Sinhal, 2013). Roof leakage is main problem faced of the age of the building. The reason that caused roof leakage is the different conditions and material used in construction. The problem that occurs when there is a roof leakage is these leakages are so small and cannot be seen with naked eyes. So, the thermal cameras are used for detecting the leaks. The technique that use is the combination of the benefits of homomorphic image processing and the additive wavelet transform. The homomorphic processing transforms the image into illumination and reflectance components while butterworth filter is to enhance separately the reflection and illumination components in the image.

Besides military applications and monitoring in medical (Azak et al., 2003; Ring & Ammer, 2012; Vilcahuaman et al., 2014), thermal camera is use for the application in food industry (Bulanon, Burks & Alchanatis, 2008; Gowen et al., 2010; Nakayama et al., 2008; Varith, Hyde, Baritelle, Fellman & Sattabongkot, 2003). One of the example is thermal imaging is used in heating process and cooking. It used pancake as an object to analyses spatial distribution and temporal variation of temperature. Two factors that control the product quality during processes are temperature and monitoring in food manufacturing process. Temperature mapping where both spatial and temporal

Comment [k11]: thermal camera in diabetics. previous thermal camera in landslide

make it sub chapter, discuss it properly and give your own opinion towards problem statement, objective etc.

temperature distribution patterns are obtained from an object have potential application for food product quality assurance, safety profiling and authenticity compliance.

From the previous history of Infrared Detectors (Rogalski, 2012), the first thermal imaging camera is developed for military applications. The example of the application for military is sniper detection using infrared cameras (Kastek et al., 2010). Sniper activities were taken in three phases which are before, during, after the shot. The targets were sniper body and muzzle flash. IR sensors can detect muzzle flash out to several kilometre or more. The infrared sensor also can detect the bullet out to several kilometres in range. The bullet is hotter than room temperature. So, it is detected effectively in the medium-wave infrared band.

After military purpose was established as first development in infrared thermal imaging technology, then wide applications in various fields such as agriculture, civil engineering and veterinary were developed (Vadivambal & Jayas, 2011). In agriculture, thermal imaging can do many operations such as estimating soil water status, estimating crop water stress and evaluating maturity of fruits and vegetables.

2.5 Thermal Image Analysis

Since 1999, the first edition of Image Processing and Fundamental book proved that Image Processing have developed rapidly in previous years (Petrou & Petrou, 2010). Image processing is developed to overcome the problems which are related with pictures. For example, image processing is used for image enhancement and restoration. The pictures can interpret more easily using image processing. Other example is image segmentation and image digitization. Image processing and computer vision are widely used in some important areas such as telecommunication, medical imaging and remote sensing (Pitas, 2000).

Image processing involves a series of steps. First step is image acquisition and pre-processing. Image acquisition is the process of data collection in a form of image while pre-processing is the process of raw images to improve the quality of the image. The technology today already has function for pre-processing in the camera such as filtering and smoothing the image.

Second step is image segmentation and feature extraction. Image segmentation is the most crucial step because the accuracy of the image is based on this step.

Furthermore, feature extraction is the process to extract the features of the image from the segmented image regions earlier. Feature extraction represents interesting parts in the image. It is usually used to solve problem in computer vision problems such as object detection and face detection.

Comment [k12]: not appropriate LR. this is basic image processing. not relevant. discuss thermal imaging by other researcher.

Next is the process which is involved interpretation process such as statistical and neural network classifiers. This process is to get the information needed to classify the image into groups.

2.6 Image Segmentation

The process of partitioning the image into some non-intersecting regions called segmentation (Pal & Pal, 1993). Segmentation is very useful in many applications. The purpose of segmentation is to make the image become more meaningful and easier to analyse. Besides, image segmentation is used to detect boundaries and objects in images.

Comment [k13]: merge with 2.5
review the image segmentation for thermal imaging.
some of the cited sentence may come from more than 1 paper. because it is common

The importance of image processing cannot be slighted because it is used in every field such as removing noise from an image, medical images like locate tumors and other pathologies, locate objects in satellite image such as landslides and forests, extracting features and recognizing object from the given image. Image segmentation can be categorized into the following categories namely statistical approaches, edge-detection approaches and region-based approaches (Heng-Da & Ying, 2000).

Region based segmentation is simple than other method. It also noise resilient. It is divided the image into different regions based on certain criteria, for example, color, intensity and object (Khan, 2013). Besides, edge detection is basic step for image segmentation process. It divides an image into object and its background. Gray histogram and gradient are two example of edge detection for image segmentation (Dass & Devi, 2012). Lastly is statistical approach. It is used in order to analyses image and provide accurate information from any image.

Comment [k14]: this is not the way you do LR. this is to explain the theory. Review the region based segementation by other researcher and relate it with thermal imaging and also with your problem

Segmentation in this study fundamentally aims at the water spots regions that saturates in the soil which is lead to landslide, using techniques as Color- Based Segmentation using K-means Clustering, Feature Matching and HSV color space. The purpose of segment the image of water spots regions is to make the image easy to

analyze. It is important to make sure there is no unwanted pixel or color inside the regions detected.

The segmentation is defined as follows (Pal & Pal, 1993) in Equation 2.1, if F is the set of all pixels and $P(\cdot)$ is a uniformity predicate defined on groups of connected pixels, the segmentation is a partitioning of the set F into a set of connected subsets or regions (S_1, S_2, \dots, S_n)

$$\bigcup_{i=1}^n S_i = F \quad \text{With} \quad S_i \cap S_j = \phi \quad i \neq j \quad 2.1$$

Furthermore, in the applications of computer visions, color can provide more additional information which can get better results of image analysis process. (Cheng, Jiang, Sun & Wang, 2001) stated that there is more information in colour of an image compared to gray level. The example application that use color segmentation such as the application for detecting the cancerous cells (Madhloom et al., 2010) and also can be used in agriculture industry such as classification of N36 pineapple (Mohammad et al., 2011). This application also can be used to find the region in the infrared camera of electrical installation (Jadin, Taib & Ghazali, 2015).

Comment [k15]: Rewrite the way you discuss LR.

UMP

2.6.1 Color-Based Segmentation using K-means Clustering

2.6.1.1 Clustering

Clustering and data grouping is a main procedure in image processing. The term of clustering means an unsupervised learning technique where the number of cluster is need to know in advance to classify the pixels (Hartigan, 1975; Jumb, Sohani & Shrivas, 2014). Figure 2.10 below shows the clustering procedure. Clustering techniques categorize the pixels with same characteristics into one cluster. A variety of applications are already applied clustering (Xu & Wunsch, 2005). The example of clustering are the applications in engineering (machine learning, electrical engineering, pattern recognition), computer science (web mining, textual document collection, image segmentation), and life and medical sciences.

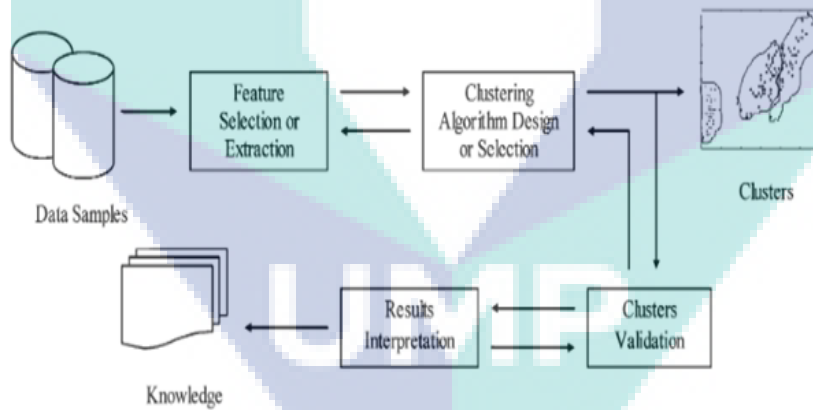


Figure 2.10 Clustering Procedure

2.6.2 K- Means Clustering

The most popular technique for image segmentation is K-means because it is fast and simple algorithm (Luo, Yu-Fei & Hong-Jiang, 2003). Research finding by

Suman Tatiraju and Avi Mehta (Tatiraju & Mehta) described that K-means is an unsupervised clustering algorithm that categorize the input set of data into various clusters based on their distance from each other. The input data is grouping into multiple clusters based on the distance metric. The points are clustered around centroids $\mu_i, \forall i = 1 \dots k$ which are obtained by minimizing the objective as shown in the Equation 2.2 below.

$$V = \sum_{i=1}^k \sum_{x_j \in S_i} (x_j - \mu_i)^2 \quad 2.2$$

Where there are k clusters S_i , $i = 1, 2, \dots, k$ and μ_i is the centroid or mean point of all the points $x_j \in S_i$.

K-Means is widely used in many applications such as medical and agriculture applications. The example of medical application is been conducted by (Juang & Wu, 2010). They used K-means clustering segmentation for tumor objects tracking method for magnetic resonance imaging (MRI) brain images. They stated that K-means can solve the MRI image by converting the input-gray level image into a color space image and labelled by cluster index. (H. P. Ng, Ong, Foong, Goh & Nowinski, 2006) was developed medical image segmentation using K-means with the improved watershed segmentation algorithm. It is used to segment magnetic resonance (MR) images.

On top of that, nowadays agriculture science and technology is already advanced. The conventional approach of fruit quality is very time consuming and expensive. Using segmentation by K- Means, defect segmentation of fruits and leaf can be seen as instance. It has been proved by (Al Bashish, Braik & Bani-Ahmad, 2011; Dubey, Dixit, Singh & Gupta, 2013; Yongsheng, Gang & Rui, 2009). They are used K-Means for defect segmentation of fruits and leaf.

2.6.3 Feature Matching

Fast and robust feature extraction is important for computer vision applications such as image matching. The examples of image features are Speeded Up Robust Features (SURF), Scale Invariant Feature Transform (SIFT) and Affine SIFT (ASIFT). SURF is a robust local feature detector which is first presented by (Bay, Tuytelaars & Van Gool, 2006). It is inspired by the SIFT descriptor. This version of SURF is several times faster than SIFT.

The SURF approach is divided into three steps (Hamid, Yahya, Ahmad & Al-Qershi, 2012). First, in the image, the keypoints are selected at distinctive locations. The examples of the locations are corners, blobs and T-junctions. Next, the feature vector is representing the neighborhood of every keypoint. Lastly, the descriptors are matched among the different images. Hessian Detector is used to find the keypoints.

(Ren, Huang, Jiang & Klette, 2009) developed a traffic sign recognition using feature matching methods (SIFT or SURF features) for Driver Assistance Systems (DAS). Traffic sign recognition is a challenging task for roads in these kinds of scenarios such as bad weather and traffic condition. This method involves a few steps. First, the RGB color input images are converted into HSV color space. Second, Hough transform is used to detect shapes (circles, triangles, squares). Third, the feature matching is used to compare potential signs and template signs in database. At the end, the traffic sign is recognized in image at real time DAS.

Besides, forensic dentistry also used feature matching in their research (Jain & Chen, 2004). Their goal is to automate the process of forensic dentistry using image processing. It involves the identification of people based on their dental record. The contour of teeth is used as feature for matching. The main steps for automated dental identification are feature extraction and feature matching.

However, there are no studies found using Feature matching in landslide prediction.

2.6.4 HSV Color Space

Color image segmentation is rapidly growing in recent years because color image bring more information than gray-level image. It is more meaningful and robust segmentation (Cheng et al., 2001). The usually color segmentation technique RGB (Red, Green, Blue) allows straight-forward representation of colors but HSV color space represents colors in term of Hue, Saturation and Intensity of the value. Other than HSV, there are also HSB (Hue, Saturation, and Brightness) and HIS (Hue, Intensity, Saturation). Hue is describes as color type such as red, blue and yellow. Saturation is a purity of the color. Value components describe the brightness of the color.

HSV color has advantages over RGB (Ikeda, 2003) such as Hue is homogenous to certain types of highlights, shading and shadows. Segmentation in HSV also performed on only one dimension (H) and it is resulted the segmentation have fewer segment than using RGB (H. Wang & Suter, 2003). According to (Bora, Gupta & Khan, 2015), HSV color space also performing better than L*A*B.

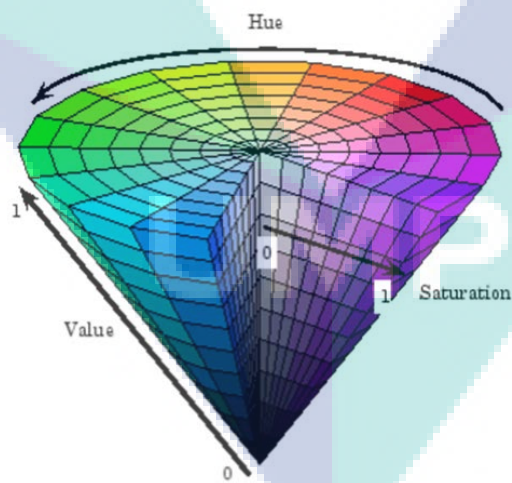


Figure 2.11 HSV Color Space

Hue is defined as an angle in the range $[0, 2\pi]$ respective to the Red axis with red at angle 0, green is located at $2\pi/3$, blue at $4\pi/3$ and red again at 2π (Sural et al., 2002). Saturation is a radial distance from the central axis. It has values between 0 at the center to 1 at the outer surface. For $S = 0$, the color goes from black to white through various shades of gray when it moves higher along the intensity axis. The HSV color space is shown in Figure 2.11 above. The pure form of the color represent by its hue if the saturation is changed from 0 to 1 (Bora et al., 2015).

HSV color space technique is a popular technique and it is often used until now (Gong, Zhang, Zhang & Li, 2016; Kawa, Khartade, Sonawane & Madole, 2016; Tigadi & Sharma, 2016; Q. Wang, Si, Xi & Zheng, 2016). A few studies using HSV for segmentation of region of interest have found in their research. (P. Ganesan et al., 2014) developed a method for extraction region from the satellite image. It used HSV to extract the reddish color from the satellite. RGB color analysis is not suitable and efficient for image analysis due to its device dependent and not uniform (P Ganesan, Rajini & Rajkumar, 2010) Device dependent means it is affected by the signal of the device while device independent not affected and it will be resulted the same color from the set of parameters (Ford & Roberts, 1998).

On top of that, there are also research finding that proposed by (Fauzi et al., 2015) that used HSV color space for detection landslide regions from satellite and also aerial image. It is to detect the greenish color of forest terrain or orange color of landslide in satellite image. Besides that, (Azman, Ghazali, Hamid, Mohamed & Nawi) have proposed a system to detect overlapping cells by nucleus detection in the sputum slide images. The system used HSV techniques to do the segmentation process of the sputum images.

As a conclusion, HSV color space is an image segmentation technique that robust and faster.

2.7 Feature Extraction

In image processing, feature extraction is an essential pre-processing step. It starts from the primary set of measured data and builds features to be informative and non-redundant. Feature extraction implemented to improve the efficiency of data storage and processing. The complexity and achievement of the analysis depends on the chosen factor as a key factor (Umbaugh, 2005).

The types of features are relying on the kind of applications which need to be actualized. The frequently used features extraction techniques in image processing are texture, color, histogram and shape (Snyder & Qi, 2010). In this study, the shape features is used which are area and perimeter. Shape is important feature and it is used to describe image content. The purpose of the shape measures is to measure geometric feature of that object and can be used for quantifying shapes (Gonzalez, 1987). Figure 2.12 below shows the classification of shape implementation and description techniques.

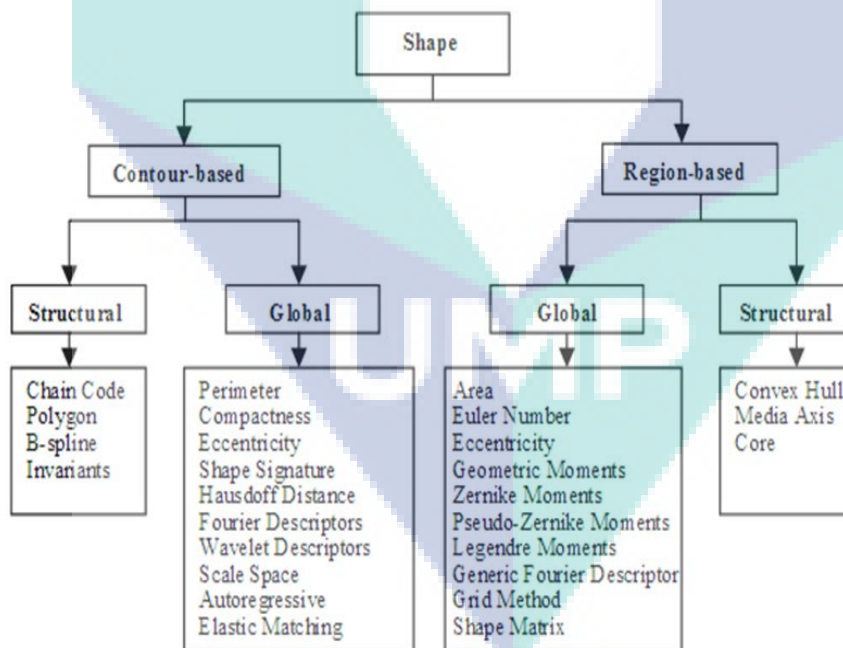


Figure 2.12 Classification of shape representation and description techniques

Source : (Zhang & Lu, 2004)

(Mehetre, Kankanhalli & Lee, 1997; Zhang & Lu, 2004) described that shape representation and description techniques are classified into two groups namely contour-based methods and region-based methods. For contour shape feature such as perimeter only pick shape boundary information while for region based techniques such as area is use all the pixels within the shape region to obtain shape representation.

Besides area and perimeter, texture features such as intensity is used in this study. Texture is a description of the spatial arrangement of intensities in an image or selected region in image. (Ojala & Pietikäinen) stated that texture features is important in applications of image analysis for segmentation of images based on local spatial variations of intensity or color.

Shape features and texture features are widely used in various applications. There is an application that used area features to examine watersheds in order to clarify characteristic properties where landslide may occur (Kusaka, Shikada & Kawata, 1992). The largest area of watershed is considered as dangerous watershed. The data is based on satellite images and map-based data. Besides, (Rosin, Hervás & Barredo, 2000) have proposed a technique using area and perimeter for performing change detection for digital aerial photographs of Tessina landslide in Italy.

Color texture feature which is intensity is used to identify of citrus disease. The disease can be seen based on darker pigmentation of the leaf (Bulanon et al., 2008). Furthermore, there is also a detection system of cervical cancer cells using color intensity. Cancerous cells have a larger distribution of darker cell compared to normal cells.

comments

Comment [k16]: revise back your LR especially 2.5 and 2.6. Rewrite the way you writing. make it like you review a paper not you tell what other people has done.

2.8 Summary

A literature review on landslides and image processing technique has been presented in this chapter. The previous works which focused on the image segmentation technique, feature extraction and classification stages have been discussed. Specifically in landslide monitoring, satellite image or aerial image is widely used by the expertise. There is no previous research reported about image processing for thermal image. One of the example, there is a research done by (Fauzi et al., 2015) which is using image processing to process image for landslide. However, they used post-event satellite image or aerial image. They propose a method to detect potential landslide region based on color and texture analysis.

Besides, previous research done by (Liu et al., 2011) and (Mineo et al., 2015) is using thermal imaging camera to detect landslide but they are not using image processing to process the result of thermal image. There are still various techniques are available for image segmentation, feature extraction and classification other than the techniques that have discussed in this chapter. However, this study is used the popular, robust and accurate techniques to process the images.

Comment [k17]: this is very important. make summary and focus on problem statement as well as methodology.

The logo for UIMP (Universitas Islam Malang) is a large, stylized letter 'U' composed of several overlapping triangles in shades of teal and light blue. The letters 'UIMP' are written in a bold, white, sans-serif font across the center of the 'U' shape.

UIMP

CHAPTER 3

METHODOLOGY

3.1 Introduction

As stated in Chapter 2, computer vision system involves image acquisition, image segmentation, feature extraction and classification. This chapter briefly discusses development of each technique. It begins with an overview of a methodology in Figure 3.2.

Comment [k18]: ??

rewrite. intro about your method. highlight again the problem statement and objective where you are going to solve the problem and achieve the objective by proposing methodology

After that, image segmentation techniques were discussed in subsection 3.4. A proposed feature extraction described in subsection 3.5. The last stage of the system is classification presented in subsection 3.6. Lastly, subsection 3.7 contains the summary of the chapter.

3.2 Research Methodology

There are two major application scopes from the significance of digital image processing method which are enhancement of graphic information for human understanding and processing of image data for storage, transmission and representing for independent machine perception (Rafael Gonzalez & Richard Woods, 2002). Computer vision system involves image acquisition, image segmentation, feature extraction and decision making. This chapter describes each technique developed and used at each stage. Figure below shows general methodology for this research.

Comment [k19]: not appropriate title

Comment [k20]: rewrite. not sound good.

The research started with collecting data of landslide image. More than 300 images of landslides with different location are taken. All samples of images will be process under several stages of the image analysis process such as image segmentation. In order to get region of interest of the images, several techniques such as HSV, K-Means and Feature Matching are used and been compared to get best result. Furthermore, as a result of image segmentation, further action is taken to the next stage

Comment [k21]: why this technique.

should explain somewhere why these techniques

which is features extraction using statistical analysis. Final stage is classification using linear thresholding for classified the landslide whether it is normal or abnormal.

There are two (2) works have been done during this research namely field work and lab work. Field work involves the collection of landslide videos in a few places at Pahang, Malaysia. The videos are extract become images to make the image processing technique easier. The study area is explained in subsection 3.3. Laboratory work involves various processes of computer vision system. The details of each step are described in the following subsection. Figure 3.1 below shows general proposed methodology of this study.

Comment [k22]: why ?

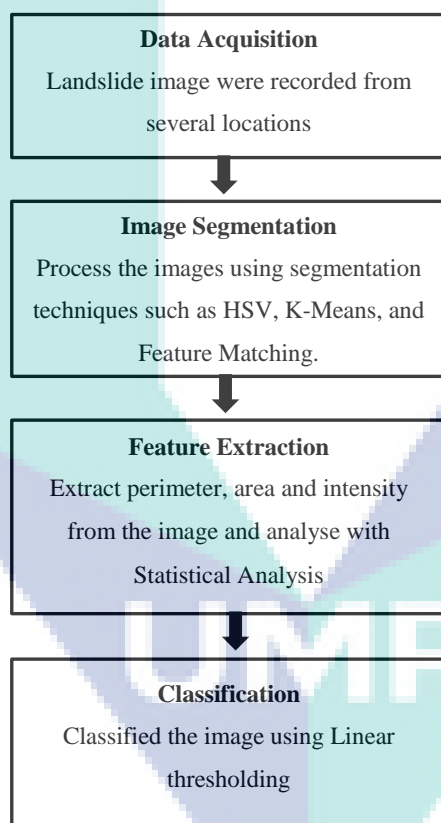


Figure 3.1 General proposed methodology of early detection of high water saturation spots for landslide prediction using thermal imaging analysis

...

Comment [k23]: explain more details each step here. explain why and how.

3.3 Study area

Field work involves the collection of data at a few places in Pahang. First data is collected at University Malaysia Pahang, Pekan, Pahang, Malaysia (UMP). It is shown in Figure 3.2 below. The data was collected around December 2014 for preliminary study. The area that investigated is inside the UMP area. There is a small slope which is located opposite of Electrical and Electronic Faculty. The data is taken after the heavy rainfall. The aim of this preliminary study is to prove that thermal camera can detect the water that saturates inside the soil.

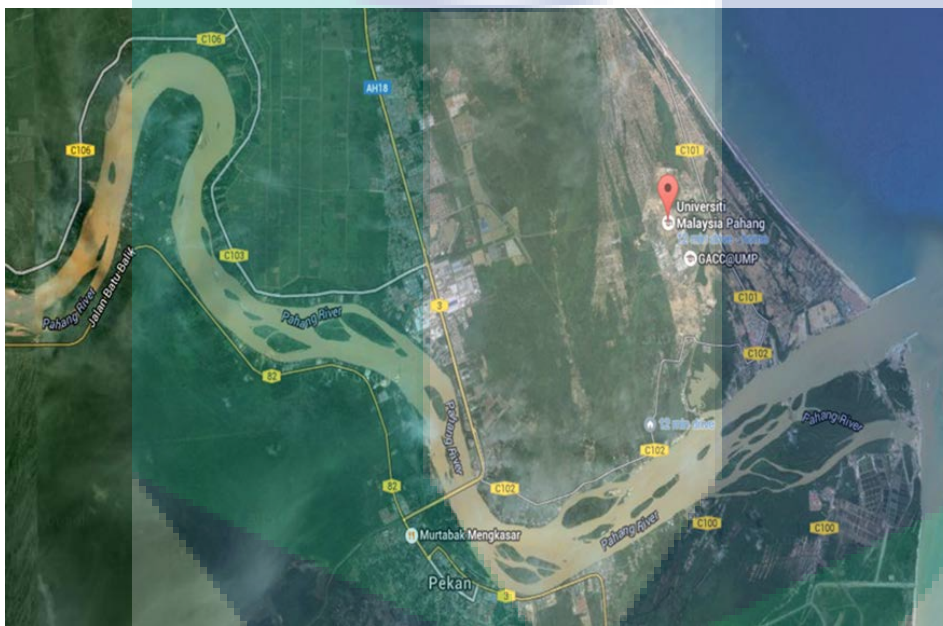


Figure 3.2 Location of first study area

Second location is at Bandar Indera Mahkota, Kuantan, Pahang. The actual investigated area is at Lorong Indera Mahkota 8/25. The geographical location for this study area is situated at latitude of 3.828669 and longitude of 103.309435. There is a landslide occur at the residential area on August, 2015. The factor of the landslide is heavy rainfall. Figure 3.3 below shows the investigated area.



Figure 3.3 The location of second study area

Third location is at Jalan Gambang, Gambang, Pahang. The sample of soil was taken from the slope here. Jalan Gambang is only 4.5 Kilometre from Universiti Malaysia Pahang. The geographical location of the study area is situated approximately latitude of 3.719728 and longitude of 103.139107. The Figure 3.4 below shows the area of the sample of soil taken.



Figure 3.4 The location of third study area

3.4 Image acquisition

The data is collected at a few places. First is preliminary study. The data for preliminary study is collected at Universiti Malaysia Pahang. The other data is at Indera Mahkota 8, Kuantan, Pahang. Lastly, the data is taken at Gambang, Pahang. The image acquired using thermal camera FLIR A615 as shown in Figure 3.6 below. The camera is placed nearest to the slope of the soil. The position of thermal camera is not static. It is for searching the high risk spots in that area. The parameters use is focus lens, camera positioning and distances. The camera resolution is 640 x 480. After recording the video of slope, that video was converted into image in JPEG (Joint Photographic Experts Group) image format by using Matlab coding. This process is shown in Figure 3.5 below.

Comment [k24]: ??? need to send it to proof reader

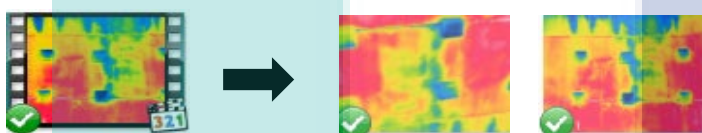


Figure 3.5 The process converts the video into image

Comment [k25]: doesn't mean any thing ... remove

For preliminary study, the video is taken about 14 seconds and after converted with one frame per second, the images become 93 images. While for second data collection at Indera Mahkota 8, there are 3 video were taken which are abnormal condition video, normal condition video and the video that combine between normal and abnormal video. Hence, three data are used in this study. First data is abnormal video which is taken about 28 seconds and after convert, the images become 181 images. Second data is normal video. It is taken about 18 seconds and the output images are 114. Lastly, third data is the video of combination of normal and abnormal condition which is 16 seconds and the output images are 71. Table 3.1 below shows the technical specification for Thermal imaging camera FLIR A615.



Figure 3.6 Thermal Imaging Camera FLIR A615

Comment [k26]: remove

Table 3.1 Technical specification of FLIR A615

Imaging & Optical Data	FLIR A615
Field of view (FOV) / Minimum focus distance	15°: 15° × 11° (19° diagonal) / 0.50 m (1.64 ft.) 25°: 25° × 19° (31° diagonal) / 0.25 m (0.82 ft.) 45°: 45° × 34° (55° diagonal) / 0.15 m (0.49 ft.) 7°: 7° × 5.3° (8.7° diagonally) / 2.0 m (6.6 ft.) 80°: 80° × 64.4° (92.8° diagonal) / 65 mm (2.6 in.)
Focal length	15°: 41.3 mm (1.63 in.) 25°: 24.6 mm (0.97 in.) 45°: 13.1 mm (0.52 in.) 7°: 88.9 mm (3.5 in.) 80°: 6.5 mm (0.26 in.)
Image frequency	50 Hz (100/200 Hz with windowing)
IR resolution	640 x 480 pixels
Object temperature range	-20 to +150°C +100 to +650°C +300 to +2000°C
Focal Plane Array (FPA) / Spectral range	Uncooled microbolometer / 7.5–14 μm
Detector pitch	17 μm
Lens identification	Automatic
Thermal sensitivity	< 0.05°C @ +30°C (86°F) / 50 mK
Focus	Automatic or manual (built in motor)
Accuracy	±2°C or ±2% of reading
Emissivity correction	Variable from 0.01 to 1.0
Ethernet	Control and image
Digital input	2 opto-isolated, 10–30 VDC
Digital output	2 opto-isolated, 10–30 VDC, max 100 mA
Digital I/O, supply voltage	12/24 VDC, max 200 mA
External power operation	12/24 VDC, 24 W absolute max
Voltage	Allowed range 10 – 30 VDC

Comment [k27]: show the sample of images

describe and explain the data/image

explain the requirement of the data
discuss type of data etc.

not enough information about the image

3.4.1 Water Content in Soil

This method is used to determine the water content in soil. The sample of soil is taken at Jalan Gambang, Kuantan, Pahang which is show in Figure 3.7. There is a slope along the road.



Figure 3.7 The location at Jalan Gambang, Pahang

The sample of soil was tested at Soil Mechanics & Geotechnical Laboratory at Universiti Malaysia Pahang. First step before drying, plant and root materials, rocks are advisable to remove it from the samples. The technique of crushing is shown as figure below. Crushing is accomplished manually using a stone rolling pin. Figure 3.8 shows crushing are done to remove aggregated soils.

Comment [k28]: method ?

why this experiment.

explain it in proper order. do not jump in without proper explanation. reader will lost.

please find a correct subchapter to explain this. and explain it properly and connect it with the methodology and with the previous chapter

what are you trying to get from this experiment and method?

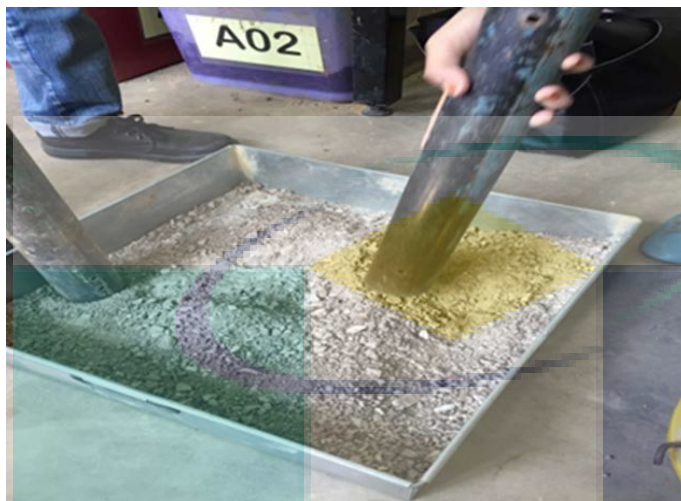


Figure 3.8 Crushing the aggregated soils

Figure 3.9 shows the soil sample is placed in a drying oven. The drying ovens are equipped with exhaust fan to speed up air moisture removal. The rate of soil drying can be control with three factors. First is the surface area of the sample is expose to the surrounding. Second is humidity of the air passing over the sample and lastly is air flow rate over the sample.



Figure 3.9 The drying oven

For soil analysis, samples are ground to pass a U.S No. 10 (2.00mm opening) sieve. The crushed aggregate was sieved into 7 size divisions which are 5mm, 3.35mm, 1.18mm, 0.6mm, 0.3mm, 0.15mm and 0.063mm. The crushed sample was placed on the top of the largest sieve ranging in size from 0.3 to 0.063mm and shaken 15 minutes with a Portable Sieve Shaker as shown in Figure 3.10 and Figure 3.11 respectively below.



Figure 3.10 The crush sample

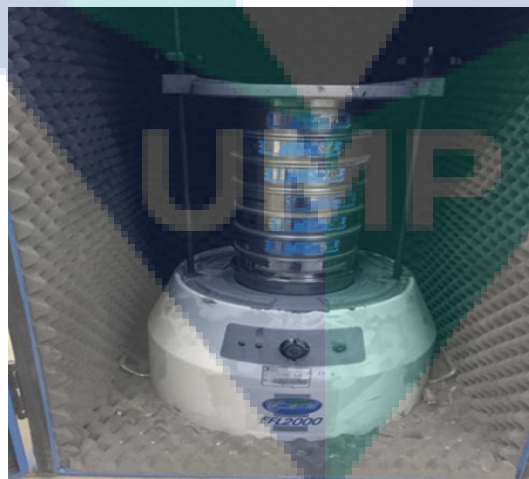


Figure 3.11 The Portable Sieve Shaker

3.5 Image Segmentation for Water Spot Detection

Image segmentation is a significant processing step in image analysis. Many segmentation techniques have been used for many applications. The image analysis procedure involves a few tasks in order to simplify and change the representation of an image into something that much easier to analyze. Image segmentation is applied to extract the target regions from its background. The target regions usually have higher intensity than its surrounding. In this study, three segmentation techniques are used for segmentation process. The techniques used are Feature Matching technique, Color-Based Segmentation using K-means Clustering and HSV technique. These three techniques used because they are accurate and robust.

Comment [k29]: explain somewhere ie in LR, intro etc about waterspot. this is your main problem statement. why, how, what.

Comment [k30]: do not need to explain the theory

Comment [k31]: why? need to have good justification why these techniques

The segmentation process is important to give effectiveness for the process afterwards such as color detection. It can be used for fine-grained recognition like classification that has very little difference between them. Furthermore, segmentation techniques also help to extract beneficial feature for recognition. The segmentation process is done to enhance the classification technique which leads to higher performance. The techniques are emphasis on getting region of interest of bluish color of water spots saturation. The purpose for image segmentation is to determine objects and boundaries such as line and curves. In this study, image segmentation is used to determine the regions of water saturations. It is to predict landslides.

Landslide prediction is very important in order to prevent the landslide from occur. Hence, segmentation for water saturation image is useful to detect the location of the high possibility of landslide. There is image segmentation used for landslide prediction previously such as thresholding but it is for aerial image for remote sensing (Rosin & Hervas, 2005). There is none of study that uses image segmentation for thermal image.

3.5.1 Feature Matching

Feature matching is a method that can be seen from two arbitrary viewpoints for matching features in images based on the similar physical point of an object (Baumberg, 2000). The kinds of feature that can be notice are specific locations in the images, for example mountain peaks or building corners. These kinds of features are called keypoint features. Another types of image features are edge, corners and ridges (Wu & Yu, 2004).

The similarity between two feature vectors is given by the Euclidean distance between them. Matching between two images involves computing the distance between all possible pairs of detected features, and selecting as matching pairs those features whose nearest-neighbour is closer than some threshold. In this study, the SURF approach is used because it is speed up version of SIFT. (Durgam, Paul & Pati, 2016) reported that SURF is performed for better performance and accuracy. It is also faster and more robust than the SIFT (Y. L. S. Ma, 2014).

Therefore, based on the characteristics of SURF feature matching, there are some improvements such as improving the integral image. Second is region of interest extraction based on the template. The region of interest will attracts more users' attention and represents more content of the image information. With reference to the region of interest, this study is used template based on region of interest. The purpose is to extract the region of interest based on the template. According to the characteristics of the template image, it is easy to find out the region that is similar to the template image in the image of detection.

There are a few steps using this Feature Matching technique. Firstly, the reference image containing the object of interest is interpreted. Each point $X = (x, y)$ of an image I , is passed through Laplacian of Gaussian filter of various sizes with corresponding standard deviation σ in different directions. This process takes the advantage of integral images and the computational time is thus independent of the size of the filter. After it read the target image, feature points in both images is detected. For example, Figure 3.12 below shows 300 strongest feature points found in the target image.

Comment [k32]: explain the theoretical explain the step feature matching

how to relate with the water spot.

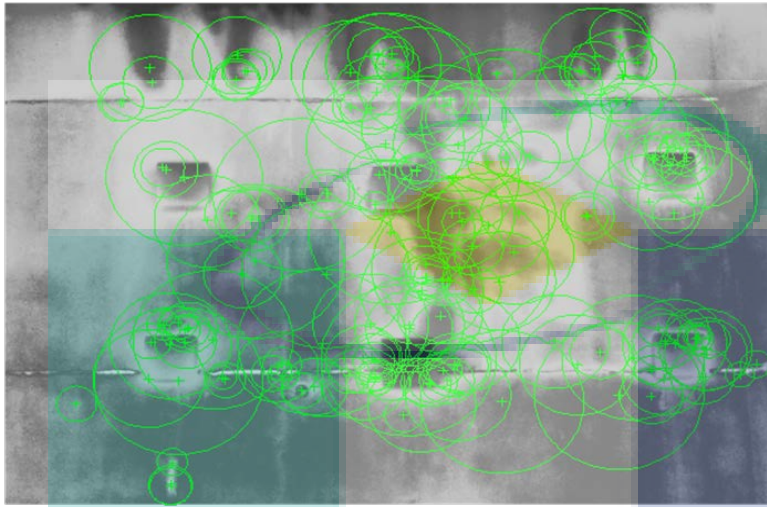


Figure 3.12 300 strongest feature points found in the target image

Interest points are detected by suppressing the non- maximal points. The next step is the feature descriptors at the interest points in both images are extracted and the features are matched using their descriptors. Figure 3.13 below displays the putatively matched features.

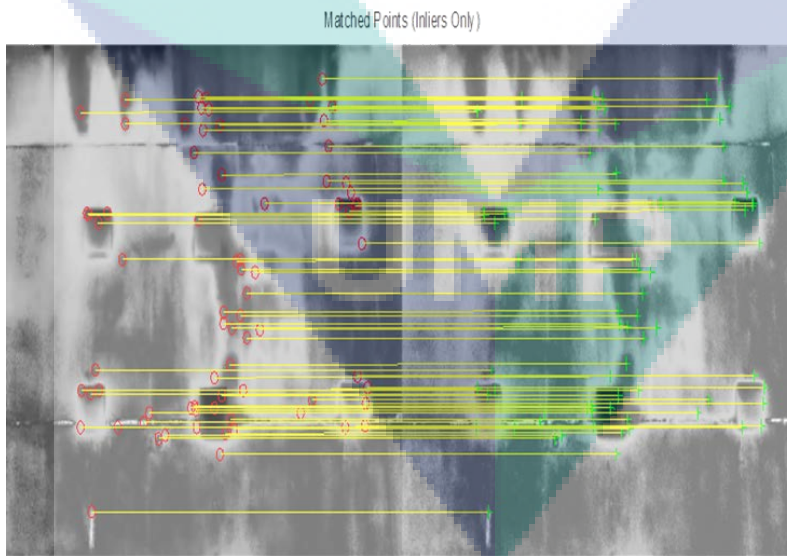


Figure 3.13 The putatively matched features image

The feature points detected on the reference image have to be matched with the feature points on the test image. The process of matching is made possible by the descriptor available for each feature point, the feature points with minimum descriptor distance are considered to be matched. Figure 3.14 below shows the detected object which is the image of water saturation spots.

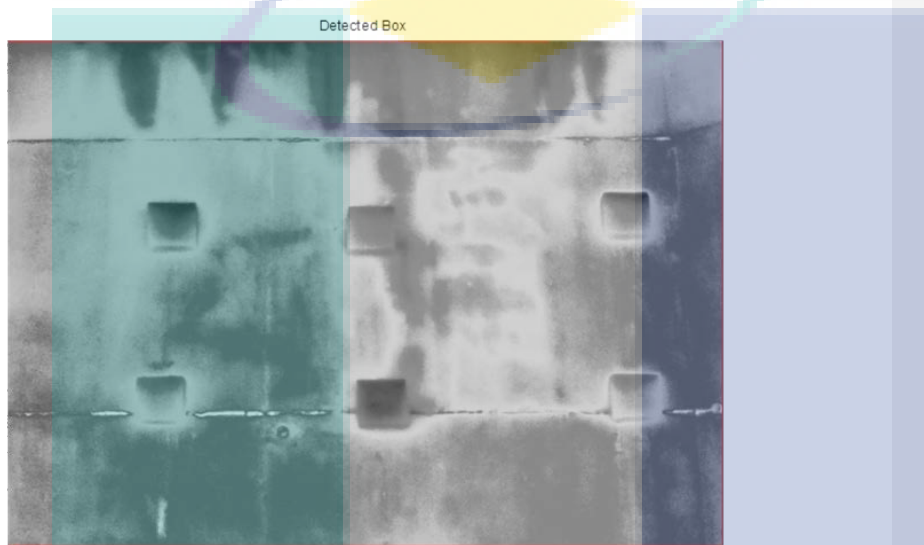


Figure 3.14 The detected box

The threshold value has been set based on the RGB value of the image. This threshold is to detect the coolest region on this image which indicates the bluish color.

3.5.2 Color-based segmentation using K-Means

Image segmentation using k-means algorithm is beneficial for the image analysis. The purpose of the proposed approach is to segment colors automatically based on the K-means clustering algorithm and L^*a^*b color space. The process of grouping data points with identical feature vectors together in a single cluster is called clustering. Hence the data points that are similar to each other in the feature space are clustered together (Juang & Wu, 2010).

In this study, K-means clustering is used to extract the meaningful part from the image. The advantages of this technique are it is computationally faster than hierarchical clustering, robust and easy to understand. K-Means is one of the simplest unsupervised learning algorithms that solve the well-known clustering problem (MacQueen, 1967). The procedure follows a simple and easy way to classify a given data set through a certain number of clusters.

The framework of segmentation operates in six steps. First step is the input image of detected regions of water spots is interpreted. The image is transform from RGB to L^*a^*b Color Space which is also known as CIELAB. L^*a^*b Space is expressed by luminosity layer ' L^* ', while color falls along the red-green axis is indicate as chromaticity layer ' a^* ' and the color falls along the blue-yellow axis is indicated as chromaticity layer ' b^* '. $L^* a^* b^*$ color space is used because it is efficient and all the color information is in the ' a^* ' and ' b^* ' layers only.

Clustering is a method of divided the groups of objects. The number of clusters to be partitioned is requires by K-means clustering. Euclidean distance metric is used to measure the difference between two colors. Every cluster is show by its mean (centroid) and variance (spread). Considering the color information exists in the ' $a^* b^*$ ' space, then the objects are pixels with ' a^* ' and ' b^* ' values. In this study, K-means is used to cluster the object into three clusters using Euclidean distance metric as shown in Figure 3.15 below.

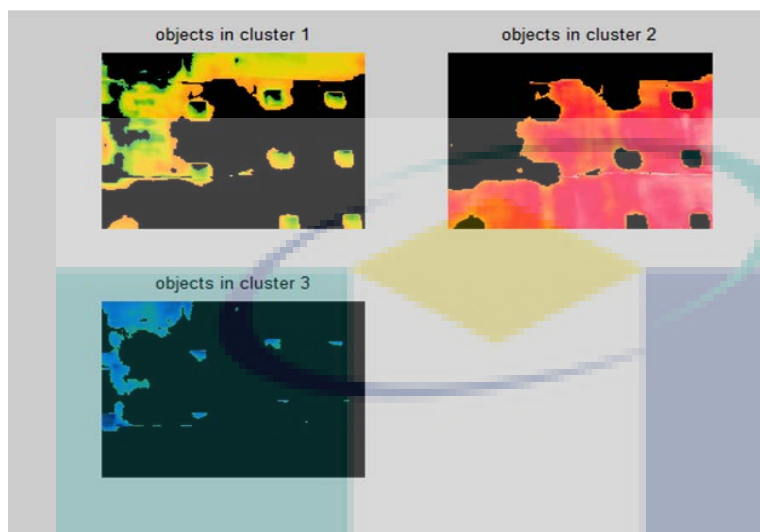


Figure 3.15 Cluster the image into three clusters using Euclidean distance metric

Each pixel in the image is labelled from the results of K-means. Every pixel of the image will be labelled with its cluster index. Lastly, the pixels in image are separated by color using pixel labels and it will result different images based on the number of clusters. In general, the propose segmentation method using K-Means summarized in Figure 3.16 below.

UMP

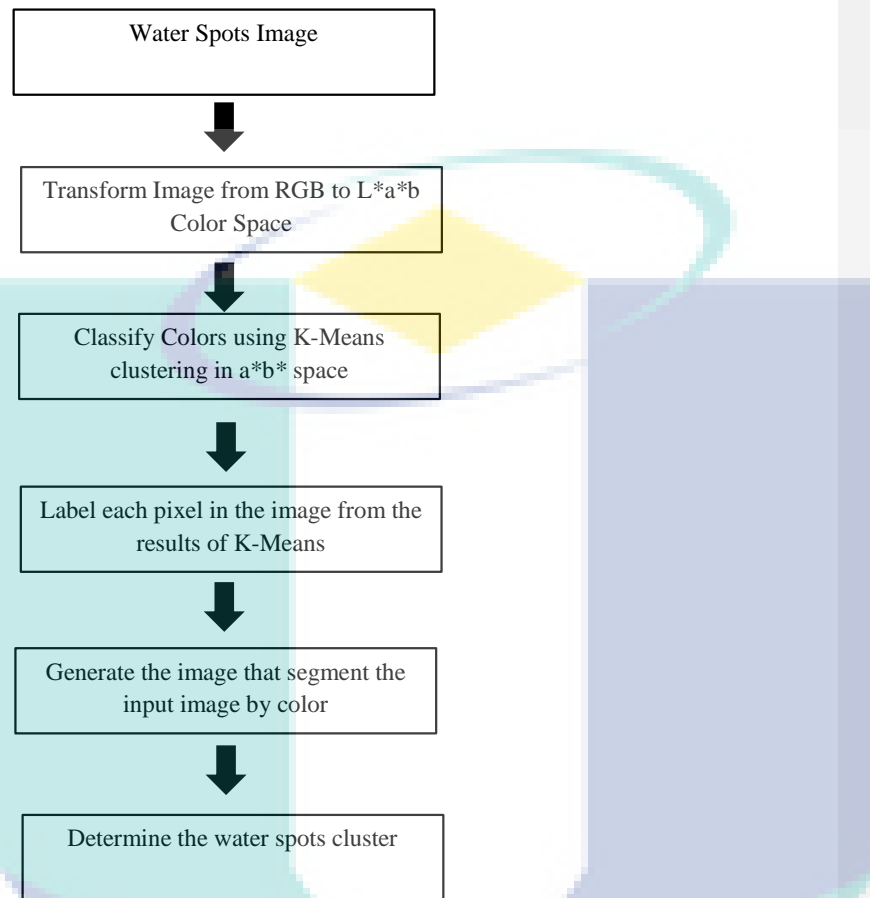


Figure 3.16 Water spots segmentation using K-means Clustering

3.5.3 HSV Color Space Technique

The image in RGB is converted to HSV color space. HSV color space is more related to human perception. The hue is angle of 360 degrees. Usually 0 or 360 degrees represents red color. 60 degree represents yellow color, 120 represents green color, 180 degree represent cyan color, 240 degree represents blue color and 300 degree represents magenta color. The transformation from RGB color space to HSV color space is given in the following Equation 3.1, Equation 3.2 and Equation 3.3:

$$H = \arccos \frac{\frac{1}{2}(2R - G - B)}{\sqrt{(R - G)^2 - (R - B)(G - B)}} \quad 3.1$$

$$S = \frac{\max(R, G, B) - \min(R, G, B)}{\max(R, G, B)} \quad 3.2$$

$$V = \max(R, G, B) \quad 3.3$$

Among three techniques which are used in this study, HSV technique is the most accurate to segment the water spots region. Details result will be discuss in chapter 4. HSV is often used in computer vision and image analysis for feature detection and image segmentation.

The flow diagram for the proposed approach is shown in Figure 3.17. There are several steps for the proposed segmentation of region of interest. Firstly, the image is in RGB color space. This color space is not suitable because it is not perceptually uniform and the disadvantage has discussed in Chapter 2. Hence, RGB is convert to HSV color space.

There are three different sub images in HSV image namely hue, saturation and value. The hue is the color type that can distinguish one color from another. The saturation defines the purity of the color. 100% saturated means there is no white. It is either a pure red or green or blue. The value describes the brightness of the color. Range for hue is 0 - 360°, ranges of saturation and value is 0 – 1.

The next step is thresholding technique. It is for remove the background pixels and detecting the regions. Then, the morphological operation such as filtering is performed. In this operation, the comparison of the corresponding pixel in the input image with its neighbour is based on the pixel value in the output image. Filtering is use to remove some noise in the image.

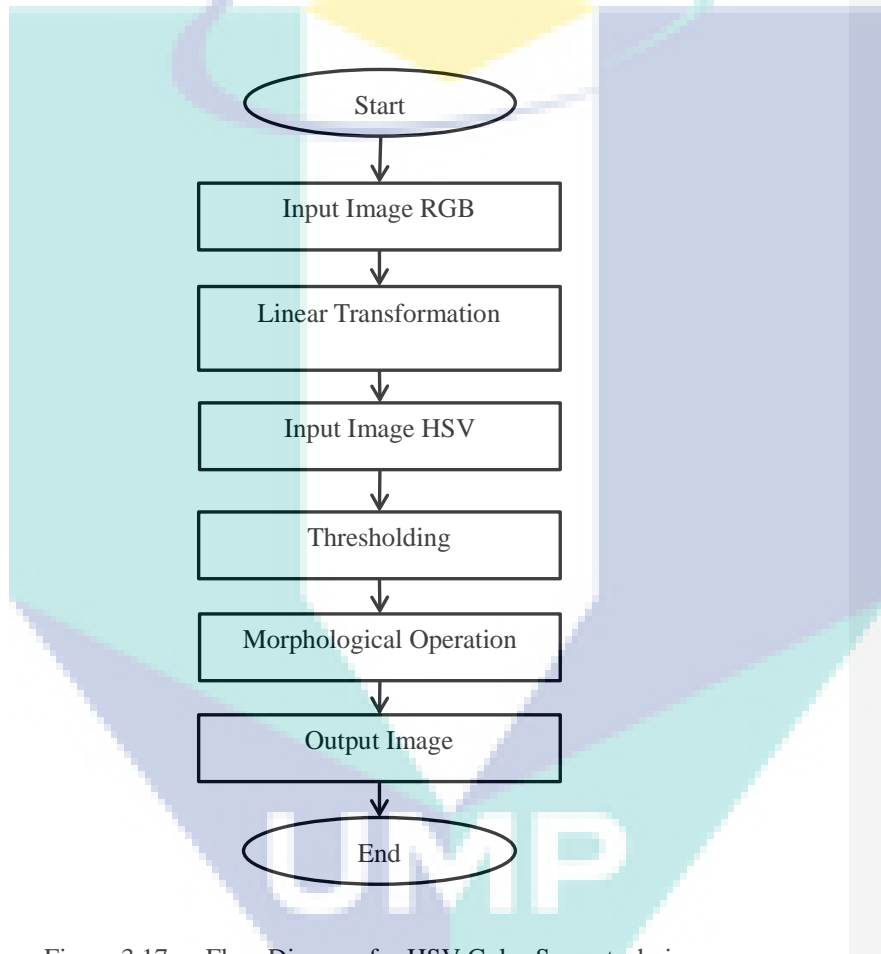


Figure 3.17 Flow Diagram for HSV Color Space technique

Comment [k33]: confusing with 3.16, 3.1. explain it properly and step by step

Comment [k34]: 3.3, 3.4 and 3.5, it is continue, separate or what ? explain and rewrite to show is comparison. and why you compare these three techniques.

3.6 Feature Extraction

The classification of water spots images into normal and abnormal is based on feature values. The decision on image is made using the pattern of the features. The object can be classified successfully if the ideal feature extraction is provided. Hence, it can make the classification process simpler (Duda, Hart & Stork, 2012).

Comment [k35]: explain the continuity from previous subchapter

There are three (3) features vector were extracted from the water saturation spots. Firstly is area feature. It is the number of pixels in a region. Second is perimeter. Perimeter will measure the distance around the boundary of the region. The Figure 3.18 below shows the pixel included in the perimeter calculation for the object. Last feature is mean intensity. It is the average intensity of pixels.

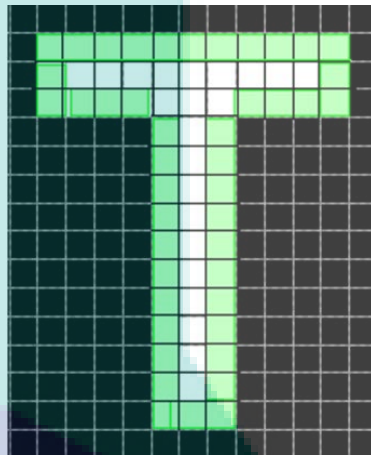


Figure 3.18 The perimeter calculation for the object

Next, after the value for these three features are measured, its values are used for statistical analysis. Statistical analysis based on minimum, maximum, mean and standard deviation of pixel values are widely used in color image analysis. The result from statistical analysis was used in the next stage of classification using linear thresholding. The value of the largest element in each row or column of the input, along vectors of a specified dimension of the input is called maximum value while the lowest value of element in each row and column of the input is minimum value. For the arithmetic average (mean) is used to measure data central tendency. Standard deviation is the dispersion of data.

Equation 3.4, Equation 3.5, Equation 3.6, Equation 3.7 below shows the mathematical equations for max, min, mean and standard deviation respectively. N refers to sample size and p_i total number of data.

$$\text{maximum (max)} = \max p_i \text{ for } i = 1, \dots, N \quad 3.4$$

$$\text{minimum (min)} = \min p_i \text{ for } i = 1, \dots, N \quad 3.5$$

$$\text{mean } (\mu) = \frac{1}{N} \sum_i^N p_i \quad 3.6$$

$$\text{standard deviation } (\sigma) = \left(\frac{1}{N-1} \right) \sum_i^N (p_i - \mu)^2 \quad 3.7$$

3.7 Classification

The final stage is classification using linear thresholding. Using the same dataset which used in statistical analysis before, the new threshold value is identified to detect the water spots image. The threshold is used to classify the image into four (4) groups namely normal and abnormal conditions. It is shown in Table 3.2.

Comment [k36]: too simple explanation on classification. explain more

Table 3.2 The groups for classification using Linear thresholding

Conditions	Specified range
Abnormal and High Intensity	Area > 26000 Intensity > 1000
Abnormal and Low Intensity	Area > 26000 Intensity < 1000
Normal and High Intensity	Area < 26000 Intensity > 1000
Normal and Low Intensity	Area < 26000 Intensity < 1000

Comment [k37]: why 2600, why 1000



3.8 Misclassification Error Measurement

There are a few measures used to evaluate the effectiveness of image segmentation algorithms. (Martin, Fowlkes, Tal & Malik, 2001) measure the effectiveness of segmentation using misclassification error (ME) while (Sezgin, 2004) measure the effectiveness of thresholding techniques using misclassification error (ME), modified Hausdorff distance, region non-uniformity (MU), edge mismatch (EMM) and relative foreground area error (RAE). In this study, misclassification error (ME) has been used to evaluate the image segmented algorithm's performance. ME measure the percentage of background pixels wrongly assigned to foreground and foreground pixels wrongly assigned to background. Hence, ME can be expressed as Equation 3.8:

$$ME = 1 - \frac{|B_0 \cap B_p| + |F_0 \cap F_p|}{|B_0| + |F_0|} \quad 3.8$$

where B_0 and F_0 denote the background and foreground of the ground-truth image respectively while B_p and F_p denote the background and foreground area pixels in the test image respectively (Sezgin, 2004). In this study, background pixels represented by black pixels and foreground pixels represented by blue pixels. The effectiveness of each segmentation algorithm is discussed in chapter 4.

In this study, the ground truth image obtained manually using Image J software. A ground truth image is the binary image that probably the best to differentiate between water spots regions and background pixels in the image obtained by human observations. The ability to distinguish an object for human being is excellent because the brain manage to do so. By using image J software, it can be simply segmented the water spots regions accurately and it does not change the image resolution.

Comment [k38]: move to chapter 4
explain more detail how you perform 3.8

CHAPTER 4

RESULTS AND DISCUSSION

4.1 Introduction

Methodologies of the image processing techniques for detection of water saturation spots using thermal images have been explained in Chapter 3 in detail. Three image segmentation algorithms have been proposed which are HSV, Color-based segmentation using K-Means and Feature Matching.

This chapter presents the experimental results obtained in developing a landslide prediction. The chapter begins by presenting the result of misclassification error for image segmentation. In the next section, the results of three segmentation techniques are discussed.

4.2 Effectiveness of image segmentation algorithm

The purpose of image segmentation is to detect region of interest (ROI). ROI is representing meaningful parts of objects. When the detection of ROI is wrong and not accurate, it will affect final classification. (Pal & Pal, 1993) proposed to use misclassification error to measure the performance image segmentation algorithm. The details results are shown in Table 4.1 until Table 4.3 and summarized in Table 4.4 below.

Based on the Tables below, the HSV techniques achieves the highest segmentation accuracy with average misclassification error (ME) equals to 0.00165 for data 1 , 0.0061 for data 2 and 0.0014 for data 3. These three data were discussed in subchapter 3.4.

Comment [k39]: what to focus on result

need to present the result based on methodology

need to relate the result with objective

Comment [k40]: you are not developing a system..

Comment [k41]: this result only ?

Comment [k42]: use ither tittle. sound not good.

Comment [k43]: do not repeat. rewrite. focus on result and discussion

Table 4.1 Misclassification error of HSV techniques

Images	Data 1	Data 2	Data 3
Image 1	0.0103	0.0046	0.0064
Image 2	0.0131	0.0036	0.0110
Image 3	0.0134	0.0032	0.0114
Image 4	0.0176	0.0034	0.0124
Image 5	0.0181	0.0035	0.0150
Image 6	0.0180	0.0040	0.0182
Image 7	0.0193	0.0041	0.0210
Image 8	0.0197	0.0048	0.0121
Image 9	0.0172	0.0046	0.0114
Image 10	0.0188	0.0048	0.0195
Image 11	0.0180	0.0039	0.0200
Image 12	0.0179	0.0043	0.0104
Image 13	0.0098	0.0042	0.0096
Image 14	0.0142	0.0089	0.0099
Image 15	0.0155	0.0084	0.0111
Image 16	0.0176	0.0088	0.0156
Image 17	0.0203	0.0086	0.0181
Image 18	0.0207	0.0084	0.0196
Image 19	0.0106	0.0085	0.0099
Image 20	0.0205	0.0167	0.0187

Comment [k44]: explain detail how you do this. show step by step and give example

Comment [k45]: what is data 1, data 2 data 3?

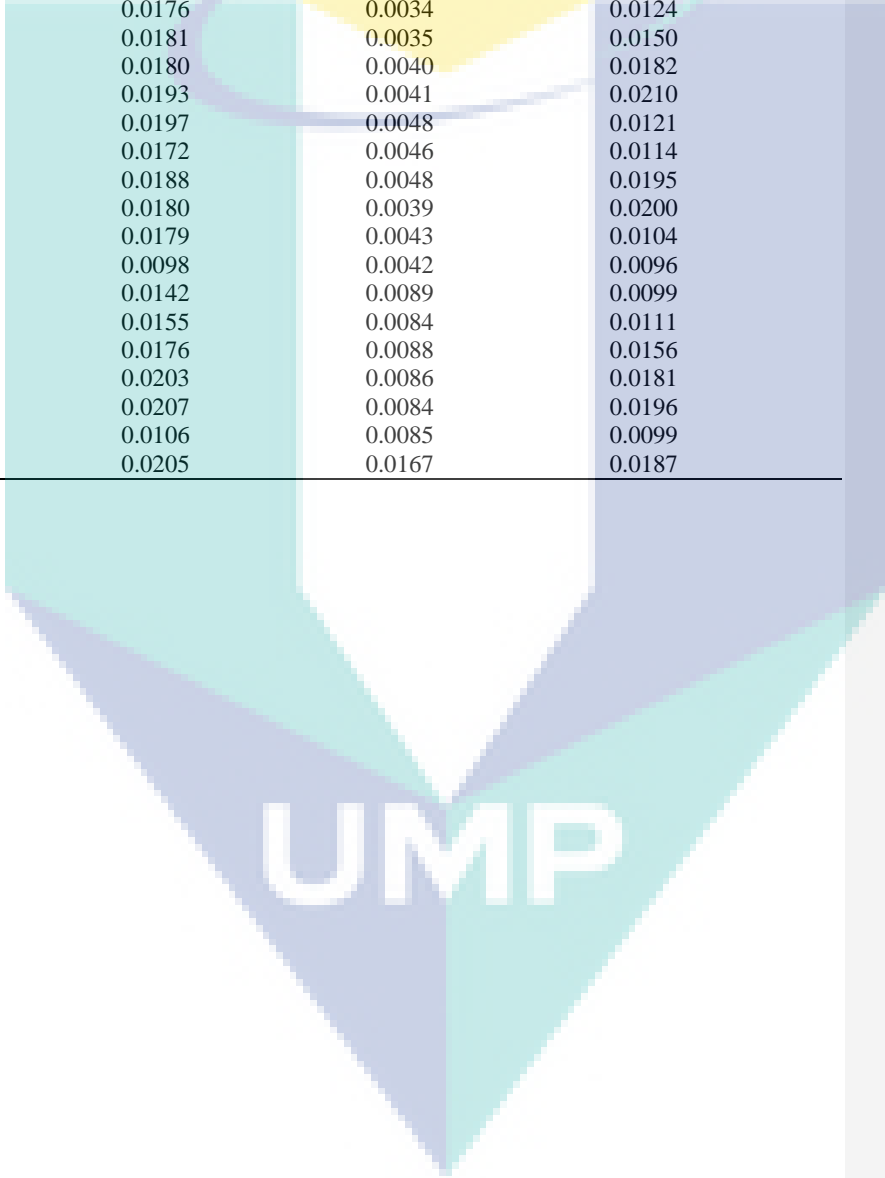


Table 4.2 Misclassification error of Color- Based Segmentation using K-Mean clustering techniques

Images	Data 1	Data 2	Data 3
Image 1	0.0486	0.0537	0.0632
Image 2	0.0684	0.0510	0.0627
Image 3	0.0589	0.0489	0.0538
Image 4	0.0597	0.0677	0.0567
Image 5	0.0823	0.0676	0.0580
Image 6	0.0421	0.0665	0.0619
Image 7	0.0687	0.0432	0.0520
Image 8	0.0751	0.0741	0.0813
Image 9	0.0726	0.0740	0.0833
Image 10	0.0734	0.0724	0.0734
Image 11	0.0871	0.0669	0.0871
Image 12	0.0478	0.0675	0.0716
Image 13	0.0729	0.0672	0.0907
Image 14	0.0456	0.0676	0.0847
Image 15	0.0447	0.0667	0.0636
Image 16	0.0894	0.0858	0.0640
Image 17	0.0789	0.0862	0.0708
Image 18	0.0847	0.0862	0.0669
Image 19	0.0475	0.0863	0.0737
Image 20	0.0470	0.0855	0.0761

UMP

Table 4.3 Misclassification error of Feature Matching techniques

Images	Data 1	Data 2	Data 3
Image 1	0.0872	0.0931	0.2984
Image 2	0.0921	0.1532	0.1799
Image 3	0.0976	0.0981	0.0914
Image 4	0.0944	0.1602	0.1687
Image 5	0.1132	0.2412	0.2497
Image 6	0.2644	0.1647	0.0892
Image 7	0.2303	0.0805	0.0932
Image 8	0.1865	0.0919	0.1658
Image 9	0.0945	0.1384	0.0934
Image 10	0.0935	0.2076	0.1874
Image 11	0.1843	0.0863	0.1365
Image 12	0.0839	0.0963	0.1576
Image 13	0.0930	0.0912	0.0915
Image 14	0.0937	0.0894	0.1712
Image 15	0.1895	0.0738	0.0871
Image 16	0.2567	0.1354	0.0954
Image 17	0.1904	0.2739	0.2477
Image 18	0.1356	0.0987	0.2584
Image 19	0.1021	0.0954	0.0987
Image 20	0.0972	0.2941	0.0972

UMP

Table 4.4 Average misclassification error of HSV, K-Means and Feature Matching techniques

Techniques	HSV			K- Means			Feature Matching		
	Data 1	Data 2	Data 3	Data 1	Data 2	Data 3	Data 1	Data 2	Data 3
	0.0165	0.0061	0.0141	0.0730	0.0693	0.0698	0.1305	0.1382	0.1529

Comment [k46]: lost. suddenly HSV, k means and feature matching.
rewrite and explain it on order. reader lost

Table 4.5 Percentage of accuracy of misclassification error of HSV, K-Means and Feature Matching techniques

Techniques	HSV			K- Means			Feature Matching		
	Data 1	Data 2	Data 3	Data 1	Data 2	Data 3	Data 1	Data 2	Data 3
	98.35	99.39	98.59	92.7	93.07	93.02	86.95	86.18	84.71

Comment [k47]: add more result here. since this part is very important towards achieving your objective.
add more discussion and analysis here. not enough result

(Apostolidis & Mezaris, 2014) stated that HSV color space gives accurate segmentation. There are many techniques for segmentation, but in this study, only three popular techniques nowadays are used. Many recent studies (Bora et al., 2015; Ha, Pham, Pham & Tran, 2016; Hidayatullah & Zuhdi, 2015; Zhao, Bu & Chen, 2002) have shown that HSV color space is a robust techniques and high accuracy. Besides, K-Means, and Feature Matching also used in this study because of the same reason which are robust and accurate (Arnfred & Winkler, 2015; Kondo, Salibian-Barrera & Zamar, 2012; J. Ma et al., 2015; Shijin Kumar & Dharun, 2016).

Comment [k48]: no need to cited any paper at result. just straight forward discuss your result.



UMP

4.3 Image Segmentation for Water Spot Detection

4.3.1 Feature Matching

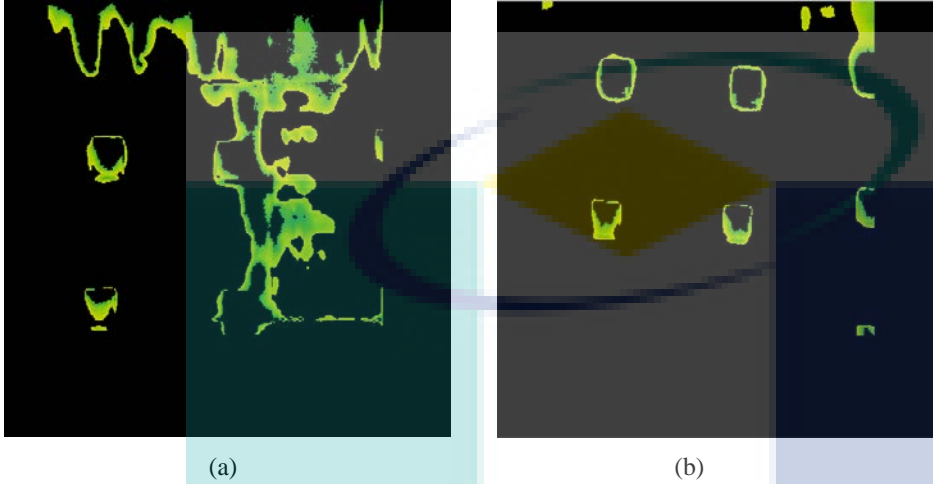


Figure 4.1 (a) the segmented result for abnormal image using Feature Matching technique (b) the segmented result normal image using Feature Matching technique.

The segmented result in Figure 4.13 above shows that Feature Matching technique has wrong segmented result. The result only detected greenish region. Greenish region is not considered as water saturation spots. The water saturation spot is blue in color which has been proven in water content experiment in section 4.7.

The comparisons for three techniques are made in the next subsection. As can be seen, the HSV technique has been chosen as the most accurate technique.

Comment [k49]: do not let subchapter after subchapter blank. explain. need ore explanation. lost..

what is the different with 4.2

ensure the contonuity between subchapter are explaining well. reader will lost.

4.3.2 Color-based segmentation using K-Means

K- Means clustering is used to partition the thermal images into certain clusters. All the color information is in the 'a' and 'b' layers. K- Means uses squared Euclidean distances to measure the difference of these two colors. Then the colors in 'a*b*' space are classified using K-means clustering. 'a*b*' space has the color information, so the objects are pixels with 'a*' and 'b*' value. K- Means is use to test the images into two (2), three (3), and four (4) clusters using the Euclidean distance metric.

Figure 4.8 below shows the dialog box that displays the options for user to choose. The dialog has three default buttons. The users can choose which clusters that segment the images accurately.

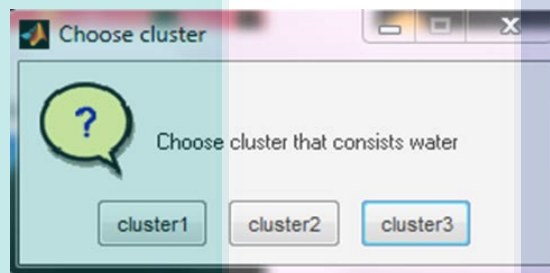


Figure 4.2 The dialog box displays the options for user.

Comment [k50]: not a result. please find a way to present result

Figure 4.9 below shows the segmentation result of water saturation spots using K-means clustering techniques. The image is segmented into two clusters. From the empirical observation, it is found that two (2) cluster does not have correct segmentation.

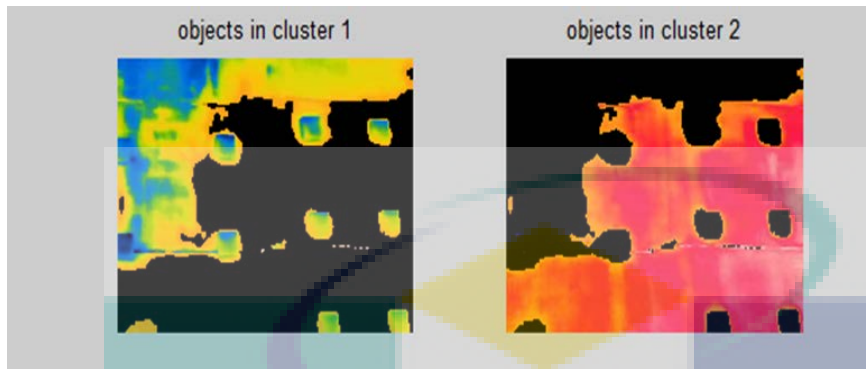


Figure 4.3 Segmentation result when number of cluster is set to 2.

The number of cluster is increased to 3. As can be seen in Figure 4.10, cluster 1 and cluster 2 are wrong segmentation but cluster 3 can accurately segment the water saturation spots. Besides, the color of segmented regions is also correct but it is not the accurate color of water spots regions.

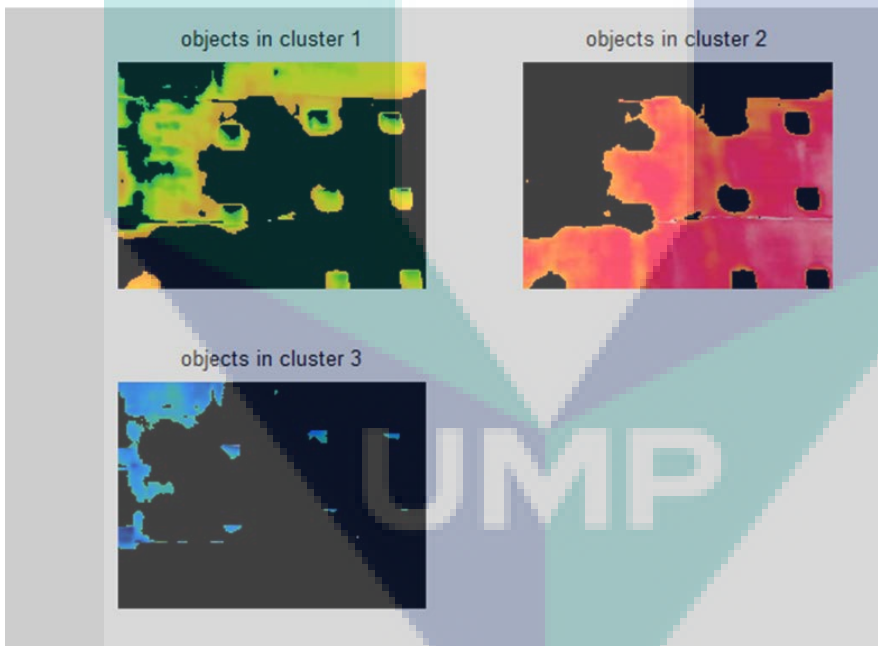


Figure 4.4 Segmentation result when number of cluster is set to 3

The image is segmented into four clusters. From the observation in Figure 4.11 below, cluster 1, cluster 3 and cluster 4 are segmented wrong regions and color. In examining a thermograph, a blue color is cold. Green is roughly room temperature and white or red is displays area of inflammation. Cluster 2 is accurately segmented with blue and a few of green color of regions.

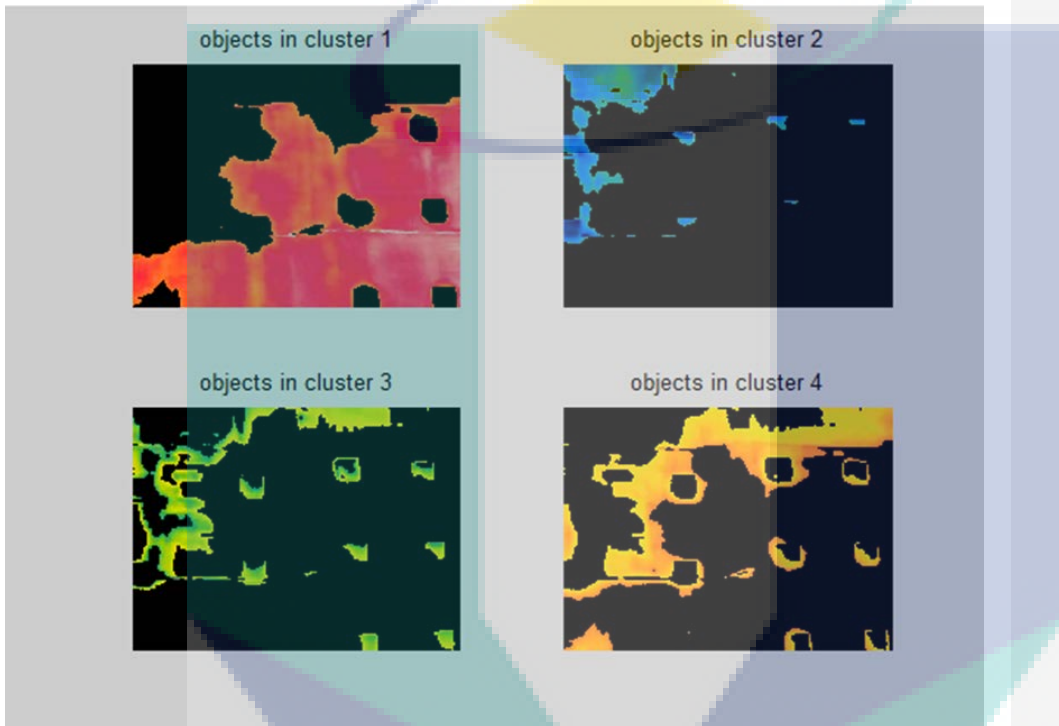


Figure 4.5 Segmentation result when cluster is set to 4

The comparison between HSV technique and K-Means techniques is being observed in Figure 4.12 below. There are a few greenish area detected in the image result using K-Means technique. The greenish area is not included as water saturation spots. The HSV technique is more accurate. It is also proved by (Bora et al., 2015). They found that HSV color space is performing better than K-Means.

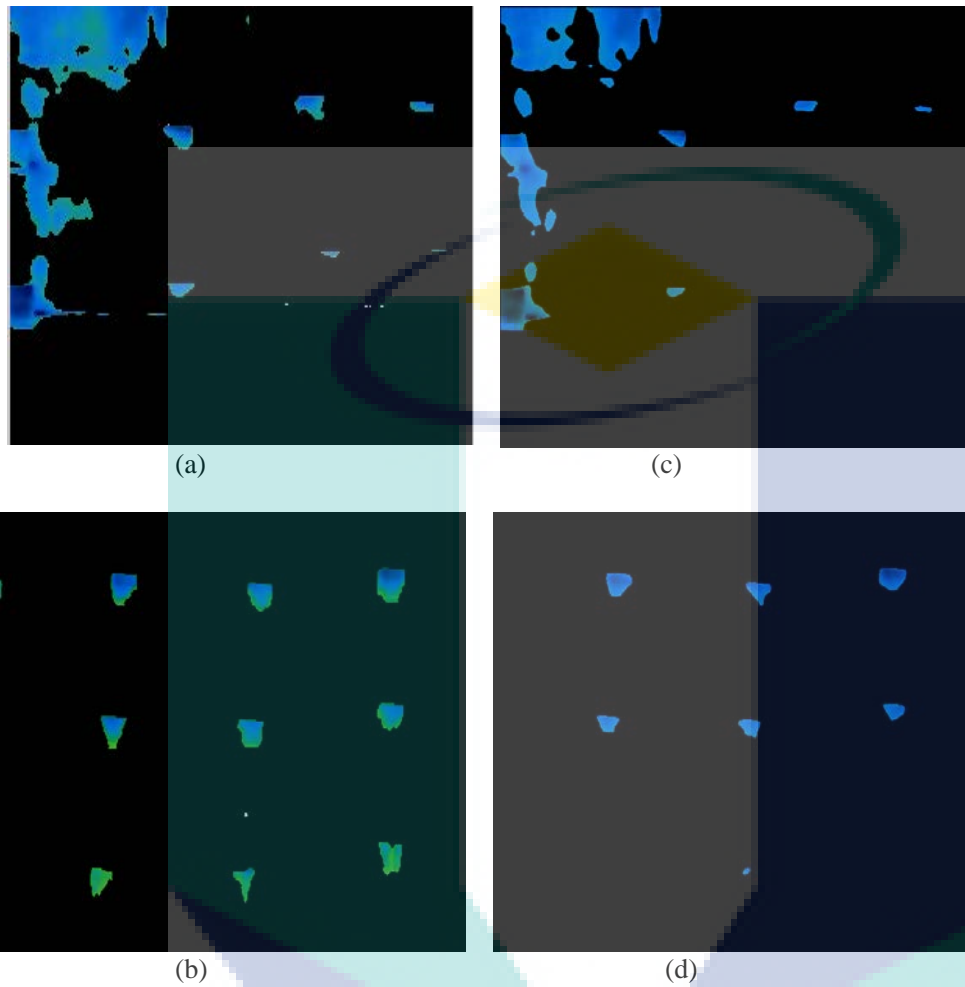


Figure 4.6 (a) The abnormal image segmented result using K-Means technique (b) the normal image segmented result using K-Means technique. (c) the abnormal image segmented result using HSV technique (d) the normal image segmented result using HSV technique.

4.3.3 HSV Color Space Technique

Hue, Saturation, Value or HSV is a color model that describes colors in terms of their shade which is saturation and their brightness which is luminance or value. Based on the explanation in methodology section 3.5.3, hue is representing color type from 0 - 360°. It is expressed hues of red starts at 0, yellow starts at 60, green starts at 120, cyan starts at 180, blue starts at 240 and magenta starts at 300. In this study, three (3) colors are used which are red, green blue. Table 4.6 below shows the hue and its value for pure red, pure green and pure blue.

Table 4.6 Hue and its values for red, green and blue in colors

Hue	Hue Value
Pure red	0
Pure green	$\frac{120}{360} = 0.333$
Pure blue	$\frac{240}{360} = 0.666$

RGB and LAB color space are not the best techniques when choosing the regions based on color. The better technique is HSV color space. This technique can define what hue range defines as blue, red or green. In this work, the blue colors in thermal images are represents as water saturation spots. Hence, the hue values in the range of 0.555 and 0.666 have been chosen. Figure 4.1 below is the original photo of concrete wall that have been used in this study and Figure 4.2 is the photo of the landslides phenomenon happen in the same location, Indera Mahkota 8, Kuantan, Pahang, Malaysia. The concrete wall that holds the slope is collapse. The collapse was cause of structural failure resulting from increased pressure developed behind the wall due to the heavy rain during the incident.



Figure 4.7 Original photo of concrete wall



Figure 4.8 The landslide phenomenon happened in Indera Mahkota 8

Figure 4.3 below shows original thermal images of water spots regions after it is convert from the videos. As can be seen, Figure 4.3 (a), Figure 4.3 (b), Figure 4.3 (c) shown the abnormal images which is contain a lot of water saturation inside the soil while Figure 4.3 (d), Figure 4.3 (e) and Figure 4.3 (f) shown the normal image, it contain a little water saturation. Figure 4.3 (g), Figure 4.3 (h), Figure 4.3 (i) are the thermal images that combine between two condition which are abnormal and normal images.

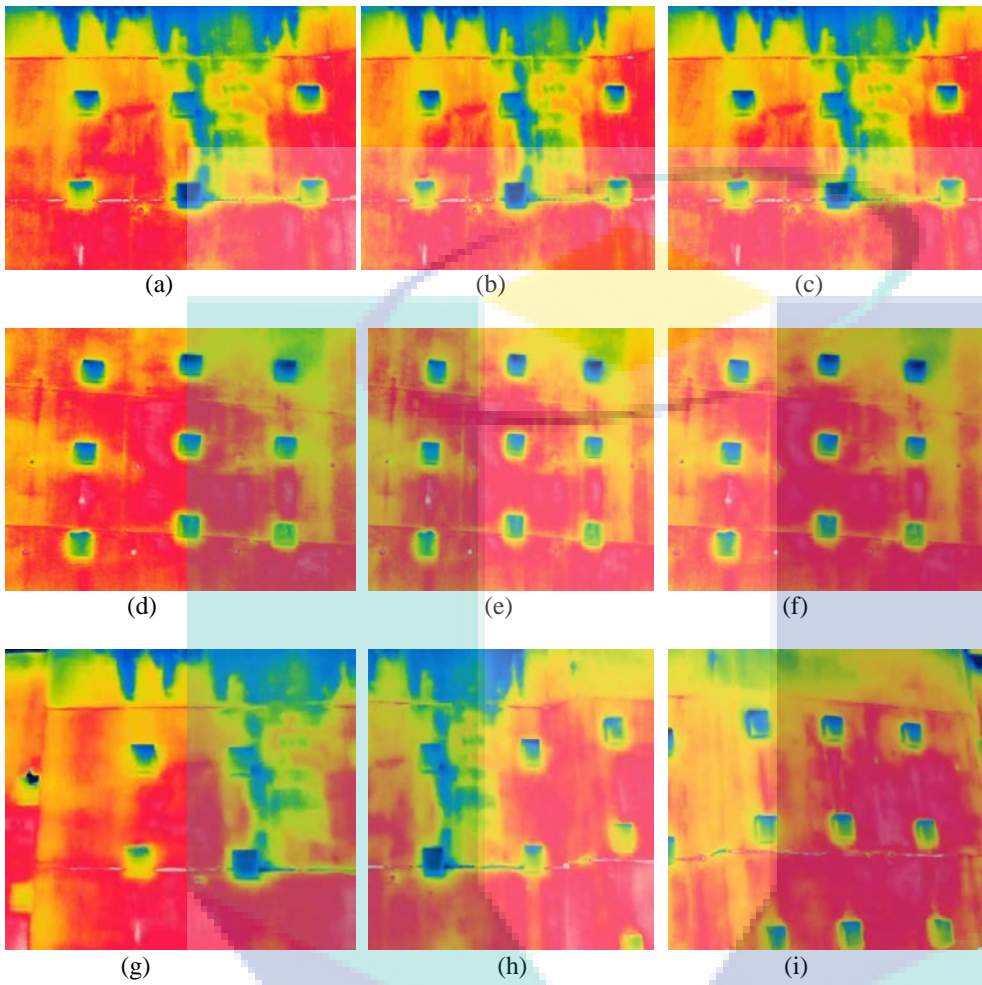


Figure 4.9 Original thermal images. (a), (b), (c) Abnormal images, (d), (e), (f) normal images (g), (h), (i) combination between abnormal and normal images

Figure 4.4 below shows the images that have been process using HSV color space technique. As can be observed, HSV color space technique has segmented the image accurately.

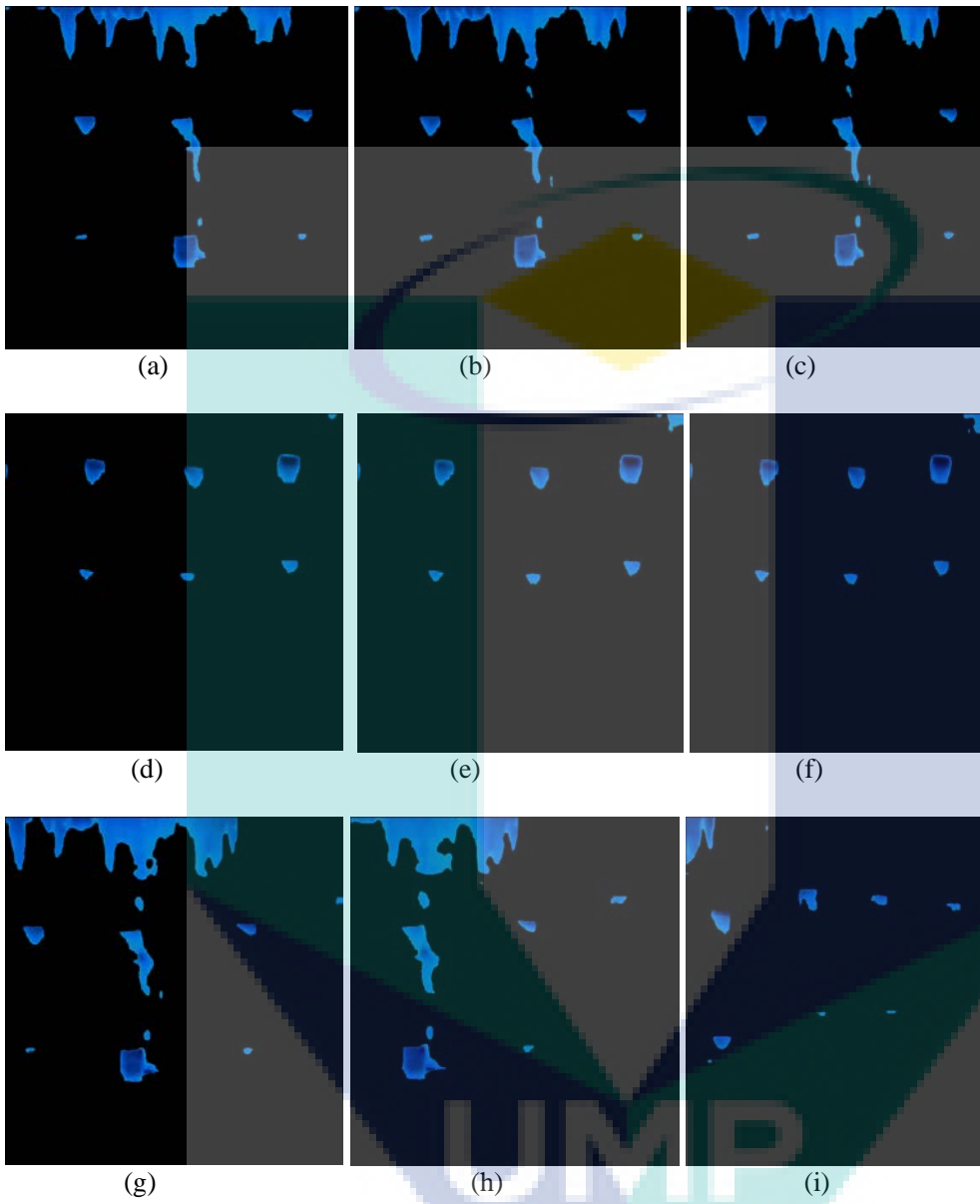


Figure 4.10 (a) – (i) The images that have been process using HSV color space technique

Figure 4.5 shows the results of thermal images using different ranges of hues values. The ranges of hues values use are between 0.33 and 0.66. Based on the table 4.7 above, green is at angle $\frac{2\pi}{3}$ and 0.333 is represented as green hue value. As can be seen, there are green color in the segmented images. The greenish area is not considered as water saturation spots.

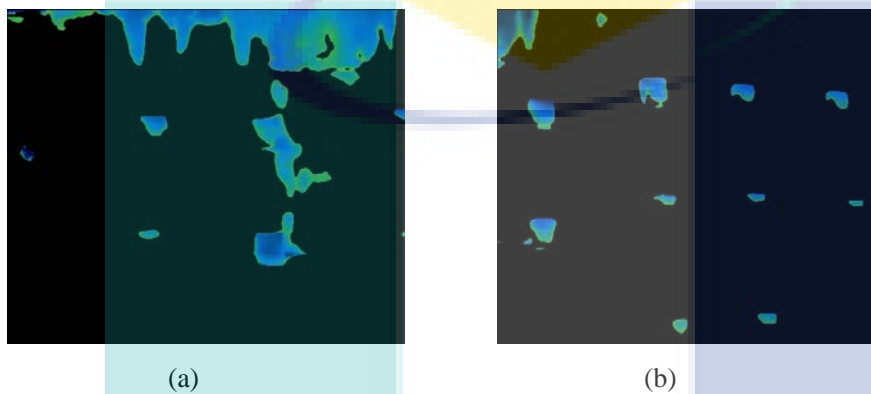


Figure 4.11 (a) and (b) The segmented images using ranges between 0.33 and 0.66

Angle in the range 0 to 2π respective to the red axis with red at angle of 0. Hence, 0 is represented as red hue value. Figure 4.6 shows images using the hue values between 0 and 0.33. From the Figure 4.6, it can be observed that the values give wrong segmented area and there are no water saturation spots which are blue regions in these result images.

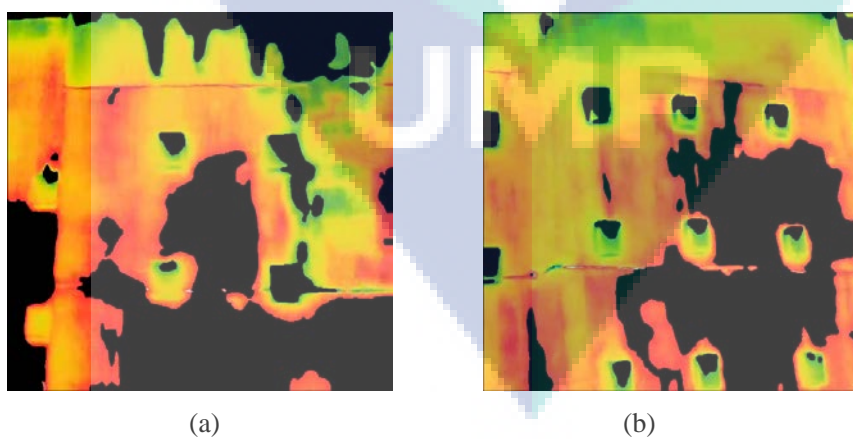


Figure 4.12 (a) and (b) The segmented images using ranges between 0 – 0.33

The comparison between RGB and HSV has been done. The RGB image is process using color thresholding operation. This thresholding technique is explored by (Rosin & Hervas, 2005) to determine landslide activity. However, they used remote sensing image for landslide monitoring. The result is shown in Figure 4.7 below.

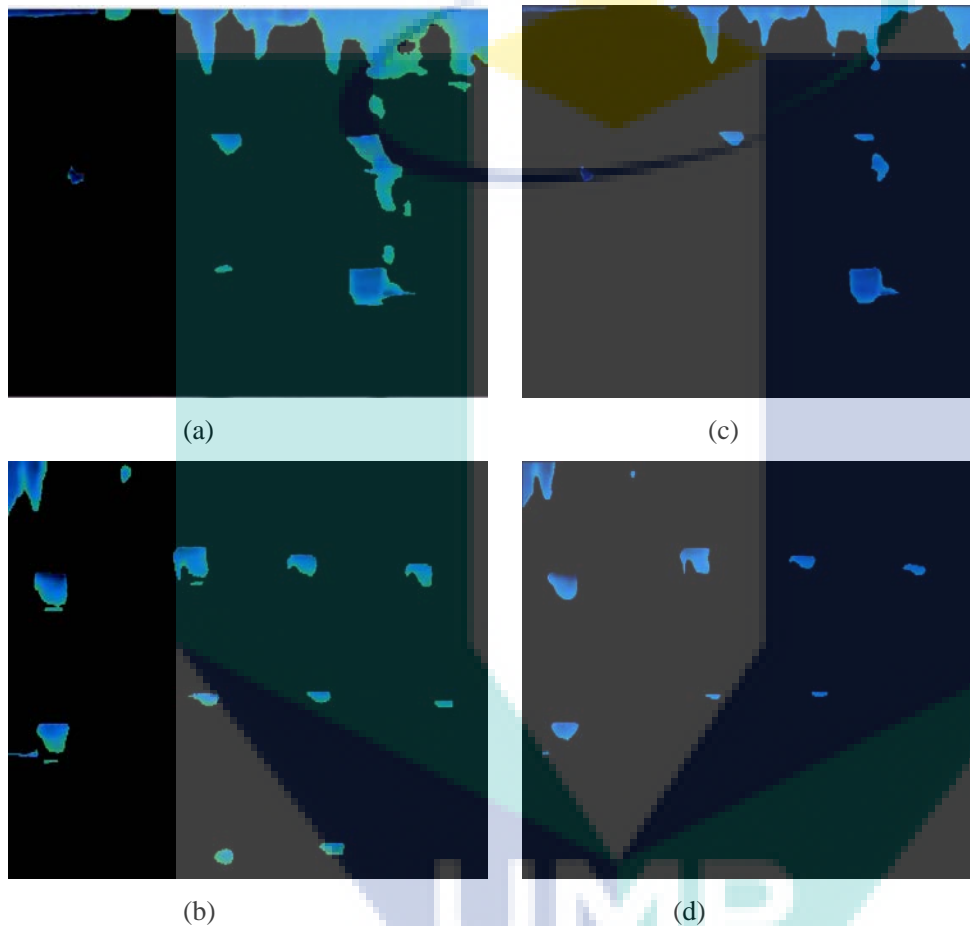
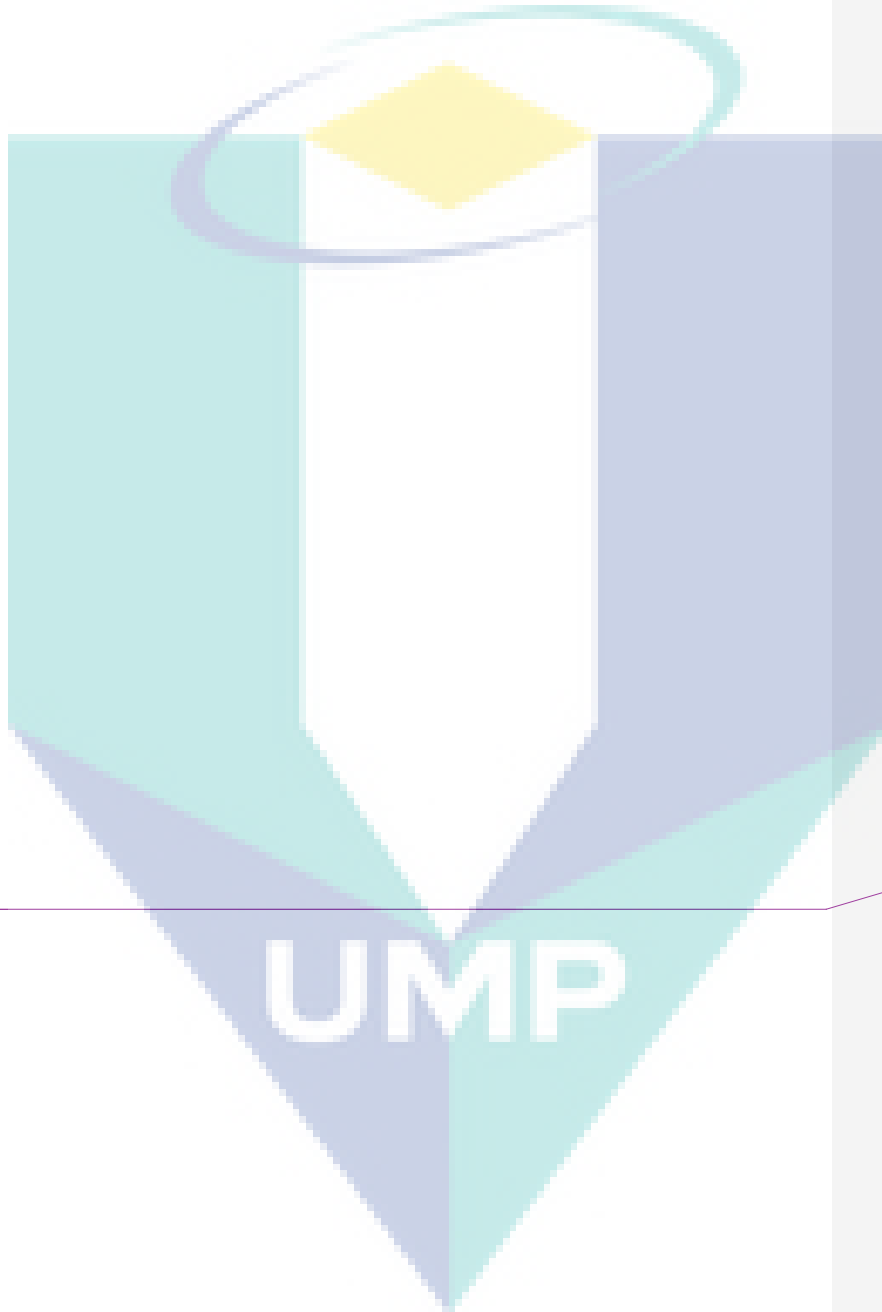


Figure 4.13 (a) and (b) The segmented RGB images using color threshold. (c) and (d) the segmented HSV images

As can be observed from Figures 4.7 above, the RGB image which is directly processed using color threshold operation is not getting accurate results. On the other hand, the RGB color space is not preferred, so it needs to convert to another color space such as HSV. The Figure 4.7 (c) and (d) shows HSV color space technique can detect only blue color of water saturation spots while RGB images get wrong segmented region and color detection.

In this study, color threshold and morphological operations also includes after processing the image using HSV color space. It is used to get the more accurate segmented images. The morphological operation which is filtering and closing are performed.



...

Comment [k51]: result must in % or in number or in graph.
add more result here

4.4 Statistical Analysis

The segmentation region is successfully detected in subchapter 4.3, 4.4 and 4.5. Next step is Feature extraction. Feature extraction has been done using region properties. The features are area, perimeter and intensity value. Min, max, mean and standard deviation from statistical analysis were used and the results are evaluated for the three techniques. The purpose of statistical analysis is to allow sets of data to be compared and make the data more meaningful. This analysis was tested using 365 images. Data 1 consists of 114 of normal images, data 2 consists of 180 of abnormal images and lastly data 3 consists of 71 of abnormal and normal images. Table 4.7 until Table 4.9 presented the example of 20 data for HSV technique. Table 4.10 until Table 4.12 shows statistical analysis for HSV image results.

Comment [k52]: why statistical. what is the connection from previous subchapter. how statistical explaining your result.

Table 4.7 20 data of abnormal condition for HSV technique

HSV Technique		
Area	Perimeter	Intensity
35863	3771.065	1165.989
37255	3842.764	1174.213
37358	3974.462	1070.397
39068	3976.563	1162.561
39147	4061.433	1071.589
39691	4027.048	1178.264
39113	3990.219	1072.564
39206	3929.249	1072.755
39463	3943.492	1073.671
39669	3927.793	1071.518
39916	3968.178	1095.993
39076	3877.793	1159.164
39013	3894.178	1070.063
39140	3886.278	968.3252
39768	3909.793	1176.546
39223	3878.864	1173.769
39073	3814.923	1173.713
39214	3782.195	1262.677
38715	3745.568	1176.95
38717	3730.739	1073.013

Table 4.8 20 data of normal condition for HSV technique

HSV Technique		
Area	Perimeter	Intensity
10947	1789.654	789.3525
11755	1893.754	677.9805
11846	1900.968	676.4609
12175	1953.252	779.5727
12433	1919.11	883.5453
12541	1904.139	883.5884
11904	1872.139	671.0895
11909	1873.997	671.1571
12652	1863.997	882.7616
13078	1886.482	676.8548
12859	1905.553	778.1251
13074	1916.139	778.5558
12813	1851.654	881.1439
13068	1936.382	777.4004
13513	1966.524	776.6416
13302	1944.725	671.0983
13390	1953.453	671.3542
13178	1895.855	775.3683
13373	1902.34	672.1916
13605	1942.039	673.6188

UMP

Table 4.9 20 data of combination normal and abnormal condition for HSV Technique

HSV Technique		
Area	Perimeter	Intensity
13460	2062.5	962.7696
13373	2072.257	766.5413
13242	2195.47	1083.234
12113	2140.985	897.5433
15120	2560.465	892.2874
19059	3042.23	985.25
21761	2919.235	1078.172
22260	2872.122	1075.822
24912	3037.092	910.9781
24260	3072.749	1244.309
23283	3071.72	1350.871
23511	3031.477	1144.065
25902	3125.82	1106.63
30298	3096.649	995.6485
31767	3153.963	1192.039
34445	3212.59	1081.48
35541	3248.347	1074.789
39540	3625.058	1297.733
40830	3630.815	1224.081
40821	3504.472	1114.618

Table 4.10 The statistical analysis for HSV abnormal images results

Statistical Analysis	HSV Technique		
	Area	Perimeter	Intensity
Min	33228	3406.715	968.3252
Max	42385	4075.291	1484.328
Mean	39454.09	3791.225	1139.479
Standard Deviation	1549.261	144.5575	81.77086

Table 4.11 The statistical analysis for HSV normal images results

Statistical Analysis	HSV Technique		
	Area	Perimeter	Intensity
Min	8317	1375.404	616.2686
Max	13906	1966.524	1102.223
Mean	11851.81	1657.727	801.5898
Standard Deviation	1161.115	165.4808	89.24729

Table 4.12 The statistical analysis for HSV normal and abnormal images results

Statistical Analysis	HSV Technique		
	Area	Perimeter	Intensity
Min	9171	1760.801	716.3007
Max	42887	3630.815	1350.871
Mean	26141.25	2756.406	1045.049
Standard Deviation	12564.72	640.9935	132.843

Table 4.13 until Table 4.15 shows the example of 20 data for K-Means technique and Table 4.16 until Table 4.18 shows statistical analysis for K-Means image results.

Table 4.13 20 data of abnormal condition for K-Means technique

	K-Means		
	Area	Perimeter	Intensity
25990	3026.751	989.6041	
26900	3043.822	1098.806	
26927	3060.349	1082.56	
28333	3111.076	1180.366	
28535	3152.047	1074.561	
29470	3069.336	771.255	
29041	3046.55	876.4183	
28929	3053.721	1083.646	
29054	3035.579	988.5424	
29411	3035.295	1194.645	
29729	3137.621	1189.671	
28867	3067.094	1098.007	
28997	3119.721	1095.192	
28995	3093.922	1093.707	
29923	3051.395	774.9627	
29580	3020.626	981.3438	
29470	3010.341	776.7229	
29445	3026.868	998.2397	
28761	3129.194	1326.588	
28824	3096.023	888.6874	

Table 4.14 20 data of normal condition for K-Means technique

K-Means		
Area	Perimeter	Intensity
6571	1137.377	2405.825
7366	1212.247	1979.632
7993	1297.36	1862.044
8157	1259.561	1962.475
8189	1313.644	2251.458
8421	1320.129	1958.734
8514	1312.431	1750.654
8107	1289.602	1960.217
8177	1278.288	1873.992
8670	1298.732	1984.798
8828	1333.703	2279.009
8646	1308.975	1974.068
8738	1334.188	2369.733
8626	1313.602	1883.011
8882	1351.845	2164.609
9087	1399.786	2457.845
8954	1359.36	2278.035
8948	1372.573	1950.62
8945	1355.644	2162.199
9070	1386.472	1960.086

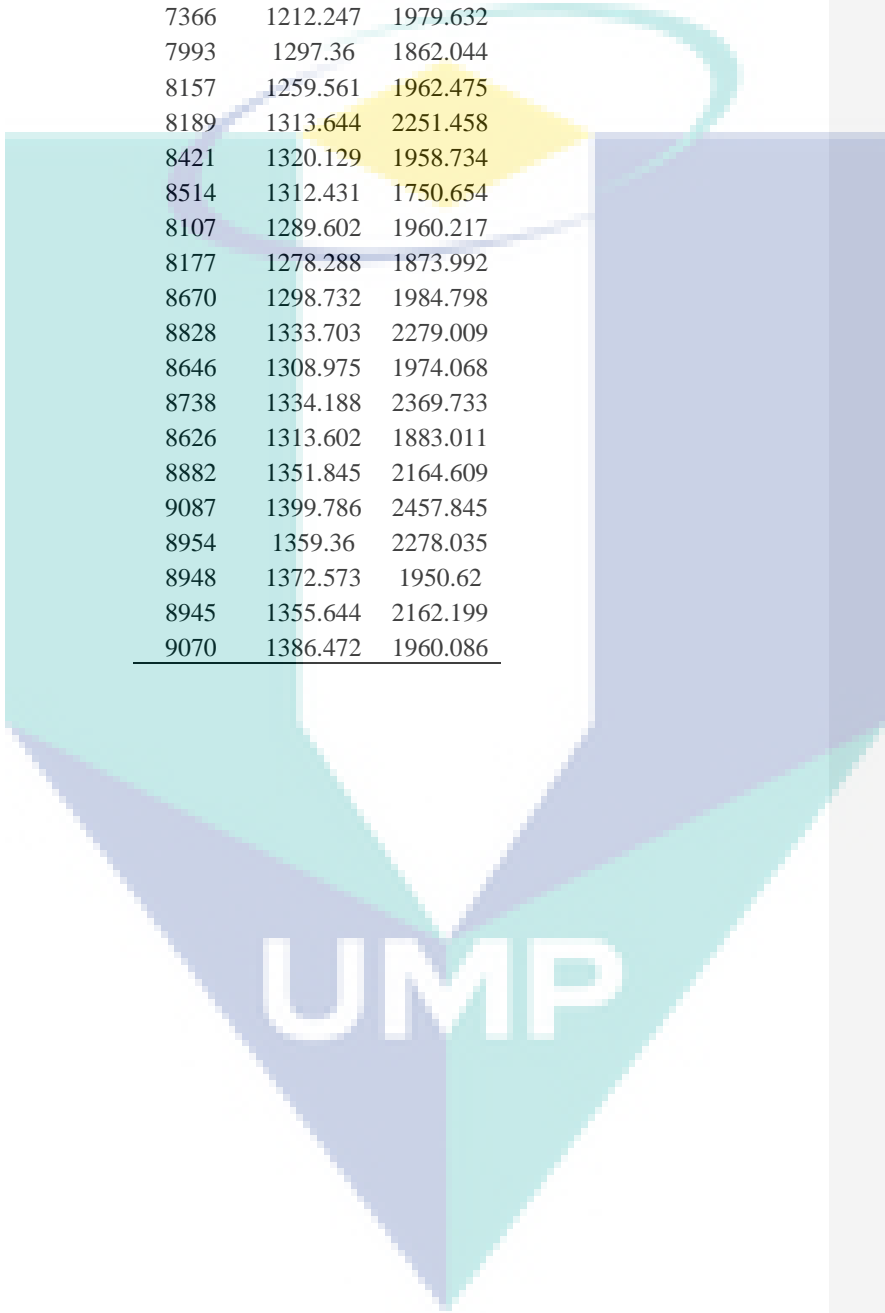


Table 4.15 20 data of combination normal and abnormal condition for K-Means Technique

K-Means		
Area	Perimeter	Intensity
9901	1695.418	1701.536
10065	1708.673	2399.533
9808	1764.815	1852.981
8965	1991.55	3057.681
10683	2101.876	3201.132
13133	2246.244	1731.317
15659	2432.871	2163.75
15977	2404.303	1748.486
18044	2481.558	1441.313
17659	2444.788	1322.52
16760	2443.859	1758.555
16718	2434.746	1128.336
18777	2594.545	1366.6
22651	2800.955	1123.122
23971	2774.913	1026.977
26502	2759.682	1108.892
27117	2845.481	1013.05
29584	3026.192	1390.193
30398	3072.092	1240.899
30776	3000.778	1188.323

Table 4.16 The statistical analysis for K-Means abnormal images results

Statistical Analysis	K-Means		
	Area	Perimeter	Intensity
Min	23539	2850.317	680.5339
Max	31284	3178.91	2119.028
Mean	28930.15	3053.817	1146.062
Standard Deviation	1298.492	56.48445	210.6288

Table 4.17 The statistical analysis for K-Means normal images results

Statistical Analysis	K-Means		
	Area	Perimeter	Intensity
Min	6571	1090.583	791.3443
Max	9774	1448.472	2625.325
Mean	8488.763	1253.372	1493.68
Standard Deviation	563.9372	82.34435	549.8933

Table 4.18 The statistical analysis for K-Means normal and abnormal images results

Statistical Analysis	K-Means		
	Area	Perimeter	Intensity
Min	5836	1269.394	608.7492
Max	65928	4350.047	3214.753
Mean	24805.09	2445.347	1418.457
Standard Deviation	12965.35	727.7802	628.554

Table 4.19 until Table 4.21 shows the example of 20 data for Feature Matching technique and Table 4.22 until Table 4.24 shows statistical analysis for Feature Matching image results.

Table 4.19 20 data of normal condition for Feature Matching technique

Feature Matching		
Area	Perimeter	Intensity
6844	1593.214	4.378611
6947	1584.67	4.084416
7102	1518.587	4.11984
7124	1550.587	4.383194
7014	1472.705	4.321028
6914	1447.45	4.347408
6878	1461.45	4.432008
6973	1461.349	4.360105
7029	1601.332	4.436752
7003	1603.918	4.416568
7071	1606.202	4.429576
7098	1599.131	4.449073
7153	1600.161	4.606804
7349	1682.788	5.081718
7321	1670.989	4.996773
7288	1651.776	4.977768
7217	1759.901	4.983103
7293	1775.7	5.184547
7279	1657.675	5.307457
6719	1520.438	3.963224

Table 4.20 20 data of abnormal condition for Feature Matching technique

Feature Matching		
Area	Perimeter	Intensity
23686	5072.968	4.452842
24105	4992.542	4.855521
24379	4339.248	5.007471
24037	4248.413	4.637542
23734	4169.092	4.623682
23673	4097.109	4.554191
23612	4095.411	4.553941
23493	4225.879	4.548287
23498	4244.849	4.616113
23480	4096.641	4.69926
23487	4095.913	4.591981
23408	4053.73	4.477599
23433	4245.879	4.93248
23342	4179.411	5.011882
23241	4140.641	5.158032
23181	4141.327	4.922658
23053	4033.605	5.287553
22997	4018.634	5.667776
23069	4043.605	5.182044
23106	4042.877	5.196081

UMP

Table 4.21 20 data of combination normal and abnormal condition for Feature Matching technique

Feature Matching		
Area	Perimeter	Intensity
9798	2173.905	3.514996
8794	2163.905	3.572134
8656	1999.194	3.090574
9875	2097.555	3.183642
9985	2116.56	3.593332
10422	2182.275	4.000187
11241	2551.211	3.673604
11309	2563.052	4.337491
11008	2599.881	4.9785
11663	2743.905	5.377049
13405	3149.184	3.283442
15289	3331.15	3.355525
15883	3569.157	3.612523
17023	3829.022	4.864084
18218	3724.713	4.786305
19631	3999.164	4.059234
19839	4160.443	4.335167
19799	4168.786	3.067458
19927	4367.421	4.013965
20181	4372.124	5.211137

Table 4.22 The statistical analysis for Feature Extraction normal images results

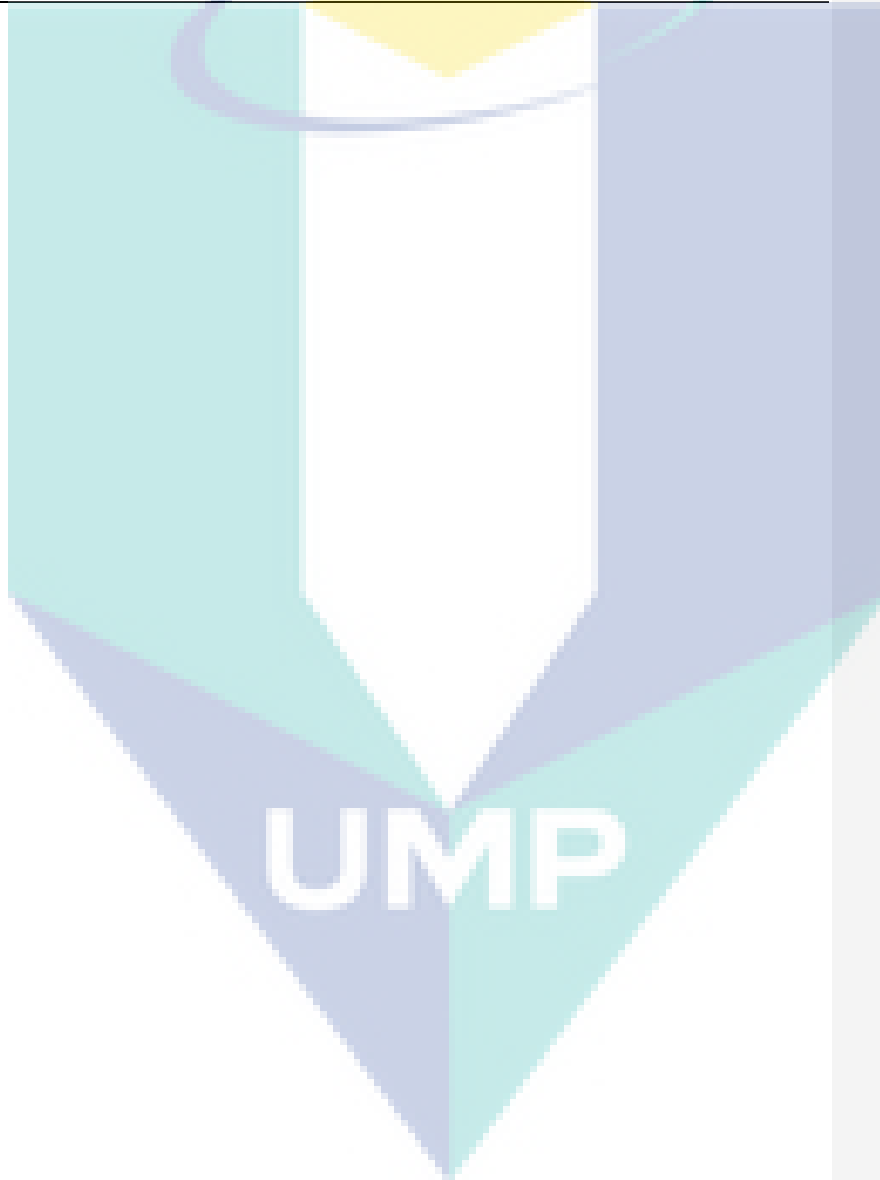
Statistical Analysis	Feature Extraction		
	Area	Perimeter	Intensity
Min	4715	1059	2.51428
Max	7349	1775.7	5.30745
Mean	5809.272	1362.64	3.514
Standard Deviation	1050.781	181.4712	1.05125

Table 4.23 The statistical analysis for Feature Extraction abnormal images results

Statistical Analysis	Feature Extraction		
	Area	Perimeter	Intensity
Min	20041	3868.218	4.413705
Max	24379	5072.968	6.981342
Mean	22183.23	4203.429	5.497287
Standard Deviation	751.7853	290.2498	0.530208

Table 4.24 The statistical analysis Feature Extraction normal and abnormal images results

Statistical Analysis	Feature Extraction		
	Area	Perimeter	Intensity
Min	8959	1999.194	3.067458
Max	23712	4756.541	8.115986
Mean	17125.32	3292.877	5.340952
Standard Deviation	3874.816	880.5384	1.211457



The quantitative findings of the HSV technique over 114 test images are presented graphically in Figure 4.14 to Figure 4.16. The graph below in Figure 4.14 is for area features. It is noticed that the range for normal condition is 10000 to 15000 and for abnormal condition is 35000 to 40000. The range between abnormal and normal condition is wide. It can be observed from the Table 4.10, Table 4.11 and Table 4.12 above, the minimum value of area for abnormal condition is 33228 and the maximum value of area for normal is 13906. The average for both conditions is around 26141.25. Hence, if the area of the water spot is higher than 26000, it is an abnormal condition. If it is below that 26000, so it is a normal condition.

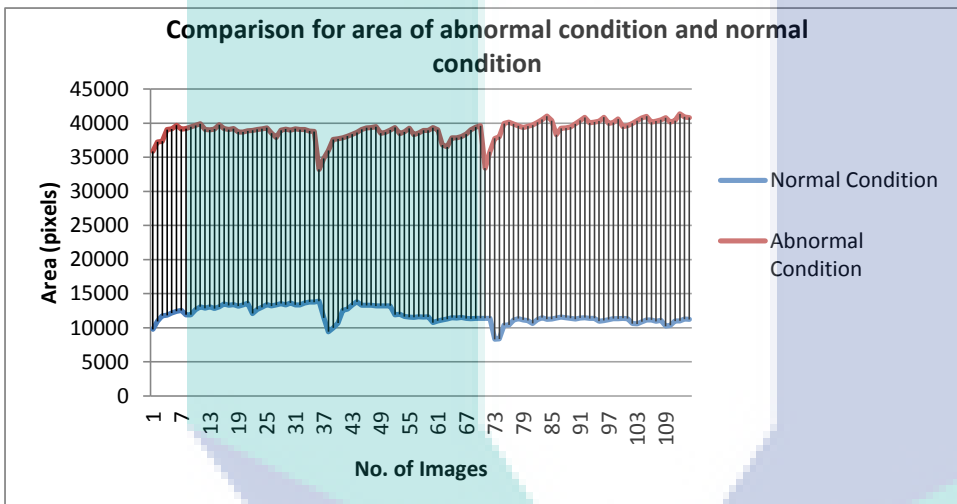


Figure 4.14 The comparison using area features between abnormal and normal condition for HSV technique.

The result in the Figure 4.15 below displays the comparison for perimeter between abnormal and normal condition. The result for perimeter features is corresponded to area features. When the area of the water spots is large, then the perimeter of the water spots is also large but the values for both features are different. The range for abnormal condition is 3400 to 4000 while for normal condition is only 1500 to 2000. The mean value for both conditions is 2756.406.

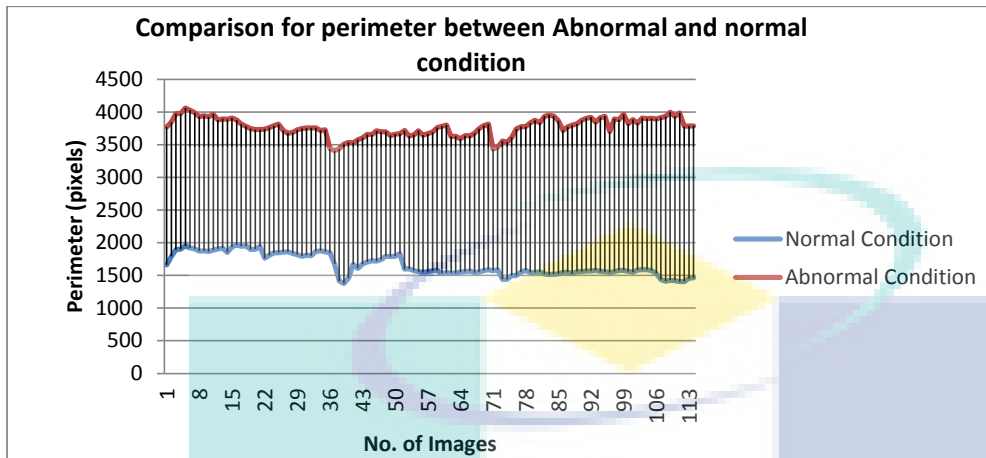


Figure 4.15 The comparison using perimeter features between abnormal and normal condition for HSV technique

The graph in Figure 4.16 below shows the result for intensity values. The graph is unstable because the regions of the water spots in each image have different value. It is discussed in Section 4.7. The range for intensity for abnormal condition is higher compared to normal condition. The highest intensity value is 1484.328 and the lowest value is 616.2686. The highest intensity means the pixel of blue color in the image is large. In thermal analysis, when the color of blue in the region is darker than other region, it means that the area of that region is colder compared to other region. Hence, that region saturates more water content.

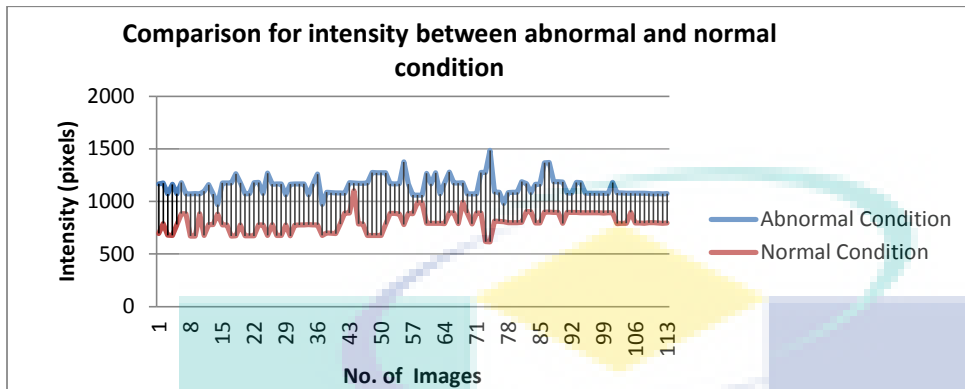


Figure 4.16 The comparison using intensity features between abnormal and normal condition for HSV technique

Next is the graph for K-Means technique. It is shown is Figure 4.17 below. First is for the area features. It can be observed that the value for abnormal condition is higher than normal condition. The range for abnormal condition is between 25000 and 30000. The range for normal condition is between 5000 and 10000. The average for both conditions is 24805. The overall results for this technique are smaller compared to HSV results. It is because the segmentation for K-Means is not accurate as HSV technique. It is not detected right region for water spots region in the image.

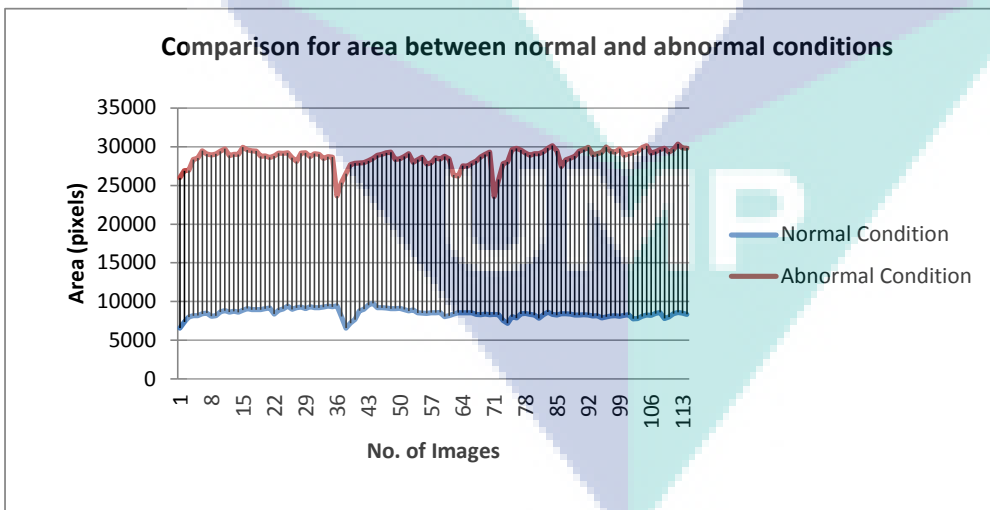


Figure 4.17 The comparison using area features between abnormal and normal condition for K-Means technique

Furthermore, the result in the Figure 4.18 below shows the perimeter features. The range for abnormal condition is small. It is between 2900 and 3100. The normal condition value is between 1000 and 1500. The value for perimeter using K- Means is also smaller than the value using HSV technique.

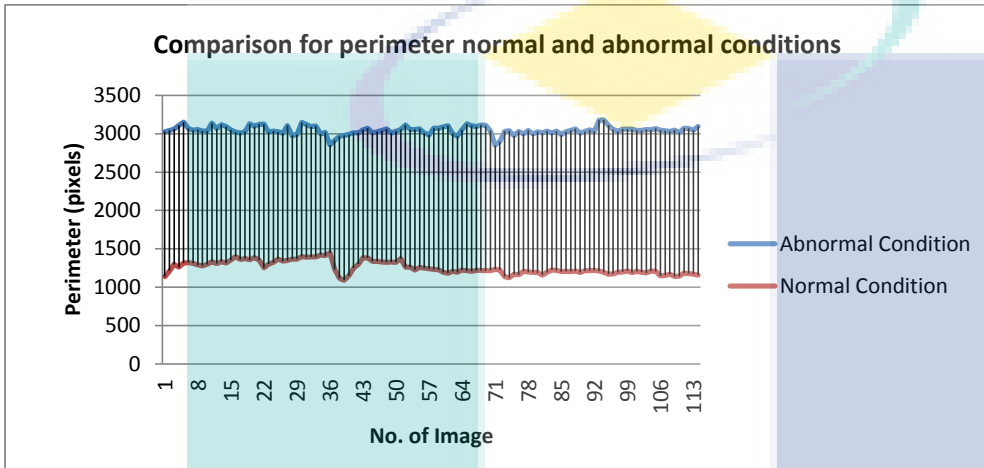


Figure 4.18 The comparison using perimeter features between abnormal and normal condition for K-Means technique

Figure 4.19 below shows the graph for intensity values. The intensity graph for K- Mean technique is unstable. For the first 49 images, the value of abnormal condition is high and normal condition is small. The value for remaining images almost similar with each other and have small values of intensity.

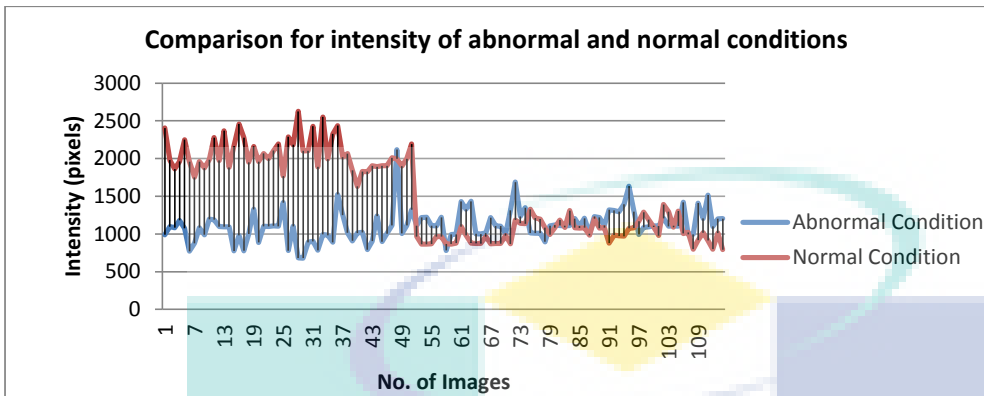


Figure 4.19 The comparison using intensity features between abnormal and normal condition for K-Means technique

Lastly, the graph in Figure 4.20 presented the results for Feature Matching technique. The range for abnormal condition is smaller compared to the HSV and K-Means technique. The value is between 20000 and 24000. The average of this technique for both normal and abnormal condition is 17125.32. From the results, it can be conclude that Feature Matching technique is not accurately segmented the image.

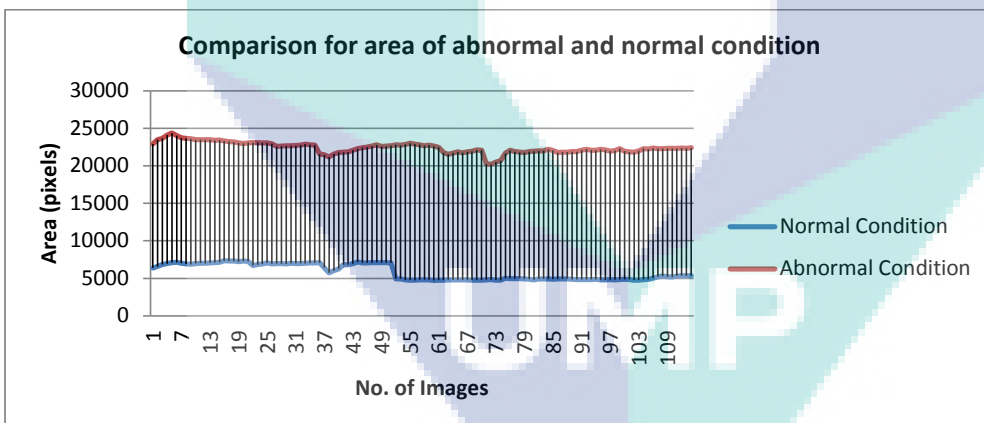


Figure 4.20 The comparison using area features between abnormal and normal condition for Feature Matching technique

The Figure 4.21 below shows the graph for perimeter features. The range for abnormal condition is between 4000 and 5000 while the range for normal condition is 1000 and 2000. The perimeter values for this technique are smaller than HSV and K-Means technique.

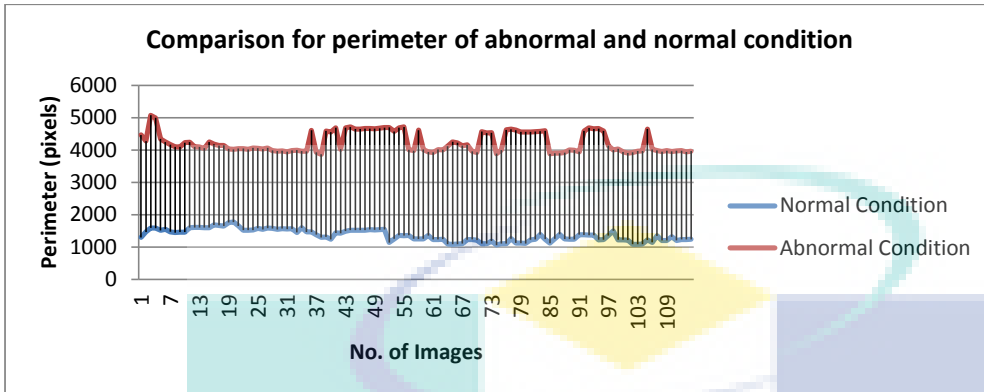


Figure 4.21 The comparison using perimeter features between abnormal and normal condition for Feature Matching technique.

Additionally, below is the Figure 4.22 for intensity features. For the first 52 images, the range between both conditions is small. The value is almost the same. But for the image from 55 to 114, the range is wide. The value of intensity for abnormal condition is higher compared to normal condition. The value for intensity is depends to each region in an image.

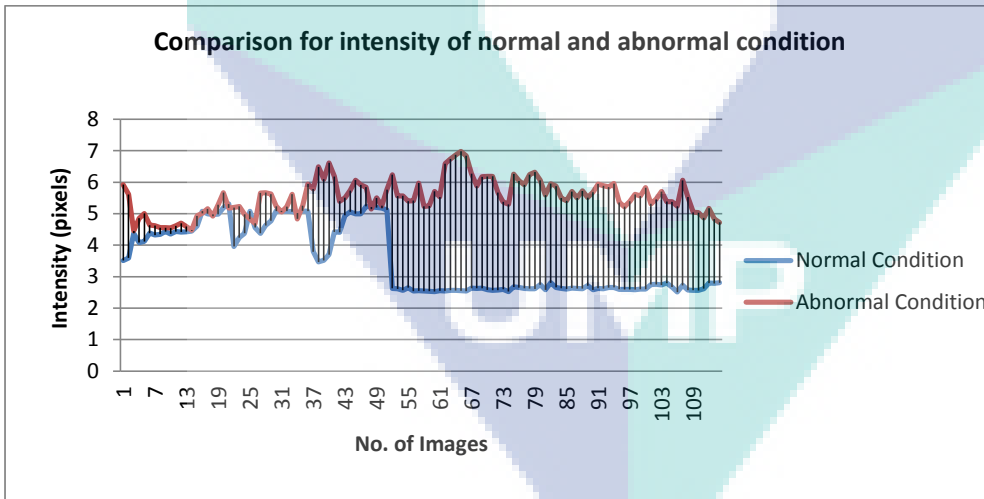


Figure 4.22 The comparison using intensity features between abnormal and normal condition for Feature Matching technique

4.4.1 Classification

This subsection discusses the result of experiment in term of classification. The outputs of the classification are normal or abnormal and high intensity or low intensity. The technique used for classification is linear thresholding. Figure 4.23 below shows the detection result for the proposed technique.

```
Command Window
Frame 1 : normal and low intensity
Frame 2 : normal and low intensity
Frame 3 : normal and high intensity
Frame 4 : normal and low intensity
Frame 5 : normal and low intensity
Frame 6 : normal and low intensity
Frame 7 : normal and high intensity
Frame 8 : normal and high intensity
Frame 9 : normal and low intensity
Frame 10 : normal and high intensity
Frame 11 : normal and high intensity
Frame 12 : normal and high intensity
Frame 13 : normal and high intensity
Frame 14 : normal and low intensity
Frame 15 : normal and high intensity
Frame 16 : normal and high intensity
Frame 17 : normal and high intensity
Frame 18 : normal and high intensity
Frame 19 : normal and high intensity
Frame 20 : normal and high intensity
Frame 21 : Abnormal and high intensity
Frame 22 : Abnormal and high intensity
```

Figure 4.23 The detection result for the proposed technique

Comment [k53]: this is not the way to present result

After detecting which frame has a high possibility for landslide to occur, the experiment is proceed with the detection of intensity of each region. It is to know which region contains high saturation of water content. Based on the Figure 4.24 below, it can be seen that region number 6 has the highest intensity of water saturation.

After the detection made, the authorities or related parties in this field such as Malaysian Public Works Department (JKR) and Department of Irrigation and Drainage (JPS) can take further actions. The further actions such as improve system of drainage at the site and the water content should be diverted away from the prone region by channeling water in sewer pipe to the base of slope. This experiment is suitable for inspection and survey.

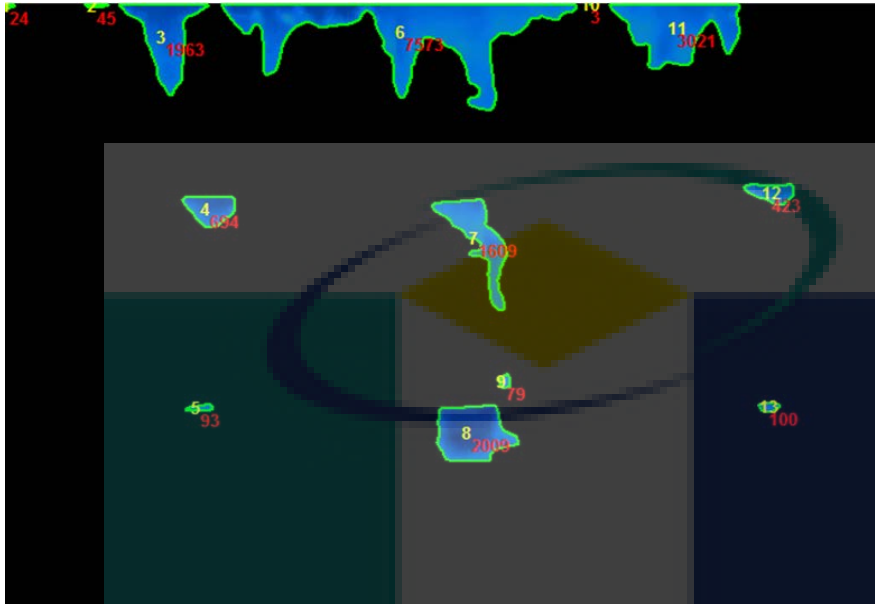


Figure 4.24 The intensity value for abnormal condition

The Figure 4.25 below is the figure for normal condition. The intensity of water is lower compared to the abnormal condition in figure above. Hence, the possibility for landslide to happen is low.

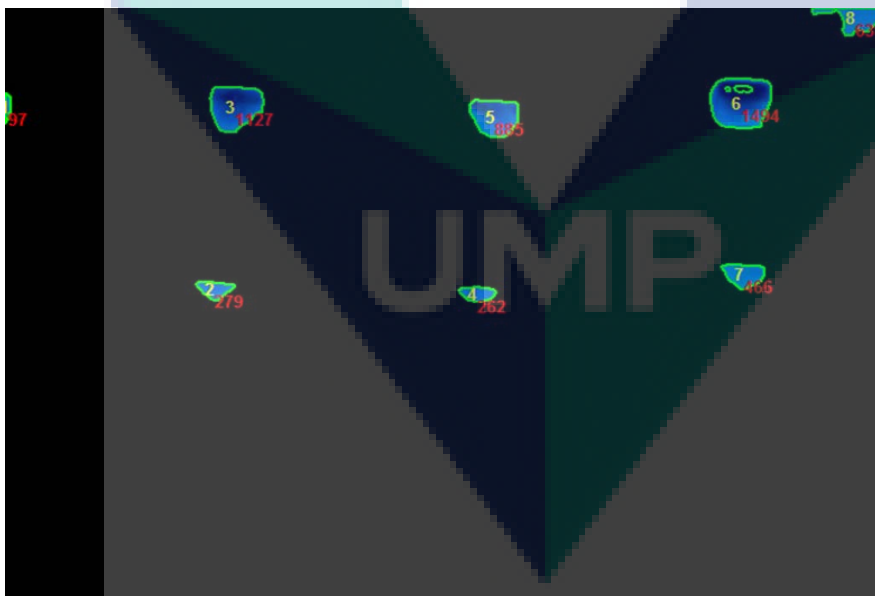


Figure 4.25 The intensity value for normal condition

4.5 Water content in soil

Comment [k54]: ???

Volumetric water content is the fraction of the total volume of soil that is occupied by water. It is because it has relationship with soil porosity. Volumetric water content is equivalent to the saturation degree when the pores are fully filled with water (Chae and Kim, 2012). Water content was calculated at measurement from Equation 4.1 below.

$$\text{Water Content (\%)} = \frac{m_{\text{wet}} - m_{\text{dry}}}{m_{\text{dry}}} \times 100 \quad 4.1$$

m_{wet} and m_{dry} are the masses of the sample before and after drying in the oven. The value of m_{dry} is 330g. Table 4.26 shows the percentage of water content and the quantity of water that be pouring into the soil. The thermal images of soil with this quantity of water are shown in subsection 4.7.1.

Table 4.25 The percentage of water content and the quantity of water

Water content (%)	Quantity of Water (ml)
0	0
5	16.5
10	33.0
15	49.5
20	66.0
25	82.5

4.5.1 The result of water content in soil

The result of the laboratory experiment that has been discussed in chapter 3.4.1 is shown in Figure 4.26 below. It is started with 0% of water content and it is increased until 25% of water content. This experiment uses thermal imaging camera to observe the changes of colors. It is to prove that thermal can detect the water content in soil and the color of water content is blue. Besides, the blue color changes into dark color when the water is increased.

It can be seen from the Figure 4.26 (a), there is no blue color detected in the image because the water content is 0%. There is no water inside the soil. While the Figure 4.26 (b), (c), (d), (e), and (f), it contain 16ml, 33ml, 49.5ml, 66ml and 82.5ml of water respectively.

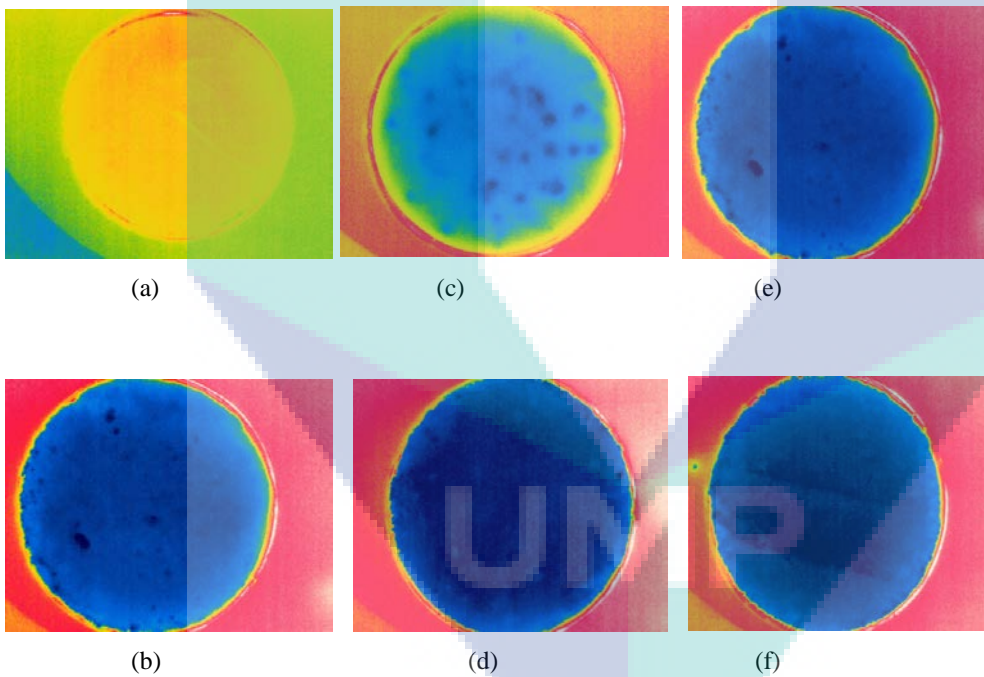


Figure 4.26 The results of laboratory experiment to prove thermal image for water content

Table 4.26 Experimental condition of soils

Sieve size (mm)	Mass of retained on sieve (g)	Cumulative mass retail	Percent passing (%)
5.00	164.31	164.31	88.47
3.35	167.43	331.74	76.71
1.18	444.54	776.28	45.51
0.60	184.36	960.64	32.56
0.30	223.39	1184.03	16.88
0.15	192.43	1376.46	3.37
0.063	25.82	1402.28	1.56
0	22.24	1424.52	0

Table 4.27 above shows experimental condition of soils. The Figure 4.27 below shows particle size distribution curve. It can be conclude that the soil used for this experiment is 11.53% is gravel, 86.91% is sand and 1.56% is silt and clay. Hence, the type of the soil is clayey.

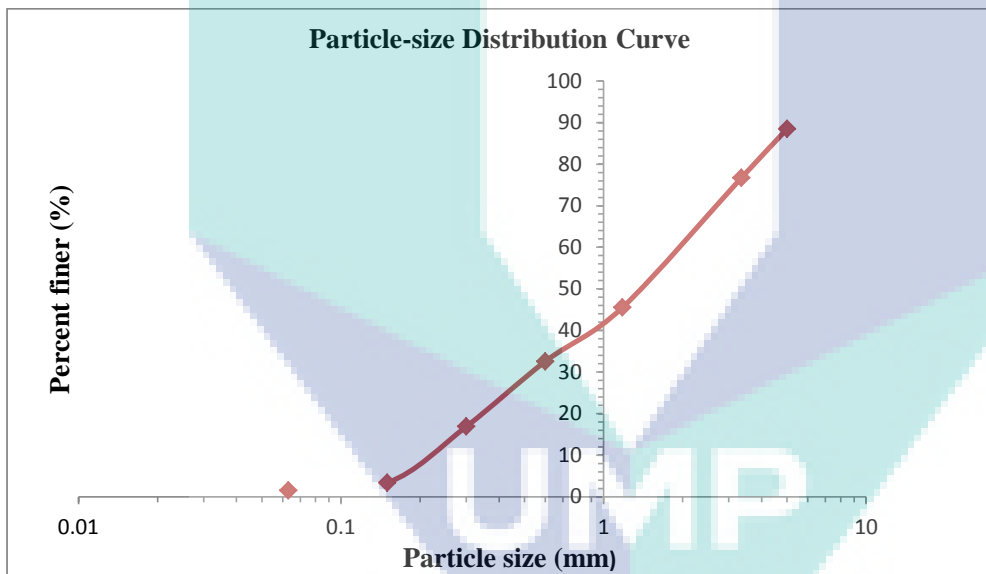


Figure 4.27 The graph of particle size distribution curve

CHAPTER 5

CONCLUSION

Comment [k55]: high light contribution.
relate with objective.

5.1 Introduction

This research develops a contribution in image processing field. The contribution is the best algorithm of image processing choose to detect water spots. The main objective in image segmentation to detect water saturation spots is accomplished. In previous techniques, there are a lot of tools that used for landslide prediction but it need installation and extra knowledge to use it. For this technique, it is practical in term of mobility and any expertise can use this system. Besides, the thermal images in this study are more accurate and clear using image processing.

The entire image involved with image segmentation, feature extraction and classification process. The performance of image segmentation was evaluated to select best algorithms for the system. HSV color space technique achieved the highest accuracy which is 98.35 for abnormal images, 99.39 for normal images and 98.59 for both conditions.

5.2 Recommendation for further research

This study has developed a computer vision system for early prediction of high water spots saturation using thermal imaging camera through the use of several proposed image processing technique. There are some recommendations that can be explored to further present work and to be used in additional application. These are outlined below:

1. Introducing real time processing

The implemented system can be control by user's smartphone or any gadget. The GUI is integrated with ANDROID or windows and then connected with thermal imaging camera to be used for direct monitoring.

REFERENCES

- Ahmad, J., Lateh, H. & Saleh, S. (2014). Landslide Hazards: Household Vulnerability, Resilience and Coping in Malaysia. *Journal of Education and Human Development*, 3(3), 149-155.
- Akyildiz, I. F. & Stuntebeck, E. P. (2006). Wireless underground sensor networks: Research challenges. *Ad Hoc Networks*, 4(6), 669-686.
- Al Bashish, D., Braik, M. & Bani-Ahmad, S. (2011). Detection and classification of leaf diseases using K-means-based segmentation and. *Information Technology Journal*, 10(2), 267-275.
- Alimohammadlou, Y., Najafi, A. & Yalcin, A. (2013). Landslide process and impacts: A proposed classification method. *Catena*, 104, 219-232.
- Alkhasawneh, M. S., Ngah, U. K. B., Tien, T. L. & Isa, N. A. B. M. (2012). Landslide susceptibility hazard mapping techniques review. *Journal of Applied Sciences*, 12(9), 802.
- Angaitkar, P. G., Saxena, K., Gupta, N. & Sinhal, A. (2013, 25-26 March 2013). *Enhancement of infrared image for roof leakage detection*. Paper presented at the Emerging Trends in Computing, Communication and Nanotechnology (ICE-CCN), 2013 International Conference on.
- Antonello, G., Casagli, N., Farina, P., Leva, D., Nico, G., Sieber, A. & Tarchi, D. (2004). Ground-based SAR interferometry for monitoring mass movements. *Landslides*, 1(1), 21-28.
- Apostolidis, E. & Mezaris, V. (2014, 4-9 May 2014). *Fast shot segmentation combining global and local visual descriptors*. Paper presented at the 2014 IEEE International Conference on Acoustics, Speech and Signal Processing (ICASSP).
- Arnfred, J. T. & Winkler, S. (2015). *Fast-match: Fast and robust feature matching on large images*. Paper presented at the Image Processing (ICIP), 2015 IEEE International Conference on.
- Arslan, A., Kelam, M. A., Eker, A. M., Akgün, H. & Koçkar, M. K. (2015). Optical Fiber Technology to Monitor Slope Movement *Engineering Geology for Society and Territory-Volume 2* (pp. 1425-1429): Springer.
- Azak, M. D., Akgun, S., Azak, S. I. & Torun, E. (2003, 22-24 Oct. 2003). *Thermal detection of buried circular objects with a rule-based fast shape detection algorithm*. Paper presented at the Sensors, 2003. Proceedings of IEEE.
- Azman, F. I., Ghazali, K. H., Hamid, R., Mohamed, Z. & Nawli, N. S. DETECTION AND SUMMATION OF SQUAMOUS EPITHELIAL CELLS IN SPUTUM SLIDE IMAGES BY NUCLEUS DETECTION.
- Baumberg, A. (2000, 2000). *Reliable feature matching across widely separated views*. Paper presented at the Computer Vision and Pattern Recognition, 2000. Proceedings. IEEE Conference on.
- Bay, H., Tuytelaars, T. & Van Gool, L. (2006). *Surf: Speeded up robust features*. Paper presented at the European conference on computer vision.
- Bitelli, G., Dubbini, M. & Zanutta, A. (2004). Terrestrial laser scanning and digital photogrammetry techniques to monitor landslide bodies. *International Archives of Photogrammetry, Remote Sensing and Spatial Information Sciences*, 35(B5), 246-251.
- Bobrowsky, P. & Couture, R. (2014). LANDSLIDE TERMINOLOGY Canadian Technical Guidelines and Best Practices related to Landslides: a national initiative for loss reduction.
- Bora, D. J., Gupta, A. K. & Khan, F. A. (2015). Comparing the Performance of L* A* B* and HSV Color Spaces with Respect to Color Image Segmentation. *arXiv preprint arXiv:1506.01472*.
- Brunetti, M., Guzzetti, F. & Rossi, M. (2009). Probability distributions of landslide volumes. *Nonlinear Processes in Geophysics*, 16(2), 179-188.

- Bulanon, D., Burks, T. & Alchanatis, V. (2008). Study on temporal variation in citrus canopy using thermal imaging for citrus fruit detection. *Biosystems Engineering*, 101(2), 161-171.
- Capparelli, G., La Sala, G., Vena, M. & Donato, A. (2015). *Analysis of hydrological and geotechnical aspects related to landslides caused by rainfall infiltration*. Paper presented at the EGU General Assembly Conference Abstracts.
- Chae, B.-G. & Kim, M.-I. (2012). Suggestion of a method for landslide early warning using the change in the volumetric water content gradient due to rainfall infiltration. *Environmental Earth Sciences*, 66(7), 1973-1986.
- Cheng, H.-D., Jiang, X., Sun, Y. & Wang, J. (2001). Color image segmentation: advances and prospects. *Pattern recognition*, 34(12), 2259-2281.
- Clague, J. J. (2013). Landslide *Encyclopedia of Natural Hazards* (pp. 594-602): Springer.
- Dass, R. & Devi, S. (2012). Image Segmentation Techniques 1.
- De Wrachien, D. (2010). *Monitoring, Simulation, Prevention and Remediation of Dense and Debris Flows III* (Vol. 67): WIT press.
- Dubey, S. R., Dixit, P., Singh, N. & Gupta, J. P. (2013). Infected fruit part detection using K-means clustering segmentation technique. *IJIMAI*, 2(2), 65-72.
- Duda, R. O., Hart, P. E. & Stork, D. G. (2012). *Pattern classification*: John Wiley & Sons.
- Durgam, U. K., Paul, S. & Pati, U. C. (2016, 5-6 March 2016). *SURF based matching for SAR image registration*. Paper presented at the 2016 IEEE Students' Conference on Electrical, Electronics and Computer Science (SCEECS).
- Fauzi, M. F. A., Wibowo, A. D. A., Lim, S. L. & Tan, W. N. (2015). *Detection of possible landslides in post-event satellite images using color and texture*. Paper presented at the Humanitarian Technology Conference (R10-HTC), 2015 IEEE Region 10.
- Ford, A. & Roberts, A. (1998). Colour space conversions. *Westminster University, London, 1998*, 1-31.
- Fredlund, D., Morgenstern, N. R. & Widger, R. (1978). The shear strength of unsaturated soils. *Canadian geotechnical journal*, 15(3), 313-321.
- Fruneau, B., Achache, J. & Delacourt, C. (1996). Observation and modelling of the Saint-Etienne-de-Tinée landslide using SAR interferometry. *Tectonophysics*, 265(3), 181-190.
- Ganesan, P., Rajini, V. & Rajkumar, R. I. (2010). *Segmentation and edge detection of color images using CIELAB color space and edge detectors*. Paper presented at the Emerging Trends in Robotics and Communication Technologies (INTERACT), 2010 International Conference on.
- Ganesan, P., Rajini, V., Sathish, B. S. & Shaik, K. B. (2014, 10-11 July 2014). *HSV color space based segmentation of region of interest in satellite images*. Paper presented at the Control, Instrumentation, Communication and Computational Technologies (ICCICCT), 2014 International Conference on.
- Giorgetti, A., Lucchi, M., Tavelli, E., Barla, M., Gigli, G., Casagli, N., . . . Dardari, D. (2016). A Robust Wireless Sensor Network for Landslide Risk Analysis: System Design, Deployment, and Field Testing. *IEEE Sensors Journal*, 16(16), 6374-6386. doi:10.1109/JSEN.2016.2579263
- Gong, Y., Zhang, W., Zhang, Z. & Li, Y. (2016). Research and Implementation of Traffic Sign Recognition System *Wireless Communications, Networking and Applications* (pp. 553-560): Springer.
- Gonzalez, R. C. (1987). *P. wintz digital image processing*. Addison-Wesley Publishing Company, 275-281.
- Gowen, A., Tiwari, B., Cullen, P., McDonnell, K. & O'Donnell, C. (2010). Applications of thermal imaging in food quality and safety assessment. *Trends in food science & technology*, 21(4), 190-200.
- Ha, S. V.-U., Pham, N. T., Pham, L. H. & Tran, H. M. (2016). Robust Reflection Detection and Removal in Rainy Conditions using LAB and HSV Color Spaces. *REV Journal on Electronics and Communications*, 6(1-2).

- Hamid, N., Yahya, A., Ahmad, R. B. & Al-Qershi, O. M. (2012). A Comparison between using SIFT and SURF for characteristic region based image steganography. *International Journal of Computer Science Issues*, 9(33-3), 110-116.
- Hartigan, J. A. (1975). Clustering algorithms.
- Heng-Da, C. & Ying, S. (2000). A hierarchical approach to color image segmentation using homogeneity. *IEEE Transactions on Image Processing*, 9(12), 2071-2082. doi:10.1109/83.887975
- Hidayatullah, P. & Zuhdi, M. (2015). Color-Texture Based Object Tracking Using HSV Color Space and Local Binary Pattern. *International Journal on Electrical Engineering and Informatics*, 7(2), 161.
- Higuchi, K., Fujisawa, K., Asai, K., Pasuto, A. & Marcato, G. (2007). *Application of new landslide monitoring technique using optical fiber sensor at Takisaka Landslide, Japan*. Paper presented at the AEG Special Publication. Proceedings of the first North American landslide conference. Vail, Colorado.
- Huabin, W., Gangjun, L., Weiya, X. & Gonghui, W. (2005). GIS-based landslide hazard assessment: an overview. *Progress in Physical Geography*, 29(4), 548-567. doi:10.1191/0309133305pp462ra
- Huat, B. B., Ali, F. H. & Low, T. (2006). Water infiltration characteristics of unsaturated soil slope and its effect on suction and stability. *Geotechnical & Geological Engineering*, 24(5), 1293-1306.
- Hungr, O., Evans, S. G., Bovis, M. J. & Hutchinson, J. N. (2001). A review of the classification of landslides of the flow type. *Environmental & Engineering Geoscience*, 7(3), 221-238. doi:10.2113/gseegeosci.7.3.221
- Ikeda, O. (2003). *Segmentation of faces in video footage using HSV color for face detection and image retrieval*. Paper presented at the Image Processing, 2003. ICIP 2003. Proceedings. 2003 International Conference on.
- Iverson, R. M. (2000). Landslide triggering by rain infiltration. *Water resources research*, 36(7), 1897-1910.
- Jadin, M. S., Taib, S. & Ghazali, K. H. (2015). Finding region of interest in the infrared image of electrical installation. *Infrared Physics & Technology*, 71, 329-338.
- Jain, A. K. & Chen, H. (2004). Matching of dental X-ray images for human identification. *Pattern recognition*, 37(7), 1519-1532.
- Jamaludin, S., Zainuddin, N. E., Abdullah, C. H. & Jaafar, K. B. (2011). MONITORING OF SLOW MOVING LANDSLIDE AT KM 8.25, JELAWANG-GUA MUSANG ROAD IN THE STATE OF KELANTAN, MALAYSIA *Geotechnical Engineering For Disaster Mitigation And Rehabilitation And Highway Engineering 2011: Geotechnical and Highway Engineering—Practical Applications, Challenges and Opportunities (With CD-ROM)* (pp. 507-512).
- Jebur, M. N., Pradhan, B. & Tehrany, M. S. (2015). Using ALOS PALSAR derived high-resolution DInSAR to detect slow-moving landslides in tropical forest: Cameron Highlands, Malaysia. *Geomatics, Natural Hazards and Risk*, 6(8), 741-759.
- Jin, S., van Dam, T. & Wdowinski, S. (2013). Observing and understanding the Earth system variations from space geodesy. *Journal of Geodynamics*, 72, 1-10.
- Jongmans, D. & Garambois, S. (2007). Geophysical investigation of landslides: a review. *Bulletin de la Société géologique de France*, 178(2), 101-112.
- Jotisankasa, A. & Vathananukij, H. (2008). *Investigation of soil moisture characteristics of landslide-prone slopes in Thailand*. Paper presented at the International Conference on Management of Landslide Hazard in the Asia-Pacific Region 11th-15th November.
- Joyce, K. E., Belliss, S. E., Samsonov, S. V., McNeill, S. J. & Glassey, P. J. (2009). A review of the status of satellite remote sensing and image processing techniques for mapping natural hazards and disasters. *Progress in Physical Geography*.
- Joyce, K. E., Dellow, G. D. & Glassey, P. J. (2008, 7-11 July 2008). *Assessing Image Processing Techniques for Mapping Landslides*. Paper presented at the IGARSS 2008 - 2008 IEEE International Geoscience and Remote Sensing Symposium.

- Juang, L.-H. & Wu, M.-N. (2010). MRI brain lesion image detection based on color-converted K-means clustering segmentation. *Measurement*, 43(7), 941-949.
- Jumb, V., Sohani, M. & Shrivasa, A. (2014). Color Image Segmentation Using K-Means Clustering and Otsu's Adaptive Thresholding. *Int. J. Innov. Technol. Explor. Eng.* 3(9), 72-76.
- Kastek, M., Dulski, R., Trzaskawka, P. & Bieszczad, G. (2010). *Sniper detection using infrared camera: technical possibilities and limitations*. Paper presented at the SPIE Defense, Security, and Sensing.
- Kawa, H., Khartade, A., Sonawane, S. & Madole, S. (2016). Smart Fire Detection System using Image Processing. *International Journal of Engineering Science*, 5485.
- Khan, W. (2013). Image segmentation techniques: A survey. *Journal of Image and Graphics*, 1(4), 166-170.
- Kondo, Y., Salibian-Barrera, M. & Zamar, R. (2012). A robust and sparse K-means clustering algorithm. *arXiv preprint arXiv:1201.6082*.
- Krishnamurthy, K., Khurana, H. K., Jun, S., Irudayaraj, J., Demirci, A., Jun, S. & Irudayaraj, J. (2009). Infrared radiation for food processing. *Food Processing Operations Modeling: Design and Analysis*, 115-142.
- Kusaka, T., Shikada, M. & Kawata, Y. (1992, 26-29 May 1992). *Extraction of Landslide Areas Using Spatial Features of Topographic Basins*. Paper presented at the Geoscience and Remote Sensing Symposium, 1992. IGARSS '92. International.
- Lee, C.-T. (2008). *GIS Application in Landslide Hazard Analysis—An Example from the Shihmen Reservoir Catchment Area in Northern Taiwan*. Paper presented at the Pacific Neighborhood Consortium (PNC) 2008 Annual Meeting program.
- Lee, S. & Min, K. (2001). Statistical analysis of landslide susceptibility at Yongin, Korea. *Environmental Geology*, 40(9), 1095-1113.
- Lillesand, T., Kiefer, R. W. & Chipman, J. (2014). *Remote sensing and image interpretation*: John Wiley & Sons.
- Liu, S., Xu, Z., Wu, L., Ma, B. & Liu, X. (2011). *Infrared Imaging Detection of Hidden Danger in Mine Engineering*. Paper presented at the Progress in Electromagnetics Research Symposium Proceedings, Suzhou, China, Sept.
- Luo, M., Yu-Fei, M. & Hong-Jiang, Z. (2003, 15-18 Dec. 2003). *A spatial constrained K-means approach to image segmentation*. Paper presented at the Information, Communications and Signal Processing, 2003 and Fourth Pacific Rim Conference on Multimedia. Proceedings of the 2003 Joint Conference of the Fourth International Conference on.
- Ma, J., Zhou, H., Zhao, J., Gao, Y., Jiang, J. & Tian, J. (2015). Robust feature matching for remote sensing image registration via locally linear transforming. *IEEE Transactions on Geoscience and Remote Sensing*, 53(12), 6469-6481.
- Ma, Y. L. S. (2014, 13-14 Dec. 2014). *Research on Image Based on Improved SURF Feature Matching*. Paper presented at the Computational Intelligence and Design (ISCID), 2014 Seventh International Symposium on.
- MacQueen, J. (1967). *Some methods for classification and analysis of multivariate observations*. Paper presented at the Proceedings of the fifth Berkeley symposium on mathematical statistics and probability.
- Madhloom, H., Kareem, S., Ariffin, H., Zaidan, A., Alanazi, H. & Zaidan, B. (2010). An automated white blood cell nucleus localization and segmentation using image arithmetic and automatic threshold. *Journal of Applied Sciences*, 10, 959-966.
- Mantovani, F., Soeters, R. & Van Westen, C. J. (1996). Remote sensing techniques for landslide studies and hazard zonation in Europe. *Geomorphology*, 15(3), 213-225.
- Martin, D., Fowlkes, C., Tal, D. & Malik, J. (2001). *A database of human segmented natural images and its application to evaluating segmentation algorithms and measuring ecological statistics*. Paper presented at the Computer Vision, 2001. ICCV 2001. Proceedings. Eighth IEEE International Conference on.
- McCauley, A. & Jones, C. Basic soil properties.

- Mehta, P., Chander, D., Shahim, M., Tejaswi, K., Merchant, S. & Desai, U. (2007). *Distributed detection for landslide prediction using wireless sensor network*. Paper presented at the Global Information Infrastructure Symposium, 2007. GIIS 2007. First International.
- Mehre, B. M., Kankanhalli, M. S. & Lee, W. F. (1997). Shape measures for content based image retrieval: a comparison. *Information Processing & Management*, 33(3), 319-337.
- Mihir, M., Malamud, B., Rossi, M., Reichenbach, P. & Ardizzone, F. (2014). *Landslide Susceptibility Statistical Methods: A Critical and Systematic Literature Review*. Paper presented at the EGU General Assembly Conference Abstracts.
- Mineo, S., Pappalardo, G., Rapisarda, F., Cubito, A. & Di Maria, G. (2015). Integrated geostructural, seismic and infrared thermography surveys for the study of an unstable rock slope in the Peloritani Chain (NE Sicily). *Engineering geology*, 195, 225-235.
- Mohammad, S., Ghazali, K. H., Che Zan, N., Radzi, M., Sofiah, S. & Abdul Karim, R. (2011). *Classification of fresh N36 pineapple crop using image processing technique*. Paper presented at the Advanced Materials Research.
- Motagh, M., Wetzel, H.-U., Roessner, S. & Kaufmann, H. (2013). A TerraSAR-X InSAR study of landslides in southern Kyrgyzstan, Central Asia. *Remote Sensing Letters*, 4(7), 657-666.
- Nakayama, C., Ikegaya, Y., Katsumata, T., Aizawa, H., Honda, M., Shibasaki, M., . . . Komuro, S. (2008, 14-17 Oct. 2008). *Thermal-imaging of foods in heating process*. Paper presented at the Control, Automation and Systems, 2008. ICCAS 2008. International Conference on.
- Ng, C. W. & Pang, Y. (2000). Influence of stress state on soil-water characteristics and slope stability. *Journal of geotechnical and geoenvironmental engineering*, 126(2), 157-166.
- Ng, H. P., Ong, S. H., Foong, K. W. C., Goh, P. S. & Nowinski, W. L. (2006, 0-0 0). *Medical Image Segmentation Using K-Means Clustering and Improved Watershed Algorithm*. Paper presented at the 2006 IEEE Southwest Symposium on Image Analysis and Interpretation.
- Ojala, T. & Pietikäinen, M. Texture classification.
- Pal, N. R. & Pal, S. K. (1993). A review on image segmentation techniques. *Pattern recognition*, 26(9), 1277-1294.
- Pascal, B., Thierry, V., Emmanuelle, K. & Yves, G. (2013). Cloud monitoring: an innovative approach for the prevention of landslide risks *Landslide Science and Practice* (pp. 665-670): Springer.
- Petrou, M. & Petrou, C. (2010). *Image processing: the fundamentals*: John Wiley & Sons.
- Pitas, I. (2000). *Digital image processing algorithms and applications*: John Wiley & Sons.
- Qasim, S., Harahap, I., Osman, S. & Baharom, S. (2013). Causal factors of Malaysian landslides: A narrative study. *Res. J. Appl. Sci. Eng. Technol*, 5, 2303-2308.
- Rafael Gonzalez, C. & Richard Woods, E. (2002). Digital image processing. *Pearson Education*.
- Rahardjo, H., Ong, T., Rezaur, R. & Leong, E. C. (2007). Factors controlling instability of homogeneous soil slopes under rainfall. *Journal of geotechnical and geoenvironmental engineering*, 133(12), 1532-1543.
- Rajbhandari, P. C. L., Alam, B. M. & Akther, M. S. (2002). Application of GIS (Geographic Information System) for landslide hazard zonation and mapping disaster prone area: a study of Kulekhani Watershed, Nepal. *Plan plus*, 1(1), 117-123.
- Ramesh, M. V. (2009, 18-23 June 2009). *Real-Time Wireless Sensor Network for Landslide Detection*. Paper presented at the Sensor Technologies and Applications, 2009. SENSORCOMM '09. Third International Conference on.
- Ramesh, M. V. (2014). Design, development, and deployment of a wireless sensor network for detection of landslides. *Ad Hoc Networks*, 13, 2-18.
- Regmi, N. R., Giardino, J. R. & Vitek, J. D. (2010). Modeling susceptibility to landslides using the weight of evidence approach: Western Colorado, USA. *Geomorphology*, 115(1), 172-187.
- Ren, F., Huang, J., Jiang, R. & Klette, R. (2009). *General traffic sign recognition by feature matching*. Paper presented at the Image and Vision Computing New Zealand.

- Riedel, B. & Walther, A. (2008). InSAR processing for the recognition of landslides. *Advances in Geosciences*, 14(14), 189-194.
- Ring, E. & Ammer, K. (2012). Infrared thermal imaging in medicine. *Physiological measurement*, 33(3), R33.
- Rogalski, A. (2012). History of infrared detectors. *Opto-Electronics Review*, 20(3), 279-308.
- Rosin, P. L. & Hervás, J. (2005). Remote sensing image thresholding methods for determining landslide activity. *International Journal of Remote Sensing*, 26(6), 1075-1092.
- Rosin, P. L., Hervás, J. & Barredo, J. I. (2000). *Remote sensing image thresholding for landslide motion detection*. Paper presented at the 1st Int. Workshop on Pattern Recognition Techniques in Remote Sensing.
- Saunders, G. M. (2014). Development of photogrammetric methods for landslide analysis.
- Savvaïdis, P. (2003). Existing landslide monitoring systems and techniques. *From Stars to Earth and Culture. In honor of the memory of Professor Alexandros Tsioumis. The Aristotle University of Thessaloniki, Greece*, 242-258.
- Scaioni, M., Longoni, L., Melillo, V. & Papini, M. (2014). Remote sensing for landslide investigations: An overview of recent achievements and perspectives. *Remote Sensing*, 6(10), 9600-9652.
- Schenk, T. (2005). Introduction to photogrammetry. *The Ohio State University, Columbus*.
- Sezgin, M. (2004). Survey over image thresholding techniques and quantitative performance evaluation. *Journal of Electronic imaging*, 13(1), 146-168.
- Sheth, A., Tejaswi, K., Mehta, P., Parekh, C., Bansal, R., Merchant, S., . . . Toyama, K. (2005). *Senslide: a sensor network based landslide prediction system*. Paper presented at the Proceedings of the 3rd international conference on Embedded networked sensor systems.
- Shijin Kumar, P. S. & Dharun, V. S. (2016). Hybrid brain MRI segmentation algorithm based on K-means clustering and texture pattern matrix. *International Journal of Applied Engineering Research*, 11(6), 4343-4348.
- Singhroy, V., Mattar, K. & Gray, A. (1998). Landslide characterisation in Canada using interferometric SAR and combined SAR and TM images. *Advances in Space Research*, 21(3), 465-476.
- Snyder, W. E. & Qi, H. (2010). *Machine vision*: Cambridge University Press.
- Tantianuparp, P., Shi, X., Zhang, L., Balz, T. & Liao, M. (2013). Characterization of landslide deformations in three gorges area using multiple InSAR data stacks. *Remote Sensing*, 5(6), 2704-2719.
- Tarchi, D., Casagli, N., Fanti, R., Leva, D. D., Luzi, G., Pasuto, A., . . . Silvano, S. (2003). Landslide monitoring by using ground-based SAR interferometry: an example of application to the Tessina landslide in Italy. *Engineering geology*, 68(1), 15-30.
- Tatiraju, S. & Mehta, A. Image Segmentation using k-means clustering, EM and Normalized Cuts.
- Terzis, A., Anandarajah, A., Moore, K. & Wang, I. (2006). *Slip surface localization in wireless sensor networks for landslide prediction*. Paper presented at the Proceedings of the 5th international conference on Information processing in sensor networks.
- Thapa, P. B. (2016). Conceptual overview of community-based landslide risk reduction. *g] kfn eff} ule {s; dfh*, 33, 57.
- Tigadi, B. & Sharma, B. (2016). Banana Plant Disease Detection and Grading Using Image Processing. *International Journal of Engineering Science*, 6512.
- Tucker, C. & Sellers, P. (1986). Satellite remote sensing of primary production. *International Journal of Remote Sensing*, 7(11), 1395-1416.
- Umbaugh, S. E. (2005). *Computer imaging: digital image analysis and processing*: CRC press.
- Vadivambal, R. & Jayas, D. S. (2011). Applications of thermal imaging in agriculture and food industry—a review. *Food and Bioprocess Technology*, 4(2), 186-199.
- Varith, J., Hyde, G., Baritelle, A., Fellman, J. & Sattabongkot, T. (2003). Non-contact bruise detection in apples by thermal imaging. *Innovative Food Science & Emerging Technologies*, 4(2), 211-218.

- Varnes, D. J. (1978). Slope movement types and processes. *Transportation Research Board Special Report*(176).
- Vilcahuaman, L., Harba, R., Canals, R., Zequera, M., Wilches, C., Arista, M. T., . . . il, H. (2014, 26-30 Aug. 2014). *Detection of diabetic foot hyperthermia by infrared imaging*. Paper presented at the Engineering in Medicine and Biology Society (EMBC), 2014 36th Annual International Conference of the IEEE.
- Wang, G., Xie, M., Chai, X., Wang, L. & Dong, C. (2013). D-InSAR-based landslide location and monitoring at Wudongde hydropower reservoir in China. *Environmental Earth Sciences*, 69(8), 2763-2777.
- Wang, H. & Suter, D. (2003). *Color image segmentation using global information and local homogeneity*. Paper presented at the Proceeding of 7th Conf. of Digital Image Computing: Techniques and Applications.
- Wang, Q., Si, H.-P., Xi, L. & Zheng, G. (2016). *Design of a tobacco leaf maturity degree detection device based on image processing technology*. Paper presented at the Materials, Manufacturing Technology, Electronics and Information Science: Proceedings of the 2015 International Workshop on Materials, Manufacturing Technology, Electronics and Information Science (MMTEI2015).
- Wu, Q. & Yu, Y. (2004). Feature matching and deformation for texture synthesis. *ACM Transactions on Graphics (TOG)*, 23(3), 364-367.
- Xu, R. & Wunsch, D. (2005). Survey of clustering algorithms. *Neural Networks, IEEE Transactions on*, 16(3), 645-678.
- Yongsheng, S., Gang, L. & Rui, G. (2009). Segmentation algorithm for green apples recognition based on K-means algorithm. *Transactions of the Chinese Society for Agricultural Machinery*, 40(Suppl 1), 100-104.
- Zhang, D. & Lu, G. (2004). Review of shape representation and description techniques. *Pattern recognition*, 37(1), 1-19.
- Zhao, M., Bu, J. & Chen, C. (2002). *Robust background subtraction in HSV color space*. Paper presented at the ITCOM 2002: The Convergence of Information Technologies and Communications.
- Zhiqiang, Z., Huili, G., Wenji, Z. & Youquan, Z. (2005, 25-29 July 2005). *Application of remote sensing to study of landslide*. Paper presented at the Proceedings. 2005 IEEE International Geoscience and Remote Sensing Symposium, 2005. IGARSS '05.



UMP